miR-155 regulates differentiation of brown and beige adipocytes via a bistable circuit

Dissertation

zur

Erlangung des Doktorgrades (Dr. rer. nat.)

der

Mathematisch-Naturwissenschaftlichen Fakultät

der

Rheinischen Friedrich-Wilhelms-Universität Bonn

vorgelegt von

Yong Chen

aus

Wuhan, China

Bonn, September 2013

Angefertigt mit Genehmigung der Mathematisch-Naturwissenschaftlichen Fakultät der Rheinischen Friedrich-Wilhelms-Universität Bonn.

1. Gutachter: Prof. Dr. Alexander Pfeifer

2. Gutachter: Prof. Dr. Dieter O. Fürst

3. Gutachter: Prof. Dr. Dr.Walter Witke

4. Gutachter: Prof. Dr. Holger Fröhlich

Tag der Promotion: 18.06.2014

Erscheinungsjahr: 2014

Acknowledgement

I would like to thank all the persons who did real supports to me during my doctoral thesis.

The most thanks are to Prof. Alexander Pfeifer for giving me an opportunity to work with him on the project, and it is him to help me to grow up. He is always showing me the way how to become a good scientist. On science, he is like my father.

Next, I will give my many thanks to Dr. Bodo Haas and Dr. Franziska Siegel. It was Bodo to bring me on the scientific "boat", and Franzi gave me all her help and much care on my doctor works and life in the lab. Without them, I couldn't finish my PhD thesis so successfully.

A lot of thanks are also to the members of my doctoral committee: Prof. Fürst, Prof. Witke and Prof. Fröhlich, thanks them for spending time on my thesis.

A special thanks, I will give to Prof. Fröhlich and Prof. Meister. Thanks them for their suggestions, and thanks for helping me to publish my doctoral works on the paper. The special thanks I shall also give to NRW International Graduate School BIOTECH-PHARMA for its funding, as well as Dr. Elisabeth Mies-Klomfass.

Here, I also would like to thanks all the colleagues of Prof. Pfeifer's group. Thank them for giving me a lot of supports. Without them, I couldn't learn so many techniques and much knowledge in the laboratory. Thank Stefanie Kipschull, Steffi helps me a lot on performing the experiments, she is very clever and my good assistant. Also I would like to thank Dr. Ana Kilič, a friend of mine; she is very smart and strong lady. She always takes care of my life in the lab. Thank Dr. Katrin Zimmerman, she is our virus "queen", without her help, I wouldn't finish my project. Thank Linda, Didier, Thorsten and Dani, they are very kind and friendly to me. I also give my thanks to our young Phd students, Anja, Jenni, Abi, Aileen, and our new colleague, Yvonne, Kamran, Kirsten, they are now working with me.

Furthermore, I thank my parents, and as well as my wife, Ruping, for many cares of my life. Special thanks to my little daughter, Zimeng, her coming in the world brings me a lot of happiness.

Table of Contents

Abbreviations

3T3-L1	white preadipocyte cell line
APS	ammonium peroxidisulfate
aP2	fatty acid binding protein 4 (Fabp-4)
BAT	brown adipose tissue
BAT-MSCs	brown adipose tissue derived mesenchymal stem cells
bp	base pair
BSA	bovine serum albumine
Ca2+	calcium ion
CaCl2	calcium chloride
cAMP	cyclic adenosine-3', 5'-monophosphate
cDNA	complementary DNA
C/EBP	CCAAT/enhancer-binding protein
ChIP	chromatin immunoprecipitation
Cidea	cell death-inducing DNA fragmentation factor α subunit-like effector A
cGMP	cyclic guanosine-3', 5'-monophosphate
CMV	cytomegalovirus promoter
DMEM	Dulbecco's Modified Eagle Medium
DMSO	dimethyl sulfoxide
DNA	deoxyribonucleic acid
dsDNA	double-strand DNA
dNTPs	deoxynucleotide triphosphate
DTT	1, 4-dithiothreitol
ECL	enhanced chemiluminescence
E. coli	Escherichia coli
EtOH	ethanol
EDTA	ethylene diamine tetraaceitic acid
FACS	fluorescence activated cell sorting
FBS	foetal bovine serum
FFA	free fatty acids

GAPDH	glycerol aldehyde-3-phosphate dehydrogenase
h	hours
HBSS	Hanks' balanced salt solution
H/E	hematoxylin/eosin
HEK293-T	human embryonic kidney cells
HEPES	N-(2-hydroxyethyl)-piperazine-N'-2-ethansulfonic acid
HIB-1B	brown preadipocyte cell line
HIV	human immune deficiency virus
HRP	horseradish peroxidase
HPRT	hypoxanthine-guanine-phosphoribosyltransferase
HSL	hormone-sensitive lipase
IBMX	3-isobutyl-methyl-xanthine
IHC	immune-histo-chemistry
ins	insulin
K	potassium
kb	kilo base
KCl	potassium chloride
kDa	kilo Dalton
KH2PO4	potassium dihydrogenphosphate
k.o.	Knock out
LB+	Luria-Bertani Medium with glucose
LBamp	Luria-Bertani Medium with ampicillin
LTD	long term depression
LTP	long term potentiation
LTR	long terminal repeat
LV-	lentiviral vector
LV-control	lentiviral vector containing no promoter and no transgene
LV-mirctrl	lentiviral vector containing CMV-GFP-scramble sequence
LV-mir155	lentiviral vector containing CMV-GFP-pre-miR155 sequence
LV-mirS155	lentiviral vector containing CMV-GFP-sponge155 sequence
ml/µl	milliliter/microliter

M/mM/µM	molar/millimolar/micromolar
MeOH	methanol
Mg	magnesium
MgCl2	magnesium chloride
mg/µg	milligram/microgram
min	minutes
miR	micro RNA
mRNA	messenger RNA
MSC	mesenchymal stem cell
n/N	number
Na	sodium
NaCl	sodium chloride
NaF	sodium fluoride
Na2HPO4	disodium hydrogenphosphate
NaN3	sodium azid
Na3VO4	sodium orthovanadate
nm	nanometer
nM	nanomolar
OD	optical density
o/n	overnight
p	passage
PAGE	polyacrylamid gel electrophoresis
PBS	phosphate-buffered saline
PCR	polymerase chain reaction
PDE	phosphodiesterase
Pen/Strep	penicilline/streptomycine
PFA	paraformaldehyde
PGK	phosphoglycerate kinase promoter
PKG	cGMP-dependent kinase, protein kinase G
PNK	polynucleotide kinase
pol	*pol*-gene of HIV-1

PPARγ	peroxisome proliferator-activated receptor γ
PGC-1α	peroxisome proliferator-activated receptor γ coactivator 1α
RIPA	adio immunoprecipitation assay
RNA	ribonucleic acid
RNase	ribonuclease
rpm	rotations per minute
RRL	lentiviral vector plasmid
RSV	respiratory syncytial virus
RT	room temperature
RTase	reverse transcriptase
RT-PCR	reverse transcription-PCR
SDS	sodium dodecyl sulfate
s.e.m.	standard error of the mean
SV40	simian virus 40
SVF	stromal vascular fraction
T2D	Type 2 Diabetes
T3	triiodothyronine
TAg	SV40 large tumor antigen
Taq	*Thermophilus aquaticus* polymerase
TBE	Tris-borate-EDTA
TBS	Tris-buffered saline
TE	Tris-EDTA buffer
TEMED	N, N, N', N'-tetramethylethylenediamine
Tris	2-Amino-2-hydroxymethyl-propane-1, 3-diol
U3	U3 region of the HIV LTR
U5	U5 region of the HIV LTR
UCP-1	uncoupling protein-1
UTR	untrancriptional region
WAT	white adipose tissue
WB	Western blot
WPRE	post-transcriptional regulatory element of the woodchuck hepatitis virus

wt	wild type
XL-1/XL-21	competent *E. coli* bacteria

1. Introduction

1.1. microRNA (miRNA)

1.1.1. Historical background of miRNA

MicroRNAs (miRNAs) are a recently discovered class of naturally occurring small RNA molecules (~22nt) that regulate specific genes post-transcriptionally. The first reported miRNA, lin-4, was cloned from C. elegans in 1993 (Lee et al., 1993; Wightman et al., 1993). This remained a singular example until 2000 when a second miRNA, let-7, was discovered (Reinhart et al., 2000). Unlike lin-4, the sequence of let-7 was found to be highly conserved in eukaryotic genomes (Pasquinelli et al., 2000). It was soon realized that similar sequences were present in eukaryotic genomes and that they represent a new class of regulatory RNA molecules, first called 'miRNA' by Ambros in 2001(Chen and Meister, 2005).

Since this time, interest in the miRNA-field has exploded resulting in hundreds of miRNAs being cloned from a wide range of animals. In human, there have been more and more experimentally confirmed miRNAs in the genome. Computational approaches suggest that their number is in a thousand (Bentwich et al., 2005; Berezikov and Plasterk, 2005). As of recent, the number of annotated human miRNAs is approximately closed to 1600 (Kozomara and Griffiths-Jones, 2010).

1.1.2. miRNA biogenesis

Many miRNAs are phylogenetically highly conserved, 20 to 22 nucleotide non-protein-coding RNA molecules that recognize target sequences of imperfect or perfect complementarity in cognate messenger RNA (mRNA) and mediate post-transcriptional gene repression by inhibiting proteins translation or destabilizing target mRNA transcripts (Monticelli et al., 2005; Shivdasani, 2006). miRNAs play an important role in cell differentiation and regulation of gene expression during development (Fazi et al., 2005), For example, miR193b-365 and miR-133 have been reported as essential factors for brown fat differentiation (Sun et al., 2011; Trajkovski et al., 2012b). miRNAs are believed to fine-regulate a diverse array of biological processes (Shivdasani, 2006). Their implication in biological processes is ranging from cell proliferation and cell death

during development to stress resistance, fat metabolism, insulin secretion and hematopoietic differentiation (Monticelli et al., 2005).

So far, over 1600 miRNAs have yet been reported in humans and are annotated in the miRNA-registry (Kozomara and Griffiths-Jones, 2010). Recent evidence suggests that the actual number of miRNA is likely to be increased.

Most human miRNAs are encoded within introns of coding or non-coding messenger-RNA (mRNA), whilst others are located intergenically or within exons (Rodriguez et al., 2004). miRNA genes are also co-transcribed together with their host gene in some cases (Mraz and Pospisilova, 2012). However, as much as 40% of miRNA genes lie in introns of protein coding genes, approximately 10% of miRNAs are located within introns of long non-coding RNA transcripts and the rest of miRNAs are found in exons of long nonprotein-coding transcripts (Rodriguez et al., 2004). miRNAs are transcribed by RNA-polymerase II as 5'-capped polyadenylated precursors known as pri-miRNAs (primary miRNAs) (Lee et al., 2004). Approximately more than half of the human miRNAs are encoded in tandems or clusters that are co-expressed within single pri-miRNAs, whilst other pri-miRNAs encode a single miRNA sequence. Pri-miRNAs are cleaved within the nucleus to form 60-70 nucleotide hairpin structures termed pre-miRNA (precursor-miRNA) by the microprocessor complex consisting of Drosha and DGCR8 (Gregory et al., 2006). Pre-miRNAs are exported from the nucleus to the cytoplasm by exportin-5 in a RAN-GTP-dependent manner. Cytoplasmic pre-miRNAs are then further cleaved to form an asymmetric duplex (the miRNA / miRNA*duplex) by Dicer in association with TRBP. The mature miRNA strand is incorporated into the translational repressor complex: RNA Induced Silencing Complex (RISC) (Figure 1A) (Lund et al., 2004).

1.1.3. Regulatory function of miRNAs

The strand with lower stability base pairing at its 5'end preferentially binds to RISC and becomes the active mature miRNA (Preall et al., 2006). The RISC-miRNA complex then binds to its cognate 3'UTR sequence in the target messenger-RNA initiating translational repression or modification (Figure 1A, B).

A

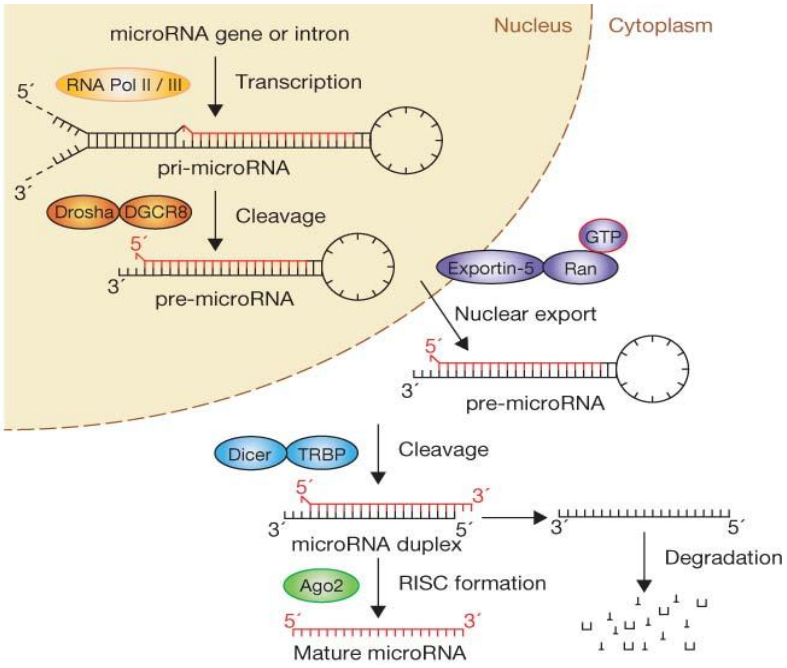

B

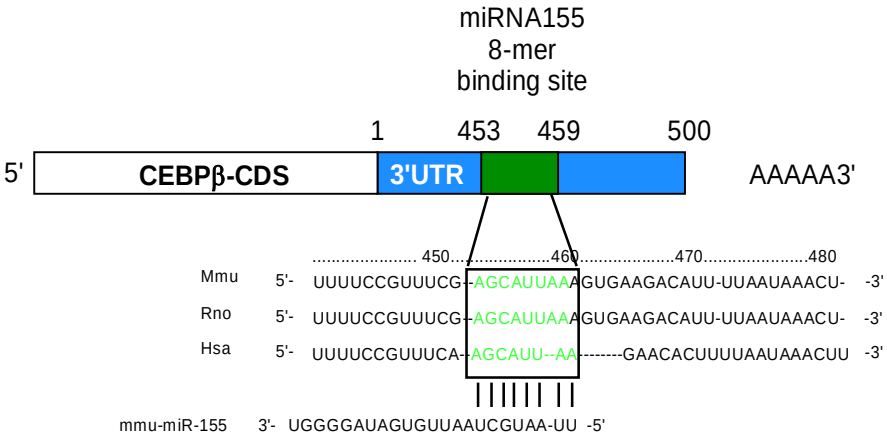

Figure 1. miRNA biosynthesis: **(A)** The miRNA is generated from the miRNA gene. With help of RNA polymerase 2, the pri-miRNA (500-3000bp) is formed. The enzyme complex Drosha cleaves the pri-miRNA to the precursor-miRNA (~70bp). During this process, the pre-miRNA is transported outside the nucleus into the cytoplasm by Exportin 5 (transporting protein). At the end, the pre-miRNA is cut to the mature miRNA by Dicer. **(B)** Example for miRNA binding to target mRNAs (ie. On 3' UTR of C/EBPβ mRNA, there is 8-mer binding site for the respective miR-155). Figure 1A is adapted from Velu's figure (Velu et al., 2012).

miRNAs perform their function by binding to complementary binding sites on the target mRNA, and thereby regulating mRNA translation or degradation. Because of imperfect binding to the 3'UTR, many mRNAs can be targeted by one miRNA. Conversely, several different miRNAs can bind to and cooperatively control one single mRNA target. Recent studies have predicted that over 30% of human genes are putatively regulated by miRNAs (Lewis et al., 2005). miRNAs negatively regulate their targets in one of two ways, depending on the degree of complementarity between the miRNA and the target mRNA: First, miRNAs binding to their mRNA targets with imperfect complementarity blocks target gene expression at the level of protein translation. Complementary sites for miRNAs using this mechanism are generally found in the 3'UTR of target mRNAs. Second, miRNAs binding with perfect (or nearly perfect) complementarity induce target mRNA cleavage. Complementary sites mediating this mechanism are usually located in the open reading frame (ORF) of mRNA targets (Figure 2).

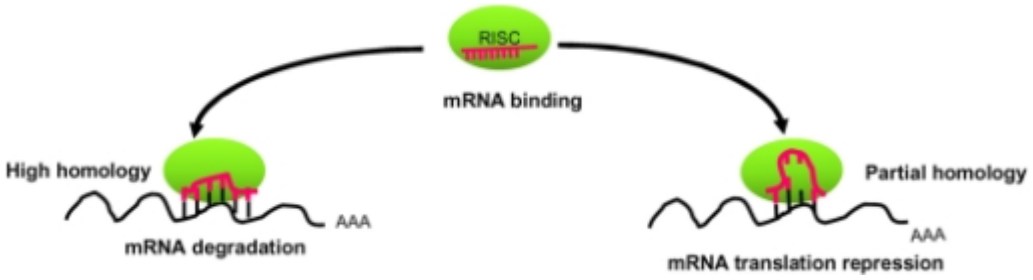

Figure 2. The miRNA/ RISC complex is binding to the target mRNA. Binding to sequences within the ORF with high homology mediates mRNA degradation (left) whereas low-complementarity binding to the target mRNA 3´UTR induces translation inhibition (right). Figure is adapted from (Liu et al., 2008).

1.2. Adipose tissue biology

There are two different types of adipose tissues in mammals: white adipose tissue (WAT) and brown adipose tissue (BAT). BAT cells have a large content of mitochondria and contain less lipids in comparison to WAT cells. The major function of BAT and WAT in mammals is about energy metabolism. BAT is responsible for energy expenditure, whereas WAT is mainly responsible for energy storage (Lowell and Flier, 1997). With regard to molecular biology, BAT

and WAT cells share the expression of many crucial "adipogenic" genes such as CCAAT Enhancer Binding Protein family members (C/EBPs), peroxisome proliferator-activated receptor gamma (PPARγ), and Fatty-acid Binding Protein 4 (FABP4 or aP2). However, high expression of so-called "thermogenic" genes is characteristic for BAT cells. These include uncoupling protein 1 (UCP1), peroxisome proliferator-activated receptor gamma coactivator 1 alpha (PGC-1α), and cell death-inducing DNA fragmentation factor α-like effector A (Cidea) (Zhou et al., 2003). These genes are essential for the major function of BAT: energy expenditure for thermogenesis (Rosen and MacDougald, 2006).

1.2.1. Brown adipose tissue (BAT) vs. White adipose tissue (WAT)

Human brown adipose tissue is mainly located in the supraclavicular region around the shoulders and is mainly found in newborns. The thermogenic activity of BAT is necessary to prevent body temperature loss after birth and in cold conditions. Importantly, recent studies have shown that BAT also exists in adults, and slim persons have higher BAT activity than obese individuals. Furthermore, more active BAT is found in females than in males (van Marken Lichtenbelt et al., 2009).

White adipose tissue is distributed widely throughout the whole body. There are two major classifications of human white adipose tissue: visceral white adipose tissue (vWAT) which is mainly surrounding organs, and subcutaneous white adipose tissue (sWAT) which is located beneath the skin, such as inguinal white adipose tissue (igWAT). Interestingly igWAT has been found to be capable to switch to brown-like adipose tissue (beige adipose tissue) (Petrovic et al., 2010; Seale et al., 2011).

These beige adipocytes show increased energy expenditure and expression of thermogenic genes, very similar to brown fat. This "browning" mechanism of white fat cells is driven by a number of transcriptional regulators and is considered therapeutically interesting with regard to the treatment of obesity (Ohno et al., 2012; Seale et al., 2008; Seale et al., 2011; Trajkovski et al., 2012a; Vegiopoulos et al., 2010).

1.2.2. Biogenesis of mesenchymal stem cells and their therapeutic potential

Stem cells are defined by their ability of self-renewal and potential to differentiate into a variety of distinct tissues. There are several different types of stem cells, which can be distinguished by their differentiation potential. Embryonic stem cells are called pluripotent, because they can be differentiated to all types of cell *in vitro*, thus it is able to rebuild the whole organism. In contrast, adult stem cells have only a limited potency of differentiation and are mostly located in the respective organ of their tissue type.

Mesenchymal Stem Cells (MSCs) are adult multi-potent stem cells that constitute a variety of adult mesenchymal tissues (Collet and Des Biens, 1975). MSCs maintain self-renewal ability with the potential to differentiated into bone, cartilage, adipose tissues, stroma, connective tissue, muscle (Pelled et al., 2002). MSCs can be isolated from bone marrow, adipose tissues or other organs and expanded to be cultured *in vitro*. MSCs play a crucial role in bone physiology and hematopoiesis (Sacchetti et al., 2007), and in part participate in the pathophysiology related to bone diseases. Furthermore, MSCs are the progenitors that give rise to adipose tissues. These features have made MSCs be a good candidate for the development of therapeutic modalities aiming to regenerate mesenchymal tissues (Pelled et al., 2002). Important methods utilizing MSCs are gene therapy or cell therapy approaches. Both exploit the current knowledge in molecular biology and biomaterial science in order to direct MSCs to differentiate *in vivo* to desired lineages and tissues, for example adipose tissues. With the powerful tools of gene therapy on hands, MSCs can be effectively transduced with viral vectors containing a therapeutic gene, as well as with complementary DNA (cDNA) for specific proteins, whose expression is therapeutically relevant for a patient (Bobis et al., 2006). Better understanding of the molecular mechanism directing the differentiation of MSCs will allow us to properly control MSCs both *in vivo* and *ex vivo* to allow the regeneration of complex tissues and organs (Saraf and Mikos, 2006).

In vitro studies, MSCs are artificially induced to differentiate into osteocytes, chondrocytes and adipocytes, such as bone marrow-MSCs (Figure 3).

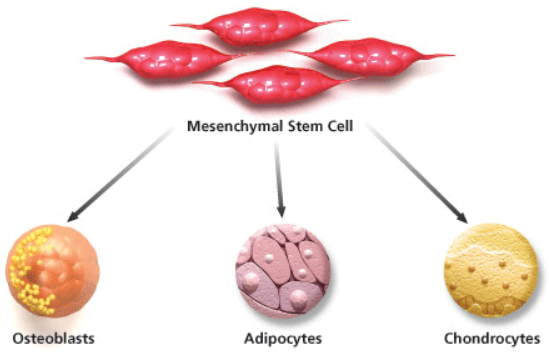

Figure 3. Lineage tree of mesenchymal cell. Source of image: website: http://articell.cz.

1.2.3. Adipogenesis of mesenchymal stem cells

MSCs can be *in vitro* differentiated to adipocytes by stimulation with certain compounds in various combinations (Jennissen et al., 2013). The MSCs used in this study were derived from brown adipose tissue (BAT-MSCs) or inguinal white adipose tissue (igWAT-MSCs). When these cells are stimulated with a cocktail of hormones, these MSCs differentiate into mature BAT or WAT cells respectively (Haas et al., 2009).

CCAAT Enhancer Binding Protein family (C/EBPs) and the hormone receptor peroxisome proliferator-activated receptor gamma (PPARγ) have been shown to play a crucial role in adipogenesis. PPARγ is frequently increased in primary mesenchymal stem cells that are differentiating to fat cells. The transcription factors which have been implicated in fat cell development in the C/EBP family are CCAAT Enhancer Binding Protein alpha (C/EBPα), CCAAT Enhancer Binding Protein delta (C/EBPδ), and CCAAT Enhancer Binding Protein beta (C/EBPβ) (Wu et al., 1999). C/EBPδ and β induce the expression of PPARγ. Ectopic expression of C/EBPδ and β leads to the induction of PPARγ This induction is a direct transcriptional effect, as the PPARγ promoter possesses C/EBP transcription factor binding sites (Shi et al., 2003). PPARγ and C/EBPs are able to induce each other's expression in a positive feedback loop that promotes and maintains the differentiated state of adipocytes (Wu et al., 1999).

However, there is evidence that C/EBPβ is more crucial in BAT than in WAT cell differentiation (Seale et al., 2008; Seale et al., 2011). Deletion of C/EBPβ (C/EBPβ$^{-/-}$) in mice induces a stronger deregulation development of brown adipose tissue, but not white adipose tissue (Tanaka et al., 1997). In contrast, C/EBPα$^{-/-}$ embryos have reduced levels of PPARγ (Wu et al., 1999) and

PPARγ$^{-/-}$ embryos die after 10 days (E9.5-E10) (Rosen et al., 2002). These phenotypes clearly underline the importance of the complex interplay of transcription factors in tissue development and especially in adipose tissue.

1.3. Brown adipose tissue (BAT)

1.3.1. BAT function in mammals

BAT is an organ unique to higher mammals that has developed parallel to endo-/homeothermy (Gesta et al., 2007). BAT is important for the thermoregulation especially during the neonatal period. The activated tissue dissipates energy in form of heat and thereby protects newborn mammals against low temperatures (e.g. after birth).

BAT has been shown to be present and functional in adult humans either. Recent PET (positron emission tomography) studies have clearly demonstrated that BAT depots can be stimulated/ metabolically activated by cold exposure in humans (Cypess et al., 2009; Nedergaard et al., 2007; Saito et al., 2009; van Marken Lichtenbelt et al., 2009; Virtanen et al., 2009). Cold-activated BAT depots can be observed around the supraclavicular region and along the spine (Figure 4). Interestingly, these PET studies also revealed that BAT activity is significantly reduced in overweight or obese subjects (van Marken Lichtenbelt et al., 2009). These findings together with the large capacity of BAT to disperse energy, suggests that increasing BAT abundance and activity could counteract obesity.

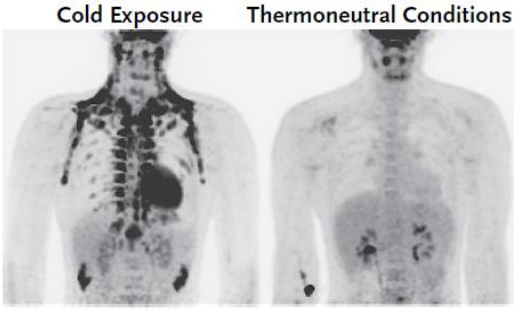

Figure 4. Cold induced brown fat tissue activation in adult human. The same patient was scanned by FDG-PET twice are shown. Cold condition (left) and RT condition (right). Figure is from (van Marken Lichtenbelt et al., 2009).

1.3.2. BAT development

Brown adipocyte development is much closer related to skeletal muscle than white adipocyte development (Figure 5). A certain transcription factor, myogenic factor 5 (Myf5), is an especially important regulator for linage determination of brown precursors. Myf5 expressing mesenchymal stem cells (Myf-positive cells) are progenitor stem cells of brown adipocytes and skeletal muscle. In contrast, Myf-negative adipoblast cells are white adipocyte progenitors. Both bone morphogenetic protein (BMP7) and PRD1-BF1-RIZ1 homologous domain containing 16 (PRDM16) can stimulate Myf5 expressing cells to differentiate to brown adipocytes, but inhibit skeletal muscle differentiation (Tseng et al., 2008). PRDM16 has been shown to be a major switch between brown adipocyte and skeletal muscle developments (Seale et al., 2008), and the transcription factor plays a key role at the early stage of brown adipocyte development.

The transcription factor C/EBPβ is an important co-factor for PRDM16. It can bind to PRDM16 and forms a protein-protein transcriptional complex (Kajimura et al., 2009). This complex drives Myf5 expressing cells towards brown adipocytes, but not skeletal muscle and plays a critical role in brown fat differentiation. However, in white fat differentiation there is no such pathway known. It implies that the transcription factor C/EBPβ is one of key factors in adipogenic differentiation, but more importantly in the early stage of brown adipogenic differentiation (Figure 5).

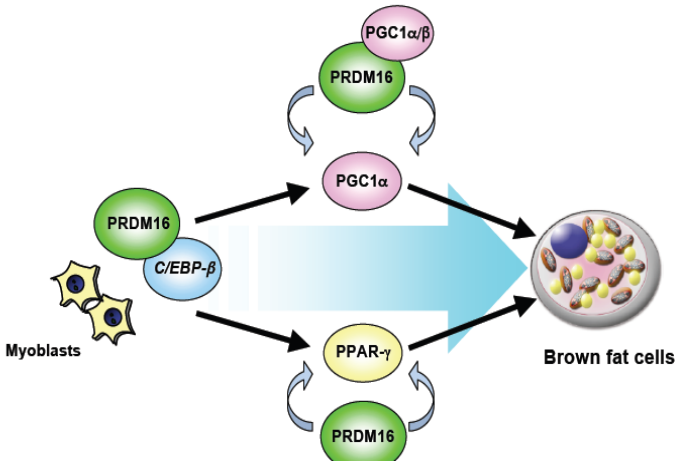

Figure 5. Brown fat differentiation requires both C/EBPβ and PRDM16. Figure is adapted from (Seale et al., 2008).

Importantly, mature brown adipocytes are rich in mitochondria and express high levels of uncoupling protein-1 (UCP-1). UCP-1 uncouples the mitochondrial respiratory chain and, thereby, leads to the energy dissipation in form of heat (thermogenesis) – the functional hallmark of BAT.

Furthermore, in the past, mature brown and white adipocytes had been shown to trans-differentiate to each other. This process is driven by hormones like catecholamines, β-agonists, as well as by cold exposure *in vivo* (Figure 6). This process is so-called "browning". Nevertheless, beige adipocyte still could be regarded as functional brown adipocyte (Nedergaard and Cannon, 2013) (Figure 6).

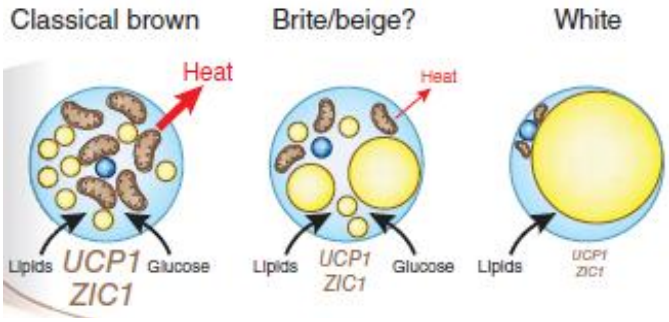

Figure 6. There are two types of adipocyte, brown adipocytes and white adipocytes. Apart from these two types, there is another type of adipocyte - beige adipocytes which are derived from white adipocytes, but has a certain function of brown adipocyte. The figure is adapted from (Nedergaard and Cannon, 2013).

1.4. miRNAs in brown fat (BAT) differentiation

As previously described, miRNAs have a very important function in biological cellular development by post-transcriptional gene regulation. They have been shown to be especially relevant as regulars of transcription factors in developmental processes (Krutzfeldt et al., 2006; Krutzfeldt et al., 2011). There are many crucial transcriptional regulators during BAT or WAT differentiation, such as C/EBPs, PPARγ, Myf-5, and PRDM16. Recent research showed that miR-193b-365 is essential for brown fat differentiation, which revealed an very important role of miRNAs in brown fat differentiation (Sun et al., 2011). In 2012, miR-196a has been found to promote appearance of beige adipocytes in WAT. This study showed the capacity of miRNAs to regulate the " browning" processing in WAT cells (Mori et al., 2012). Moreover, PRDM16, has

been found to directly regulated by miR-133 (Trajkovski et al., 2012b). In this term, miRNAs may become an effective factor to turn on the beneficial thermogenic functions of BAT or switch the "unhealthy-white fat (WAT)" to energy dissipating "healthy brown-like fat (beige fat)" in order to treat diabetes and obesity. Thus, the regulatory potential of miRNAs in brown or beige fat differentiation becomes more and more therapeutically relevant.

1.5. TGFβ1-Smad signaling pathway in adipogenesis

Transforming growth factor beta (TGF-β) regulates many biological processes, and aberrant TGF-β signaling is implicated in tumor development (Amanda et al., 2010). Moreover, TGFβ1/Smad3 signaling is involved in adipogenesis: TGFβ1 inhibits adipocyte differentiation via Smad3 interaction with C/EBPs (Choy and Derynck, 2003), This indicates that there is some kind of interaction existing between TGFβ and the C/EBP transcription factor family in adipogenesis. Smad3 also has been shown to regulate BAT-specific genes, like PGC-1α and PRDM16, which co-operate with C/EBPβ in the brown adipocyte differentiation (Seale et al., 2008). Deletion of Smad3 causes white adipocytes to trans-differentiate to beige adipocytes (Yadav et al., 2011; Yadav and Rane, 2012). TGFβ1 has been shown to induce the expression of several miRNAs, among them miR-155 in epithelial cells. Smad4 is a co-factor with other Smads in TGFβ1-signaling pathway. It is also called co-Smad and works together with such as Smad3, Smad5, by forming heteromers. TGFβ1 cannot induce miR-155 expression without Smad4 activity in epithelial cells (Kong et al., 2008). This indicates that TGFβ1 may also induce miR-155 expression via the TGFβ1/Smad4 signaling pathway in adipocytes; thereby TGFβ1/Smad4/miR-155 pathway may be involved in regulation of adipogenesis (Figure 7).

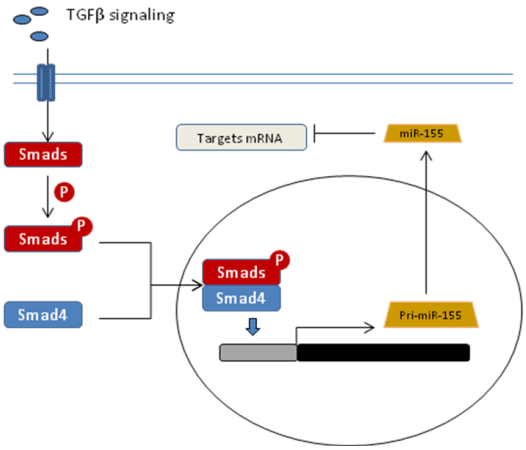

Figure 7. miR-155 expression is activated by TGFβ / Smads signaling in epithelial cell.

1.6. Aim of the PhD thesis

miRNAs are small non-coding RNAs that can regulate many cellular processes via targeting e.g. signal transduction proteins or transcription factors. To date, not much is known about the regulatory function of miRNAs in brown adipose tissue (BAT) – the major site of energy expenditure in form of heat (thermogenesis) in mammals.

Therefore, the aim of this thesis is to identifiy miRNAs that are differentially regulated during BAT differentiation and that play a role in BAT development and function. The following main questions are addressed:

- Which miRNAs are significantly up- or down- regulated during brown fat differentiation?
- Which signaling pathways regulate these miRNAs?
- Does over-expression or knock-down of these miRNAs influence brown fat differentiation *in vitro*?
- What are the major mRNA targets of the identified miRNA in BAT cells and what is the targets´ function in brown fat differentiation?
- Does over-expression or deletion of this miRNA affect brown fat differentiation and function in *in vivo* models?

2. Materials and Methods

2.1. Materials

2.1.1. Reagents

Acetic acid	Sigma-Aldrich
ADP	Sigma-Aldrich
ammonium persulfate (APS)	Merck
Agarose	PeqLab
Ampicillin	Roth
ATP	Sigma-Aldrich
BSA	Roth
BSA (essential fatty acid free)	Sigma-Aldrich
Bromphenol blue	Roth
β-mercaptoethanol	Sigma-Aldrich
$CaCl_2$	Roth
Chloroform	Roth
Complete® EDTA-free	Roche
Coomassie brilliant blue G-250	Merck
Digitonin	Sigma-Aldrich
Desoxy-cholic acid-Na	Sigma-Aldrich
Dithiothreitol	Sigma-Aldrich
ECL reagent	Amersham Biosciences
EGTA	Sigma-Aldrich
Ethanol	Roth
Ethidium bromide	Carl Roth GmbH
Ethylendiamintetraacetate (EDTA)	Sigma-Aldrich

Eosin G	Merck
Ficoll Typ 400	Sigma-Aldrich
Free Glycerol Reagent	Sigma-Aldrich
Glucose	SERAG
Glutamate	Sigma-Aldrich
Glycerol Standard Solution	Sigma-Aldrich
HCl	Roth
Hydrogen peroxide	Roth
HEPES	Sigma-Aldrich
Imidazole	Sigma-Aldrich
IMMU-MOUNT	Thermo Scientific,Waltham
Isopropyl alcohol (99%)	Roth
Kanamycin	Roth
KCl	Roth
KH_2PO_4	Roth
LightCycler® SYBR Green I Master mix	Roche
L-(-)-Norepinephrine bitartate salt monohydrate (NE)	Sigma-Aldrich
Malate	Sigma-Aldrich
Mannitol	Sigma-Aldrich
Methanol	Roth
$MgCl_2$	Roth
Mayers hemalaun	Merck
4-Morpholineethanesulfonic acid	Sigma-Aldrich
NaCl	Roth
NaF	Roth

Na_2HPO_4	Roth
Na_3VO_4	Sigma-Aldrich
Na-Citrate	Roth
NP-40	Roth
Oil RedO	Sigma-Aldrich
Oligomycin	Sigma-Aldrich
Paraffin	Roth
Paraformaldehyde	Sigma-Aldrich
PeqGOLD TriFast®	Peqlab
Phosphoric acid	Sigma-Aldrich
Precision plus All Blue Standard	BioRad
Protease inhibitor cocktail, Complete® EDTA-free	Roche
Proteinase K	Roche
Restriction enzymes	New England Biolabs
Roti®-Histokitt	Carl Roth GmbH
Roti® Phenol/C/I	Carl Roth GmbH
Rotiphorese®Gel 30	Carl Roth GmbH
Sodium ascorbate	Sigma-Aldrich
SDS	Sigma-Aldrich
Succinate	Sigma-Aldrich
Skimmed milk	Sigma-Aldrich
Taurine	Roth
T4 DNA ligase	Invitrogen
Tween 20	Sigma-Aldrich
TEMED	Sigma-Aldrich
Triglyceride Reagent	Sigma-Aldrich

Triton X-100	VWR
Xylencyanol FF	Sigma-Aldrich
Xylol	Sigma-Aldrich

2.1.2. Cell culture

Collagenase II	Worthington, Lakewood
Dexamethason	Sigma-Aldrich
DMSO	Roth
DMEM	Gibco
DMEM, liquid (4.5 g/L D-glucose)	Gibco
Fetal bovine serum (FBS)	Biochrom AG
Insulin	Sigma-Aldrich
Isobutylmethylxanthine (IBMX)	Sigma-Aldrich
Lipofectamine™ 2000	Invitrogen
Penicillin, Streptomycin (P/S)	Biochrom AG
Triiodothyronine-Na	Sigma-Aldrich
Trypan blue 0.4% solution	Sigma-Aldrich
Trypsin-EDTA 0.05%	Invitrogen

2.1.3. Lab wares

Cell scraper	Labomedic
Chemiluminescence films, Hyperfilm®	Amersham Biosciences
Cryogenic vials	Sarstedt
100 mm dish	Sarstedt
15 ml / 50 ml Falcon tube	Sarstedt
Microscope Cover Glasses	Marienfeld GmbH

5 ml / 10 ml / 25 ml pipette	Sarstedt
6-well / 12-well plate	Sarstedt
PVDF membranes, Immobilon®P 0.45µm	Millipore
Sterile filter 0.22 µm	VWR

2.1.4. Equipments

Autoclave, Varioklav 135 T	Faust
Casting platforms	EmbiTech
Centrifuge, Biofuge Primo	Heraeus
Centrifuge, 5415R	Eppendorf
Centrifuge, Sigma 8k with 12510-H rotor	Sartorius
DatLab Version 4.2.0.73 Software	Oroborus Instruments
Electrophoresis/blotting system, Mini Trans Blot System	BioRad
Electrophoresis chamber	Peqlab
Film processor, CP100	Agfa
Fluorescence microscope, LEICA DMIL4000 B	Leica
Incubator, Certomat IS	Sartorius
Incubator, HeraCell 150	Heraeus
Laminar air flow, HeraSafe	Heraeus
Leica Application Suite V3	Leica Microsystems GmbH
Luminometer, Lumat LB 9507	EG&G BERTHOLD
Micro plate reader, SUNRISE-BASIC TECAN	Tecan
Microsystems GmbH, WetzlarCamera, LEICA DFC425C	Leica
Microsystems GmbH, WetzlarAxioCam camera and AxioVision software	Zeiss
Microwave	Severin

Neubauer counting chamber	Labomedic
Photometer, Biophotometer	Eppendorf
Power supply, Consort E835	Peqlab
QuantityOne® Software	BioRad
Oxygraph-2k	Oroborus Instruments
Real-time PCR machine, StepOnePlus™ Real-Time PCR System	Applied Biosystems
Thermocycler, T1	Biometra
Thermomixer, 5350	Eppendorf
UV light transilluminator, GelDoc®XR	BioRad
WetzlarMicrotome, HM335E	Microm

2. 2. Methods

2.2.1. Animals

2.2.1.1. Animal breeding

Transgenic mice used in this study were established, maintained and bred in the animal facility of H.E.T (House of Experimental Therapy Centre) at University of Bonn in Germany. To obtain miR-155 transgenic mice, a *PGK* or *UCP1* promoter driven *eGFP* mRNA/pre-miR-155 cassette was cloned into a lentiviral vector. High titer virus was used to transduce preimplantation embryos as described previously (Pfeifer et al., 2002). Genotypes were assessed by PCR detection of the *eGFP*-cassette in genomic DNA. miR-155 knock-out mice (Thai et al., 2007) were purchased from Jackson Laboratory in USA. All the animals were maintained on a daily cycle of 12 h light (06:00 to 18:00) and 12 h darkness (18:00 to 06:00) at steady room temperature around 24°C and were allowed free access to standard rodent diet and water. Mice were separated by sex and marked with ear tags at the age of 4 weeks after birth. Mice at young age (1 or 2 weeks old) which were taken to be sacrificed had been marked by toes cut.

2.2.1.2. Cold exposure experiments

The analysis of the influence of miR-155 deletion on BAT *in vivo* was performed using littermates' male mice at the age of 12 – 16 weeks. Mice were fasted for 3 h at 24°C (room temperature) with free access to water but without access to chow to exclude the possibility of different feeding states. Afterwards, mice were exposed to 4°C (acute cold exposure), for 4 h without access to chow. Subsequently, mice were sacrificed and dissected.

2.2.1.3. Mouse body surface or core temperature

The body temperature was measured as ability of BAT activity *in vivo*. The infrared camera was used to measure the body surface temperature of all mice pups at age of 1 week. In Cold exposure experiments, 12 to 16 weeks old littermates' male mice were shaved to expose back without furs. The rectal temp-meter was used to measure body core temperature of mice at age of 10 to 16 week.

2.2.1.4. Metabolic cage measurement (TSE)

Male mice at 16 weeks of age were kept in TSE cages over weekend before starting measurement. Fat mass and lean mass of the mice were measured by NWR minispec analyzer instrument (LF50H, Bruker), and also body weights were weighted before starting TSE data recording at measuring day. TSE cages temperature were set to 24°C at first measuring day, 30°C at second day, and then 4°C for 4 h at third day. Food intake, oxygen consumption and carbon dioxide emission, etc. were recorded by TSE sensors and output data by the system.

2.2.1.5. Measurement of lipolysis in brown adipose tissue (BAT)

To measure the basal lipolytic activity in BAT from cold stimulated wild type or miR-155$^{-/-}$ mice, BAT tissues were isolated from the animals immediately after cold exposure. Half a lobe of BAT was taken and shredded with scissors (Everhards, ES19) completely for the assay. The homogeneous mixture was incubated in lipolysis medium which consist of DMEM, liquid (4.5 g/L D-glucose) (Gibco) supplemented with 1% P/S and 2% essential fatty acid free BSA (Sigma-Aldrich). The first 50µl of medium were taken after half hour incubation at 37°C and 5% CO_2, then after 2 h incubation at same condition, again 50µl of medium were taken. Then, the lipolytic activity was measured by quantifying the glycerol concentration. 750 µl of the Free Glycerol Reagent (Sigma) were added to the 50 µl of medium, the samples were incubated at 37°C for 5

minutes afterwards the absorbance was measured at 540 nm (SUNRISE). A glycerol standard (Glycerol Standard Solution; Sigma-Aldrich) was used to calculate glycerol concentrations. The glycerol release was normalized to the protein content of the samples. Therefore, the remaining medium was removed from the cells, total cell lysates were prepared and protein concentration was determined as described in 2.3.1. The finial lipolysis values from BAT of mice were calculated by 2 h value subtracting to half an hour value.

2.2.1.6. Preparation of paraffin sections

Interscapular BAT and inguinal WAT were fixed overnight in PFA (4% in PBS pH 7.4) at 4°C. Afterwards tissue samples were dehydrated by successive incubations in ethanol with ascending concentrations (from 50%, 70%, 96% to 100%) for 1 h each at room temperature (RT). Subsequently, samples were incubated 3 times in xylol for 10 minutes each at RT and 3 times in paraffin for 1 h each at 60°C. Tissue samples were embedded in fluid paraffin (60°C) and cooled down to RT. Paraffin blocks were then stored at RT. Sections with 4-5 µm thickness of tissue samples were cut using a microtome (Microm).

2.2.1.7. Hematoxylin/Eosin (H/E) staining

H/E staining was performed at RT. Paraffin sections were incubated separately for 2 minutes each in xylol (deparaffinization), ethanol with descending concentrations (from 100%, 96%, 70%, to 50%) and PBS (rehydration). Afterwards, slides were treated with hematoxylin (Mayers hemalaun) for 1 minute, washed shortly with water, and then stained with eosin for 1 minute, followed by being washed shortly again with water. Sections were dehydrated separately for 2 minutes each in ethanol with ascending concentrations (from 50%, 70%, 96%, to 100%) and xylol. Finally, tissue samples were mounted in Roti®-Histokit mounting medium. Images were taken using a LEICA DMI4000 B microscope (Leica Microsystems GmbH) or Zeiss AxioVision microscope.

2.2.1.8. Immunocytological staining of UCP1 on inguinal white adipose tissue sections

Immunocytological staining of UCP1 on inguinal white adipose tissue was carried out on 5µm paraffin sections. The sections were incubated at 37°C overnight or 42°C for 2 h, then dewaxed and rehydrated as described before (2.2.1.6). Antigen retrieval of sections were carried out by warming the sections up to 75°C-80°C in 10mM Na-Citrat buffer (pH 6.0) for 20min.

Afterwards, the sections were washed 3 times with H_2O for 5 min each and incubated in 3% H_2O_2 for 10 min. Tissue sections were blocked with 2.5% goat serum in PBS-T for 1 h at RT and incubated overnight with the anti-UCP1 (Abcam, ab10983) antibody which is diluted 1:500 in 0.25% goat serum (in PBS-T) at 4°C. After 3 times washing in PBS-T for 5min, the secondary antibody (anti-rabbit HRP, Santa Cruz) were applied 1:200 in 0.25% goat serum (in PBS-T) for 1 h at RT. Afterwards the slides were washed 3 times again with PBS-T, dehydrated in ethanol with ascending concentrations as described before (2.1.5) and counter-stained with Hematoxylin for 3-5min. Finally, sections were mounted in IMMU-MOUNT mounting medium (Thermo Scientific).

2.2.2. Cell culture

2.2.2.1. Isolation of primary BAT-MSCs

BAT-MSCs were isolated from interscapular brown fat of newborn littermatched wild type and miR155$^{-/-}$ mice. The interscapular BAT was resected and transferred to collagenase digestion buffer (123 mM NaCl, 5 mM KCl, 1.3 mM $CaCl_2$, 5 mM Glucose, 100 mM HEPES, adjusted to pH 7.4, freshly added 1.5% BSA and 0.2% Collagenase II). After incubation in a shaking water bath for 30 min at 37°C, tissue remnants were removed by filtration through a 100 µm nylon mesh (Millipore). Afterwards the cell suspension was placed on ice for 30 min. The resulting infranatant, which contained the MSC fraction, was filtered through a 30 µm nylon mesh (Millipore) and centrifuged at 700 g for 10 min. The cell pellet was resuspended in dissection medium (DMEM Glutamax I + 4500 mg/l Glucose supplemented with 10 % FBS, 1 % P/S, 4 nM insulin, 4 nM Triiodothyronine-Na, 10 mM HEPES and 25 µg/ml sodium ascorbate). Cells were counted with trypan blue (1:1) (Sigma-Aldrich) in a Neubauer counting chamber (Labomedic) and 5.7 x 10^5 cells per well were seeded on 6-well plates and incubated in a humidified incubator with 5 % CO_2 at 37 °C.

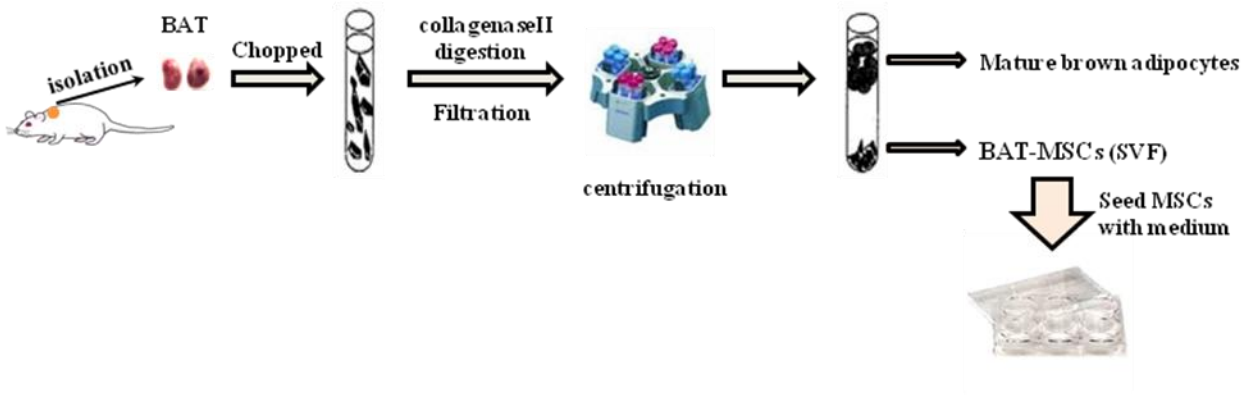

Figure 8.1. Isolation scheme of BAT-MSCs from interscapular BAT of newborn mice. BAT-MSCs were isolated from interscapular BAT of newborn wt or miR155$^{-/-}$ littermates. The BAT tissue was collagenase digested; BAT-MSCs (BAT preadipocytes) were separated from mature brown adipocytes by centrifugation and seeded on 6-well plates.

2.2.2.2. Immortalization of primary BAT-MSCs

Primary BAT-MSCs at p0 (passage 0) were immortalized 24 h after isolation by infection (2.2.2.6) with lentivirus expressing the Simian Virus 40 (SV40) large T-antigen under control of the phosphoglycerate kinase (PGK) promoter. Immortalized cells were expanded in Dulbecco's modified Eagle's medium (DMEM) growth medium (Glutamax I + 4500 mg/l Glucose without pyruvate, Gibco) supplemented with 10% fetal bovine serum (FBS) and 1% penicillin/streptomycin (P/S) at 37°C and 5% CO_2 and were not used beyond p5 (passage 5).

2.2.2.3. Isolation of WAT stromal cells

WAT-MSCs/stromal cells were isolated from inguinal and gonadal white fat of 8-12 weeks old mice of newborn litter-matched wild type or miR155$^{-/-}$ mice. 1g white fat collected from 4 mice is always required for the isolation. The inguinal WAT was shredded with scissors (Everhards, ES19) completely and transferred to 7 ml WAT collagenase digestion buffer (1.5 mg/ml collagenase II and 0.5% BSA in DMEM). After incubation in a shaking water bath for 30-45 min at 37°C, same volume of WAT growth medium (DMEM GlutaMAX™ I + 4500 mg/l glucose with pyruvate, supplemented with 10% FBS and 1% P/S) was added and incubated at RT for 10 min. The floating adipocyte fraction was removed by taking off the upper phase (about 1 ml). Afterwards, the cells were centrifuged at 200 g for 10 min and the pellet was resuspended in 2 ml

WAT growth medium. Then the suspension was filtered through a 100 µm nylon mesh (Millipore). Cells were counted and 2 x 10^5 cells per well were seeded on 6-well plates and incubated in a humidified incubator with 5 % CO_2 at 37 °C. On the next day, cells were washed 2-3 times with growth medium to remove dead cells, tissue remnants and mature fat cells.

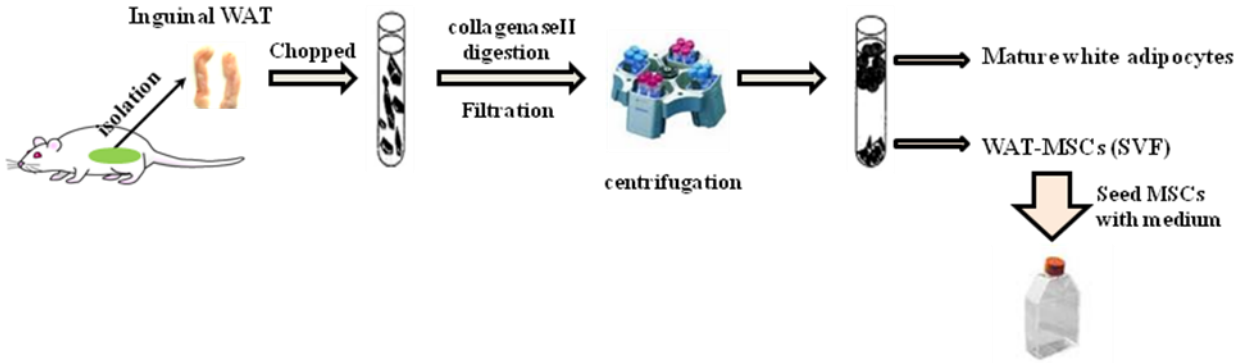

Figure 8.2. Isolation scheme of WAT-MSCs from inguinal WAT of adult mice. WAT-MSCs were isolated from inguinal WAT of newborn wt or miR155$^{-/-}$ littermates. The WAT tissue was collagenase digested; WAT-MSCs (igWAT preadipocytes) were separated from mature white adipocytes (igWAT) and seeded on flask or 6-well plates.

2.2.2.4. Cultivation and storage of immortalized BAT-MSCs and WAT-MSCs

The cells were always cultured in a humidified incubator with 5 % CO_2 at 37 °C and subcultured when they were confluent. In order to detach cells from the well plate, cells were washed in prewarmed PBS (37°C) and detached by incubation with trypsin-EDTA (Invitrogen) for approximately 5 minutes at 37°C. Detached cells were collected and resuspended in growth medium. An appropriate number of cells were seeded on new dishes for further culture.

To store cells for longer periods of time, cells were trypsinized and resuspended in prewarmed (37°C) growth medium. Cell suspensions were centrifuged for 5 minutes at 160 g. The pellets were resuspended in growth medium, mixed with freezing medium in a ratio of 1:1 to achieve a final dimethyl sulfoxide (DMSO) concentration of 10% and transferred to cryogenic vials (Sarstedt). Cryogenic vials were incubated on ice for 15 minutes and were finally stored at -80°C. After 24 h, cryo-cultures were transferred to liquid nitrogen (-196°C).

In order to thaw cryo-preserved cells, cryo-vial was quickly placed in a water bath at 37°C for 30 seconds. Afterwards cells were transferred to prewarmed (37°C) growth medium, and

centrifuged for 5 minutes at 1000 rpm. The cell pellet was resuspended in growth medium and seeded on well plates.

2.2.2.5. Adipogenic differentiation of immortalized BAT-MSCs and WAT-MSCs

To differentiate immortalized BAT-MSCs into mature brown adipocytes, 1.5 x 10^5 cells/well were seeded on 6-well plates or 0.9 x 10^5 cells/well on 12-well plates (day -4) in growth medium and after 48 h the medium was exchanged with differentiation medium containing additionally 20 nM insulin, and 1 nM T3 (triiodothyronine) (day -2) for 48 h. Adipogenesis was induced by treating confluent cultures (day 0) with induction medium (IM) which is supplemented with 20 nM insulin, 1 nM T3, 0.5 mM isobutylmethylxanthine (IBMX), and 1 µM dexamethasone (Dexa) for 48 h. After this induction phase cells were changed back to differentiation medium (day 2), which was replenished every second day until day 7 or 8 when the cells had differentiated into brown adipocytes (Haas et al., 2009; Jennissen et al., 2013).

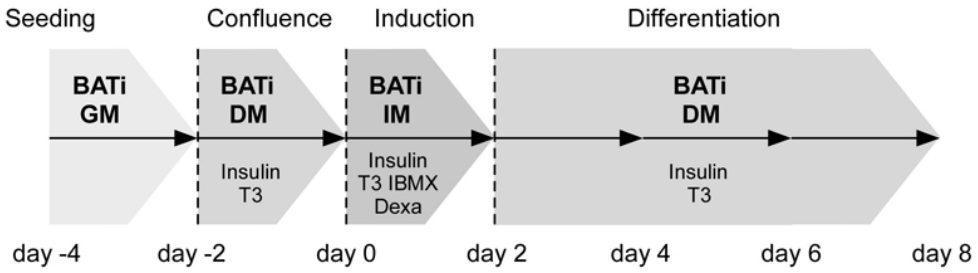

Figure 9.1.BAT-MSCs (BAT preadipocytes) were differentiated by following from the protocol (Jennissen et al., 2013)

For WAT *in vitro* differentiation, fully confluent cells were kept in growth medium for 2 days, and then treated with IM supplemented with 1µg/ml insulin, 1nM T3, 0.25µM dexamethason, 0.5mM IBMX, 1µM rosiglitazone, and ABP (50µg/ml L-Ascorbat, 1µM Biotin, and 17mM Panthothenat). After 6 days, the cells were kept in medium supplemented with 1µg/ml insulin, 1nM T3, and ABP for another 4 to 5 days. Medium was exchanged every 2 days.

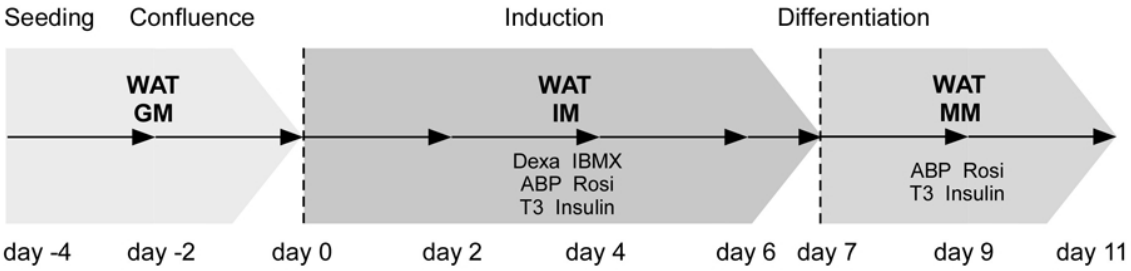

Figure 9.2.WAT-MSCs (WAT preadipocytes) were differentiated by following from the protocol (Jennissen et al., 2013)

2.2.2.6. Infection of cells with lentiviral vectors

For infection, 1.5 x 10^5 cells / well were seeded in a 6-well plate. When attached, cells were infected with 200 ng RTase of the virus (corresponding to physical titer of the virus) in 800 µl growth medium. The next day, the medium was exchanged with either fresh growth medium and cells were incubated overnight. Afterwards, the infected cells were subjected to further experiments.

2.2.2.7. Oil RedO staining of differentiated adipocytes

Oil RedO is a dye used for staining of lipids in tissues and cells. Lipid droplets, stained by accumulated Oil RedO, appear in a red color.

Differentiated brown adipocytes (day 7/8) were washed with PBS, fixed in 4% PFA in PBS for 15 minutes at RT and washed again with PBS for 3 times. Afterwards, the cells were incubated with Oil RedO working solution for 4 h at RT and were washed 3 times with PBS.

5mg/ml Oil RedO stock solution (Sigma-Aldrich) was prepared by dissolving 0.5% Oil RedO overnight in 99% isopropyl alcohol with a magnetic stir bar at RT. 3mg/ml Oil RedO working solution was then prepared by dissolving 40% of stock solution in H_2O one day before use and filtering through a paper filter before use.

2.2.2.8. Quantification of triglyceride (TG) accumulation in differentiated brown adipocytes

TGs are esters of fatty acids and glycerol. To determine TG accumulation in differentiated brown adipocytes, an assay was performed based on coupled enzyme reactions resulting in an increase in the absorbance at 540 nm that is directly proportional to the glycerol concentration. Therefore, Free Glycerol Reagent (Sigma-Aldrich, F-6428) and Triglyceride Reagent (Sigma-Aldrich, T-2449) were used according to the manufacturer's instructions. In brief, differentiated adipocytes (day 7/8) grown in 6-well plates were washed with PBS, 200 µl TG-Tx-lysis buffer (150 mM NaCl, 10 mM Tris/HCl pH 8.0, 0.05% Triton-X 100, freshly added 40 µl/ml Complete® protease inhibitor cocktail) were added and cells were immediately frozen at -80°C. After thawing on ice, cells were resuspended and centrifuged for 10 minutes at 15000 g at 4°C. Afterwards 2 µl of the supernatant were used for protein content determination applying the Bradford method. The remaining part of the sample was resuspended, added to 1 ml of the TG assay reagent (80% Free Glycerol Reagent and 20% Triglyceride Reagent), incubated at 37°C for 5 minutes and centrifuged for 2 minutes at 15000 g at RT. Afterwards the absorbance was measured at 540 nm. A glycerol standard (Glycerol Standard Solution; Sigma-Aldrich) was used to calculate glycerol concentrations according to the manufacturer's instructions.

2.2.2.9. Luciferase reporter assay

Luciferases are commonly used as reporters to assess the activity of promoters in cells which are transfected with constructs containing the luciferase gene under control of the promoter of interest. In the luciferase reaction, light is emitted when enzymes act on the appropriate luciferin substrate.

HIB-1B brown adipose cells, kindly provided by Prof. M. Klingenspor (Technical University Munich, Germany) were transiently co-transfected with firefly and Renilla luciferase expression vectors at a ratio of 1:1 using Lipofectamine 2000 (Invitrogen) according to the manufacturer's instructions on day -2. Luciferase reporter assays were accomplished on day 0 or day 2 using the Dual-Luciferase® Reporter Assay System (Promega) according to the assay protocol. In these assays the activities of firefly and Renilla luciferases are measured sequentially from a single sample by adding different substrates. Cell lysates were prepared following the instructions for passive lysis. The activity of the firefly luciferase was normalized to the corresponding Renilla

activity value for each sample. pGL3-BIC/miR-155 promoter assays were normalized to Renilla luciferase activity from the co-transfected pRL-TK vector (Promega).

2.2.2.10. Proliferation assay

Cell number was determined using the PrestoBlue Cell Viability Reagent (Invitrogen) according to manufacturer´s instructions.

2.2.3. Protein analysis

2.2.3.1. Preparation of total protein lysates from adherent cells and tissues

For the extraction of total proteins, cells were washed once in 4°C cold PBS and scraped in 100-200 µl of 4°C cold RIPA-lysis buffer (10mM Tris/HCl pH7.4, 150 mM NaCl, 1% NP-40, 1% Desoxy-cholic acid-Na, 0.1% SDS, 40 µl/ml Complete® EDTA-free, 10 mM NaF, 1 mM Na_3VO_4). Tissues were lysed in 500 µl of ice cold RIPA-lysis buffer and disrupted using an Ultra-turrax® (IKA). Lysates were centrifuged at 15000 g for 10 minutes at 4°C, and the supernatant was transferred into a new tube. The protein concentration of the supernatant was determined using the Bradford protein assay. After adjusting the protein concentration, the appropriate amount of 3 x Laemmli buffer (125 mM Tris/HCl pH 6.8, 20% Glycerol, 17 % SDS, 0.015% Bromphenol blue, 5%β-mercaptoethanol) was added and samples were incubated at 97°C for 5 minutes. Samples were either frozen at -20°C or directly subjected to SDS-PAGE.

2.2.3.2. One-dimensional SDS-polyacrylamid-gelelectrophoresis (SDS-PAGE)

To perform discontinuous gel electrophoresis, 40-100 µg proteins were applied in Laemmli buffer as described before (2.3.1). Proteins first passed through a stacking gel to become concentrated and then passed through the separating gel to be separated according to molecular size under denaturating conditions. The SDS polyacrylamide gel was prepared with the help of the mini-protean II cell system (BioRad, Munich, Germany), whose components are shown in table 1. SDS-PAGE was performed in SDS-PAGE running buffer (Table 1) at 100 volt at RT using the Mini Trans Blot system (BioRad).

Table 1. Different concentrations of SDS-PAGE gel compounds

	Seperating gel		**Stacking gel**
Concentration	**8 %**	**10 %**	**5 %**
Double distilled water	4.6 ml	4.0 ml	3.4 ml
Rotiphorese®Gel 30	2.7 ml	3.3 ml	0.83 ml
Buffer (1.5 M Tris-HCl, pH 8.8)	2.5 ml	2.5 ml	-
Buffer (1 M Tris-HCl, pH 6.8)	-	-	0.63 ml
10 % SDS	100 µl	100 µl	40 µl
20% ammonium persulfate (APS)	50 µl	50 µl	20 µl
N, N, N', N'-Tetramethylethylenediamine (TEMED)	6 µl	4 µl	8 µl

2.2.3.3. Western blotting and immunodetection

Western blot analysis is an immunological method to detect specific proteins by antibodies. After separating the proteins by SDS-PAGE (2.2.3.2), a transfer sandwich was assembled using a methanol activated and transfer buffer equilibrated PVDF membrane. Proteins were electrically transferred in the transfer buffer (Table 2) under different conditions depending on their size (Table 2).

Table 2. Transferring conditions of proteins with different sizes

Protein size	**Voltage**	**Current**	**Time**	**Temperature**
15 – 30 kDa	100 V	250 mA	1 hour	4°C
30 – 50 kDa	100 V	275 mA	1 hour	4°C
50 – 75 kDa	100 V	300 mA	1 hour	4°C
75 – 250 kDa	100 V	300 mA	1-1.5 hour	RT

After disassembling the transfer sandwich, membranes were incubated in methanol for 30 seconds and dried for at least 30 minutes at RT. After drying, membranes were incubated in methanol for 30 seconds and blocked in 5% Skimmed milk or BSA in Tris-buffered saline supplemented with 1% Tween-20 (TBST, table 3) for 1 h at RT. Blocked membranes were washed 3 times in TBST and incubated with the primary antibody at 4°C over night in blocking buffer according to the manufacturer's instructions. After 3 times washing with TBST, the membranes were incubated with a horseradish peroxidase (HRP)-coupled secondary antibody for 1 h at RT in blocking buffer according to the manufacturer's instructions. Finally, the membranes were washed 3 times in TBST and subjected to chemiluminescence based detection using an enhanced chemiluminescence (ECL) reagent and chemiluminescence films (Amersham Biosciences) which were developed in an automatic film processor (CP-100, Agfa). Densitometric analysis was carried out using the QuantityOne software (BioRad). The primary and secondary antibodies are listed in table.

Table 3. Buffers used for western blot

10 x running buffer	250 mM Tris 2 M glycine 35 mM SDS dest. H_2O
Transfer buffer	25 mM Tris 192 mM glycine 20 % (v/v) methanol dest. H_2O
TBST	100 mM NaCl 10 mM Tris 0.2 % (v/v) Tween 20 dest. H_2O

Table 4. Antibodies used for western blot

Antibodies	**Company**	**Species**	**Dilution**
anti-FABP4 (aP2)	Santa Cruz, sc-18661	Goat	1:1000
anti-C/EBPα	Santa Cruz, sc-61	Rabbit	1:1000
anti-C/EBPβ	Santa Cruz, sc-150	Rabbit	1:800
anti- UCP1	Sigma-Aldrich, U6382	Rabbit	1:500
anti-PGC-1α	Santa Cruz, sc-5816	Mouse	1:1000
anti-PPARγ	Santa Cruz, sc-7273	Mouse	1:800
anti-Pref-1	Cell Signalig Technology, #2069	Rabbit	1:1000

anti-β-Tubulin	Dianova, DLN-09992	Mouse	1:1000
anti-Smad4	Santa Cruz, SC-7154	Rabbit	1:1000
anti-RhoA	Santa Cruz, sc-418	Mouse	1:1000
anti mouse-HRP	Dianova, 115-035-146		1:10000
anti rabbit-HRP	Cell Signalig Technology, 7074		1:5000
anti goat-HRP	Chemicon, AP309P		1:5000

2.2.3.4. ELISA

Cell culture supernatants were collected every 2 days throughout *in vitro* differentiation. TGFβ1 ELISAs were performed according to the manufacturer's instructions (R&D Systems).

2.2.4. DNA/RNA analysis

2.2.4.1. Isolation of ribonucleic acids (RNA) from cells and tissues and reverse transcription

Total RNA from cultured cells and tissues was isolated using the TriFast® reagent (Peqlab) according to the manufacturer's instructions. For real-time PCR analysis 0.5 µg RNA were reverse transcribed into cDNA using the Transcriptor First Strand Synthesis Kit (Roche) and random hexamer primers according to the manufacturer's instructions. For cloning, RNA was reverse transcribed into cDNA using oligo-dT primers.

2.2.4.2. Isolation of desoxyribonucleic acids (DNA) from tails (genotyping) and tissues

Genomic DNA from mice tails or toes was quickly isolated by protease K (table) for mice genotyping PCR. The purified genomic DNA was isolated from tissues with Phenol/Chloroform extraction method according to the manufacturer's instructions.

Table 5. The quick genomic DNA isolation Substances

Substances	**Volume in µl**
Protease K	2
10 x PCR buffer with $MgCl_2$	10
Double distilled H_2O	88

Table 6. The quick genomic DNA isolation procedure

Incubation temperature (°C)	**time**
55	overnight
97	15 min
4	Stored

2.2.4.3. Polymerase-Chain-Reaction (PCR)

To perform PCR reactions, the DNA template, a forward primer, a reverse primer, a DNA Taq polymerase and deoxynucleotide triphosphates (dNTPs) are required. The amplification of DNA fragments occurs in 3 steps: denaturation at 95°C, annealing of the primers to the DNA template at 52 - 65°C depending on the primers and DNA extension at 72°C. The primer sequences, components of the reaction mixture and PCR programs are shown as following.

Table 7. Sequence of genotyping primers

Primer Name	**Primer sequence**
oIM7859	5' - GTG CTG CAA ACC AGG AAG G- 3'
oIM7860	5' - CTG GTT GAA TCA TTG AAG ATG G- 3'
oIM7861	5' - CGG CAA ACG ACT GTC CTG GCC G - 3'

Table 8. Master mixture of regular PCR

Substances	**Volume in µl**
Isolated DNA	1
Primer oIM7859 (10 pmol/µl)	1.25
Primer oIM7860 (10 pmol/µl)	1.25
Primer oIM7861 (10 pmol/µl)	1.25
dNTPs (1.25 mM each)	4
10 x PCR buffer with $MgCl_2$	2.5
Taq polymerase	0.25
H_2O	13.5

Table 9. Procedure of regular PCR

Step	**Temperature [°C]**	**Time [seconds]**	**Comments**
1	94	300	
2	94	30	
3	61.8	60	
4	72	60	steps 2 – 4 were repeated 10 times
5	72	120	
6	10	-	Hold

2.2.4.4. Agarose gel electrophoresis

Agarose gel electrophoresis is used for separating, identifying and purifying DNA fragments. For gel preparation, the appropriate amount (0.7 – 2%) of agarose was added to 1x Tris-acetic acid-EDTA (TAE) buffer (100mM Tris, 0.11% acetic acid, 1mM Na_2-EDTA) and boiled in a microwave (Severin). 800 ng/ml ethidium bromide were added and the solution was poured into casting platforms (EmbiTech), allowed to harden at RT and placed in an electrophoresis chamber (Peqlab) containing 1x TAE buffer. For electrophoretic separation, 6x loading buffer (18% Ficoll Typ 400, 0.12 mM EDTA, 0.15% Bromphenol blue, 0.15% Xylencyanol FF in 1x TAE buffer) was added to the DNA and samples were loaded on the agarose gel. Electrophoresis was performed at 80 – 120 V at RT. DNA bands were visualized using a UV light transilluminator (GelDoc®XR, BioRad) at 366 nm using QuantityOne® Software (BioRad).

Extraction of DNA fragments was performed using the illustra™ GFX™ PCR DNA and Gel band purification kit according to the manufacturer's instructions.

2.2.4.5. Quantitative real-time (RQ) PCR

Quantitative real-time (qRT) PCRs were performed according to the SYBR Green kit on mRNAs analysis or TaqMan®MicroRNA Kit (Applied Biosystem, USA) on miRNAs analysis.

SYBR Green I is a dye which intercalates into double-stranded DNA thereby producing a fluorescence signal. The intensity of the signal is proportional to the amount of double-stranded DNA present in the reaction. Therefore, the intensity increases with each cycle of the PCR reaction as the amount of the product increases. SYBR Green qRT-PCRs were accomplished using the LightCycler® SYBR Green I Master mix (Roche) on a StepOnePlus™ Real-Time PCR System (Applied Biosystems; 96-well format). The primer sequences, components of the reaction mixture and PCR programs were run as following.

Table 10. Primers' sequence of qRT-PCR

Primer Name	**Primer sequence**
UCP1 forward	5' - GGT GAA CCC GAC AAC TTC CGA AGT G - 3'
UCP1 reverse	5' - GGG TCG TCC CTT TCC AAA GTG TTG A - 3'
PGC-1α forward	5' - GCA CAC ACC GCA ATT CTC CCT TGT A - 3'
PGC-1α reverse	5' - ACG CTG TCC CAT GAG GTA TTG ACC A - 3'
Cidea forward	5' - ATT TAA GAG ACG CGG CTT TGG GAC A - 3'
Cidea reverse	5' - TTT GGT TGC TTG CAG ACT GGG ACA T - 3'
HPRT forward	5' - ACA TTG TGG CCC TCT GTG TGC TCA - 3'
HPRT reverse	5' - CTG GCA ACA TCA ACA GGA CTC CTC GT - 3'
C/EBPα forward	5' - CGA GGA GGA CGA GGC GAA GCA - 3'
C/EBPα reverse	5' - TGC GCA GGC GGT CAT TGT CAC - 3'
C/EBPβ forward	5' - CAC CAC GAC TTC CTC TCC GAC CTC T - 3'
C/EBPβ reverse	5' - GTA CTC GTC GCT CAG CTT GTC CAC C - 3'
aP2 forward	5' - TGA AAG AAG TGG GAG TGG GCT TTG C - 3'
aP2 reverse	5' - CAC CAC CAG CTT GTC ACC ATC TCG T - 3'
PPARγ2 forward	5' - TCC GTA GAA GCC GTG CAA GAG ATC A - 3'
PPARγ2 reverse	5' - CAG CAG GTT GTC TTG GAT GTC CTC G - 3'

Table 11. Master mix of qRT-PCR

Substance	**Volume in µl**
2 x SYBR Green I Master mix	4 µl
Primer forward (5 pmol/µl)	1 µl
Primer reverse (5 pmol/µl)	1 µl
cDNA	5 µl

Table 12. Procedure of qRT-PCR

Step	**Temperature [°C]**	**Time [seconds]**	**Comments**
1	95	600	
2	95	10	
3	72	15	steps 2 – 5 were repeated 40 times
4	72	90	
5	82	1	single acquisition
6	95	1	Melting Curve begins
7	65	15	20 acquisitions per °C
8	95		from 65°C to 95°C
9	4	hold	

Single miRNA is reverse transcribed to cDNA with specific RT-primer, and then the the cDNA is amplified by primer with TaqMan® probe, both primers are from TaqMan®MicroRNA Kit. The probe will be activated to produce fluorescence signal, when the extending step is end at per

cycle. The intensity frequently increases with each cycle of the PCR reaction as the amount of the activated probe increases.

miRNAs' specific RT-primers and qRT-PCR primers were purchased from Applied Biosystems (Table 13). ABi qRT-PCRs accomplished using the TaqMan® Universal PCR Master Mix (Applied Biosystems) on a StepOnePlus™ Real-Time PCR System (Applied Biosystems; 96-well format) according to the manufacturer's instructions (Table 14 and Table 15).

Table 13.miRNAs' assay kits (including RT-primers and qRT-PCR primers) ID from Applied Biosystem

miRNAs	**Assay ID (ABi)**
mmu-miR-155	002571
mmu-miR-146a	000468
mmu-miR-148a	000470
mmu-miR-673	001954
mmu-miR-615	001960
mmu-miR-30e	002223
mmu-miR-340	002258
mmu-miR-223	002295
mmu-miR-409-3p	002332
mmu-miR-805	002045
mmu-miR-21	000397
mmu-miR-27b	000409
mmu-sno-202	001232

Table 14. Master mix of qRT-PCR on miRNA

Substance	**Volume in µl**
Product from miRNA RT reaction	1.33 µl
TaqMan® Universal PCR Master Mix	10 µl
TaqMan® Small RNA Assay (20x)	1 µl
H_2O	7.67 µl

Table 15. Procedure of qRT-PCR on miRNA

Step	**Temperature [°C]**	**Time [seconds]**	**Comments**
1	95	600	
2	95	15	
3	60	60	steps 2 – 3 were repeated 40 times
4	4	hold	

Relative quantification of mRNA levels was performed based on the crossing point (CP) values of the amplification curves using the ΔΔCT method. Hypoxanthine-guanine-phosphoribosyltransferase (HPRT) served as an internal control to mRNA, and snoRNA202 were set as the endogenous control to miRNA.

2.2.4.6. Generation of lentiviral miRNA or mRNA expression constructs

Lentiviral expression constructs were used to stably express proteins of interest (Table 16). The constructs were derived from the pRRL.SIN-18 vector, containing sequences of HIV-1 and the transgene of interest. The pRRL.SIN-18 vector system contains no wild type copies of the HIV-long terminal repeats (LTRs): the 5'-LTR is chimeric and contains an enhancer and promoter of the respiratory syncital virus (RSV) instead of the U3-region of the wild type HIV (RRL). The U3-region in the 3'-LTR was nearly completely deleted. Therefore, both LTRs are transcriptionally inactivated (self-inactivating (SIN) vector) (Dull et al., 1998). The original virus plasmids were provided by Inder Verma (The Salk Institute for Biological Studies, Laboratory of Genetics, and La Jolla, CA, USA). Preparation of the lentivirus was accomplished by the lentiviral vector platform of the Institute of Pharmacology and Toxicology at University of Bonn.

miRNA precursors were amplified from genomic DNA according to normal PCR procedure. Fragments were ligated into two restriction enzyme sites of target vector (Table 17). Briefly speaking, fragments of miRNA precursors were amplified by PCR, and then brought into pCR®2.1-TOPO® vector (Invitrogen) using The Original TA Cloning® Kit (Invitrogen) according to the manufacturer's instructions. The two designed restriction sites of the cDNA fragments were used to retrieve the cDNA fragment from the pCR®2.1-TOPO® vector and ligate it into the target vector CMVpRRL.SIN18 or PGKpRRL. SIN18 expression vectors which carries green fluorescent protein (GFP) as reporter.

mRNA *C/EBPβ* cDNA was digested with two restricted enzymes (NEB) from pcDNA3.1-C/EBPβ purchased from Addgene (www.addgene.org) and sub-cloned into target vector CMVpRRL.SIN18 or PGKpRRL without GFP.

Anti-miR-155 construct, miR-155 Sponge, is carried 10 repetitive miR-155 binding sites to soak up endogenous miR-155(Table 18) (Ebert et al., 2007). The sponge construct was sub-cloned in to CMVpRRL.SIN18 with GFP as reporter.

Insertions were checked by specific restrict enzymes (NEB) digestion, then the made plasmid vectors were sent to Eurofins MWG for sequencing confirmation.

Table 16. Basic information of lentiviral plasmids concerning to the study

Vector	**Backbone**	**Promoter**	**Transgene**	**Source**
LVcontrol	pRRL.SIN18	----------	----------	AG Pfeifer
LVC/EBPβ	pRRL.SIN18	CMV	*C/EBPβ*	Y. Chen
LVC/EBPβ	pRRL.SIN18	PGK	*C/EBPβ*	Y. Chen
LVmiRctrl	pRRL.SIN18	CMV	*GFP-miR-scramble*	H. Lehman / Y. Chen
LVmiR155	pRRL.SIN18	CMV	*GFP-miR-155*	Y. Chen
LVmiR155	pRRL.SIN18	PGK	*GFP-miR-155*	Y. Chen
LVmiR155	pHPWLM	mu-UCP1	*GFP-miR-155*	M. Von Osten/ B. Haas
LVmiR155	pHPWLM	rat-UCP1	*GFP-miR-155*	M. Von Osten/ B. Haas
LVmiR146a	pRRL.SIN18	CMV	*GFP-miR-146a*	Y. Chen
LVmiR223	pRRL.SIN18	CMV	*GFP-miR-223*	H. Lehman / Y. Chen
LVmiR143	pRRL.SIN18	CMV	*GFP-miR-143*	F. Siegel
LVmiR9*	pRRL.SIN18	CMV	*GFP-miR-9**	AG Pfeifer
LVmiR195	pRRL.SIN18	CMV	*GFP-miR-195*	AG Pfeifer
LVmiR145	pRRL.SIN18	CMV	*GFP-miR-145*	AG Pfeifer
LVmiRS155	pRRL.SIN18	CMV	*GFP-Sponge-155*	S. Kipschull / Y. Chen
LVT/OmiR155	pLenti6.3	CMV/TO	*GFP-miR-155*	S. Kipschull / Y. Chen

Table 17. Primers' sequence for cDNA amplification of miRNA precursors

Primer names	**Primer sequences**
miR-155 fwd PstI	5'- CTAC ctgcag TCAAAGCTGAAGTCTACCTTGCC -3'
miR-155 rev EcoRv	5'- CTAC gatatc AGCAGGGTGACTCTTGGACTTG-3'
miR-146a fwd EcoRv	5'- CTAC gatatc TGTCCCAGATCCTTATGCATCA-3'
miR-146a rev SalI	5'- CTAC gtcgac TCAATCCAACATGACTCCCTCC-3'
miR-223 fwd EcoRv	5'- CTAC gatatc TCTTTCCAGTTGCACATCTTCC-3'
miR-223 rev SalI	5'- CTAC gtcgac GCATTCATATGTAGGCAGCAGG-3'

Table 18. Sponge-miR-155 sequence of anti-miR-155 casstte in LV-mirS155 plasmid

Sponge name	**Sponge sequence**
Sponge-miR-155	5'*actagt*ACCCCTATCAGTCTAGCATTAAGGGTTTACCCCTATCAATGTAGCATTAACACAGAACCCCTATCAGAGTAGCATTAAGAGCAGACCCCTATCATTGTAGCATTAAGTGGAAACCCCTATCAACTTAGCATTAACCTTGAACCCCTATCAAGGTAGCATTAAGGACCAACCCCTATCATACTAGCATTAACGAGATACCCCTATCATCTTAGCATTAACCAGGTACCCCTATCAGGATAGCATTAAGGTGCTACCCCTATCAGCCTAGCATTAA*tctaga*-3'

2.2.4.7. Generation of constructs for luciferase reporter assays on mRNA 3'-UTR

In luciferase reporter assays on miRNAs and 3'-UTR of mRNAs, constructs are used containing the luciferase gene as reporter of the 3'-UTR including miRNAs binding "seed" site of interest mRNAs. To generate a plasmid carrying the firefly luciferase with 3'-UTR of *C/EBPβ*, a 550bp fragment of the *C/EBPβ* 3'-UTR region was cloned into the SpeI and SacI sites of the firefly and Renilla luciferase Dual-expressing vector pMIR-RNL-TK (Figure 10) which contains herpes simplex virus thymidine kinase (TK) and SV40 promoters that promote firelyfly and Renilla

genes expression, therefore firefly expression can be used as reporter and Renilla gene expression can be used as control.

The 550bp fragment of the *C/EBPβ* 3'-UTR region was generated from genomic DNA by PCR using the following primers which exhibited a SpeI and SacI recognition site (Table 19).

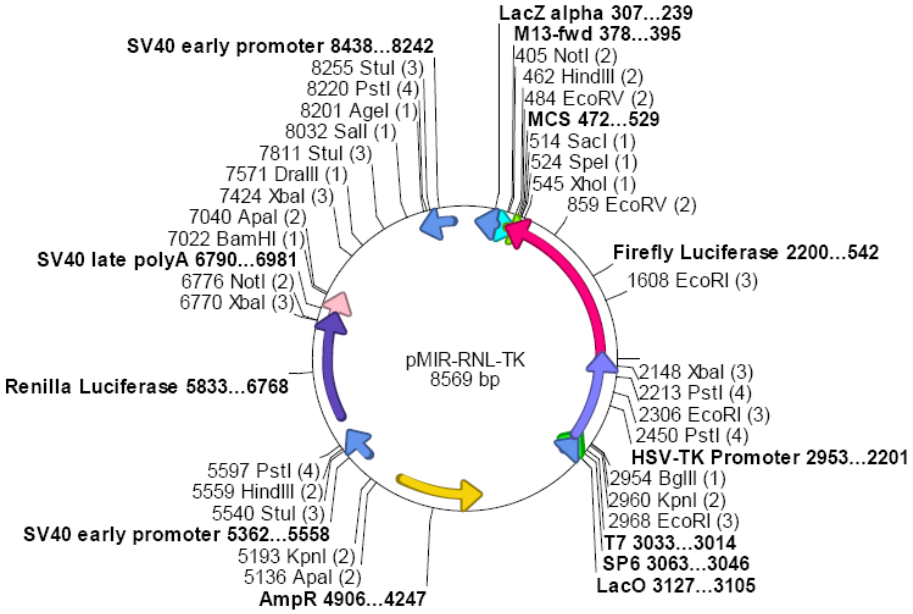

Figure 10. The plasmid vector map for pMIR-RNL-TK which was used to carry mRNA-3'UTR cassette.

Table 19. Primer sequences for amplification of C/EBPβ-3'UTR and mutation of miR-155 binding sites

Primer names	**Primer sequences**
C/EBPβ-UTR fwd SpeI	5' - TAT act agt GAG AAA AGA GGC GTA TGT ATA T - 3'
C/EBPβ-UTR rev SacI	5' - ACC gag ctc CCA AAC AGG CGT GCG GTC TCC - 3'
C/EBPβ-UTR fwd mut	5'- GAG AAC CTT TTC CGT TTC GTT GTG ACG CGT GAA GAC ATT TTA ATA AAC - 3'
C/EBPβ-UTR rev mut	5'- GTT TAT TAA AAT GTC TTC ACG CGT CAC AAC GAA ACG GAA AAG GTT CTC - 3'

The resulting fragment was ligated into the pCR®2.1-TOPO® vector (Invitrogen) using The Original TA Cloning® Kit (Invitrogen) according to the manufacturer's instructions. The SpeI and SacI recognition sites of the DNA fragment were used to retrieve the fragment from the vector and ligate it into the pMIR-RNL-TK dual-luciferase vector. The "seed" mutation has been performed using the Quick-Change Site Directed Mutagenesis Kit (Stratagene) with primers designed according to the manufacturer's instructions.

Insertion was checked by EcoRV digestion. The finial plasmid DNA was sent to Eurofins MWG for sequencing confirmation.

2.2.4.8. Promoter analysis and luciferase assay

Computational analysis of the *BIC*/miR-155 promoter sequence for identification of putative transcription factor binding sites was performed using the TFSEARCH ver.1.3 database.

For the luciferase reporter assay on promoter of miR-155, miR-155/BIC promoter construct in pGL3 plasmid was a kind gift from Prof. Flemington. The pGL3-miR-155/BIC construct is formed with miR-155 promoter and luciferase firefly gene as reporter. The pRL-TK vector (Promega) was co-operated to serve as an internal control expressing Renilla luciferase under control of the TK promoter.

2.2.4.9. Deep sequencing

Deep sequencing (including miRNA cloning and library sequencing) was performed by Vertis Biotech (Munich, Germany).

2.2.4.10. Chromatin immunoprecipitation

Wild type primary brown preadipocytes were transduced with LVC/EBPβ or LVcontrol. ChIP assay was performed following the manufacturer's instructions (Agarose ChIP kit, Pierce). An anti-C/EBPβ antibody (Santa Cruz) was used to precipitate C/EBPβ-bound DNA. qRT-PCR analysis on recovered DNA fragments was performed using primers that span the putative C/EBPβ binding sites A, B/C/D, or E respectively. qRT-PCR results were normalized to input values.

Table 20. Primer sequences for C/EBP binding site ChIP assay

Primer names	Primer sequences
ChIP C/EBPβ A fwd	5' – TGT GTG GTA GGA AGA AAA CCT TCA - 3'
ChIP C/EBPβ A rev	5' – TGT CAG ATT CGT GGA CAC AGA AA - 3'
ChIP C/EBPβ B/C/D fwd	5' – CCA GAT ACT ACA GGG ATC TAA AGA GGT T - 3'
ChIP C/EBPβ B/C/D rev	5' – TCA GGC CTT CCC CTA AAA CTC - 3'
ChIP C/EBPβ E fwd	5' – CAG AGT GAC CTG CCT TAT CTT AAA AA - 3'
ChIP C/EBPβ E rev	5' – GAC CCT TTA ATA CAG TTC CTT CTG TTG - 3'

2.2.5. Respiratory measurements in cultured adipocytes and tissue

Analysis of mitochondrial function is central to the study of energy metabolism and thermogenic activity in brown fat cells. However, important properties of mitochondria differ *in vivo* and *in vitro*. To study mitochondrial function in BAT and in cultured brown adipocytes, a protocol for the *in situ* analysis of functional mitochondria in selectively permeabilized cells using digitonin, without the isolation of organelles, was applied (Kuznetsov et al., 2008).

Adipose tissue (about 3-6 mg BAT or 30-50 mg inguinal WAT) from 12-16 week old, cold-exposed (4 h, 4°C) wt, miR-155$^{+/-}$, or miR-155$^{-/-}$ mice was isolated immediately before oxygraphic measurements (Oxygraph 2K, Oroboros Instruments). Tissue was dissected into small pieces and transferred to the oxygraph chamber containing 2ml incubation medium (0.5mM EGTA, 3mM $MgCl_2.H_2O$, 60mM K-lactobionate, 20mM Taurine, 10mM KH_2PO_4, 20mM HEPES, 110mM Sucrose, 1g/l BSA, and pH7.1) with 25µg/ml digitonin. Ex vivo respiration levels of the adipose tissues were recorded when reaching a steady state. Respiration rates were normalized to total protein content.

Additionally, the maximal mitochondrial oxygen consumption in permeabilized cells and tissue under maximal substrate availability conditions as well as the UCP-1-dependent fraction were

determined. Therefore, a substrate/inhibitor titration protocol was applied. The following substances were added to the chamber using Hamilton syringes to the indicated final concentrations in the stated order. After adding a substance, it was waited until the respiration rate reached a steady state, then the next substance was added.

Table 21. Substances used in respiratory measurements

Substance	**Final concentration**	**Function**
Digitonin	25 µg/ml	Permeabilization
Glutamate/Malate	10 mM each	Substrate
Succinate	10 mM	Substrate
ADP	2 mM	Substrate
Oligomycin	10 µg/ml	Inhibitor

To measure cold-induced thermogenesis in differentiated brown adipocytes *in vitro*, the cells were pretreated with 1 mM 8-Br-cAMP for 24 h prior to the respiratory measurements to mimic cold exposure.

The obtained respiration rates were normalized to the protein content of determined by the Bradford method from reference wells.

2.2.6. Statistics

Values are presented as means ± standard error of means (SEM). Statistical differences between two means were determined using Student's *t*-test (unpaired, two-tailed), one-way ANOVA was used to compare differences among multiple groups. GraphPad Prism 5 or Excel software was used to calculate P-values (*$P < 0.05$; **$P < 0.01$; ***$P < 0.001$).

3. Results

3.1. Identification of miRNAs with a function in brown adipogenesis

3.1.1. Genome-wide profiling of miRNAs in brown fat

Mature brown adipocytes are derived from BAT-MSCs. To identify miRNAs that play a role during brown adipogenesis, we compared miRNA expression profiles of preadipocytes isolated from the SVF of BAT (Haas et al., 2009) with *in vitro* differentiated mature brown adipocytes by a global deep sequencing analysis. 288 miRNAs could be detected in this screen: 16 miRNAs were >2fold higher expressed in mature adipocytes compared to preadipocytes, whereas 12 miRNAs were >2fold down-regulated during differentiation (Figure 11).

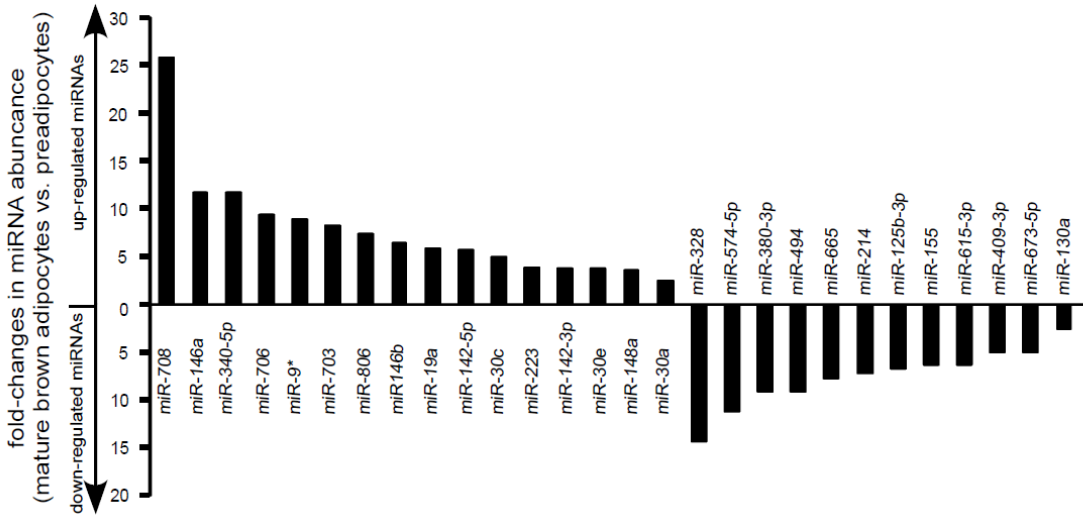

Figure 11. Genome-wide deep sequencing screen to identify differentially regulated miRNAs in brown adipocytes. Shown are the 16 up-regulated and 12 down-regulated miRNAs with fold changes > 2.

3.1.2. Validation of miRNA candidates

In order to confirm the most differentially regulated miRNA candidates, we selected 12 miRNAs according to relevance of their putative target genes (www.targetscan.org), as well as by literature search on known function of the identified miRNA candidates (www.ncbi.nlm.nih.gov/pubmed). The expression of these selected miRNAs was validated by

quantitative Real-time PCR (qRT-PCR) in preadipocytes and *in vitro* differentiated brown fat cells (Figure 12).

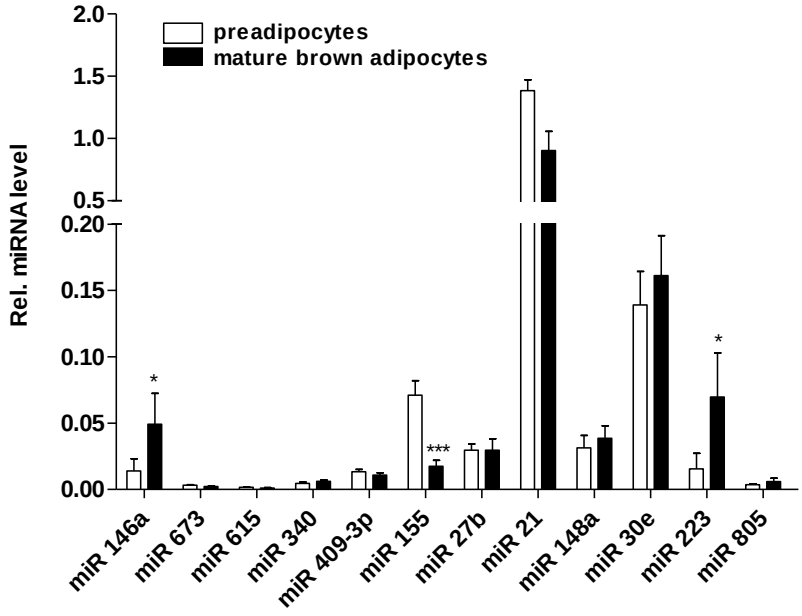

Figure 12. qRT-PCR analysis of miRNA expression in preadipocytes (stromal vascular fraction) isolated from brown fat tissue (BAT-SVF) versus *in vitro* differentiated mature adipocytes. Data are normalized to sno202RNA expression and are represented as means ± SEM. (*$p<0.05$, ***$p<0.001$, n=6).

Three miRNA candidates from the deep sequencing screen could be validated by qRT-PCR: miR-146a (about 3.57 fold increased in mature brown adipocytes , $p<0.05$), miR-155 (about 4.12 fold decreased, $p<0.001$), and miR-223 (about 4.6 fold increased, $p<0.05$).

3.1.3. Lentiviral expression vectors for efficient miRNA expression

To analyze these miRNAs in more detail lentiviral expression vectors carrying optimized miRNA precursor expression cassettes for efficient miRNA expression under control of the constitutively active CMV promoter were generated. The miRNA precursor sequences were cloned into the 3´UTR of the GFP reporter gene open reading frame (ORF). A non-matching scrambled sequence was used as control (miRctrl) (Figure 13).

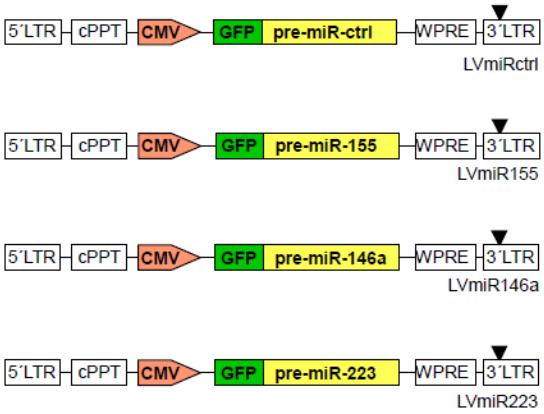

Figure 13. Lentiviral expression vectors; LVmiRs express miRNA precursors (yellow) coupled to GFP mRNA as reporter (green), LVmiRctrl contains a scrambled, non-targeting sequence. LTR, long terminal repeat; cPPT, central polypurine tract; CMV, cytomegalovirus promoter; GFP, green fluorescent protein; pre-miR-155, precursor miR-155; WPRE, woodchuck hepatitis responsive element; triangle, self-inactivating mutation.

The miRNA-carrying lentiviruses effectively infected the cultured BAT preadipocytes (BATi cells). At 48 h post transduction, GFP reporter expression was observed under the florescence microscope to evaluate transduction efficiency (Figure 14)

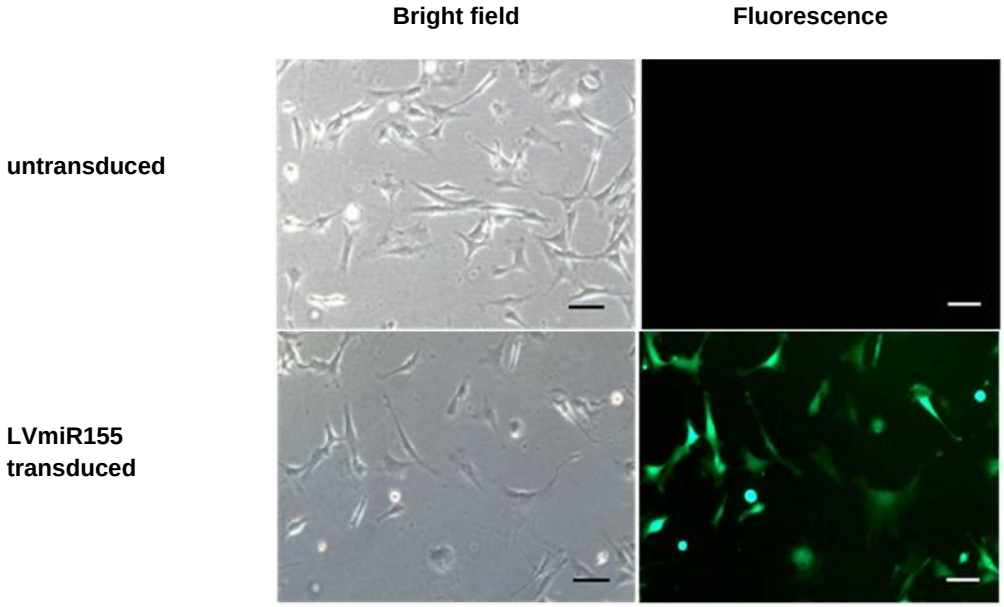

Figure 14. Lentiviral transduction efficiency in preadipocytes (BATi). LVmiR155 transduced cells were observed under the microscope to evaluate the percentage of GFP positive cells. Un-transduced preadipocytes served as controls (representative images are shown).

Transduction of preadipocytes with GFP/ miRNA carrying lentiviruses showed high efficiencies. Between 99.2% and 99.9 % cells were detected as GFP positive by using flow cytometry (FACS) analysis.

3.1.4. Role of identified miRNA candidates in brown adipogenesis

To investigate miRNA function in brown fat differentiation, preadipocytes (BATi) were infected with the miRNA-expressing viruses (day -4) and fully differentiated until day 8 *in vitro* using the standard brown fat differentiation protocol (see 2.2.2.5.).

To measure fat differentiation *in vitro*, lipid droplets of mature differentiated brown fat cells were stained with Oil Red O substrate.

As shown in Figure 15, miR-146a slightly reduced lipid accumulation, whereas miR-155 strongly reduced the number of lipid droplets. In contrast, overexpression of miR-223 had a slightly increased amount of lipid droplets.

These findings suggest that miRNAs can both activate and inhibit the accumulation of lipid droplets of brown fat cells *in vitro*.

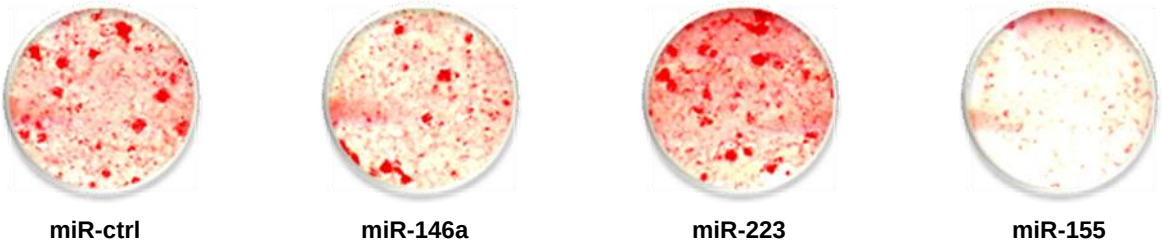

Figure 15. Oil Red O staining shows the effects of miRNA overexpression on brown fat lipid accumulation, and differentiation *in vitro*

3.2. Role of miR-155 in brown adipocytes

3.2.1. Regulation of miR-155 in brown adipogenic differentiation

Since miR-155 has such a strong effect on lipid accumulation, we selected it for further studies during brown adipocyte differentiation. miR-155 was shown to play a role in the context of hematopoiesis, immune response, and tumor formation (Eis et al., 2005). In contrast the knowledge of miR-155 function in adipose tissue is very limited.

First, I studied *ex vivo* expression of miR-155 in brown fat cell types, total RNA was isolated either from the stromal vascular fraction or the mature fat fraction of BAT. I found that miR-155 expression is remarkably lower in the mature fat fraction than in the SVF of BAT (Figure 16A).

To further elucidate the role of miR-155 in adipogenesis, SVF-derived preadipocytes were purified by FACS sorting. Purified BAT progenitors positive for the preadipocyte/stem cell marker Sca1 and negative for the hematopoietic markers CD45 and Mac1 (Schulz et al., 2010) were then cultured on cell culture dish for 48 h *in vitro*. Comparative qRT-PCRs were performed in unsorted vs. FACS-sorted BAT-SVF cells. Data showed that there was no significant difference of miR-155 expression between the sorted and unsorted BAT-SVF cells (Figure 16B). Finally, total RNA was isolated from unsorted preadipocytes, and from *in vitro* differentiated BAT cells at day 7/8. The results indicated miR-155 expression is strongly reduced in differentiated brown fat cells (Figure 16C). These experimental data demonstrated that miR-155 is downregulated during brown fat differentiation *in vivo* (Figure 16A), as well as *in vitro* (Figure 16C).

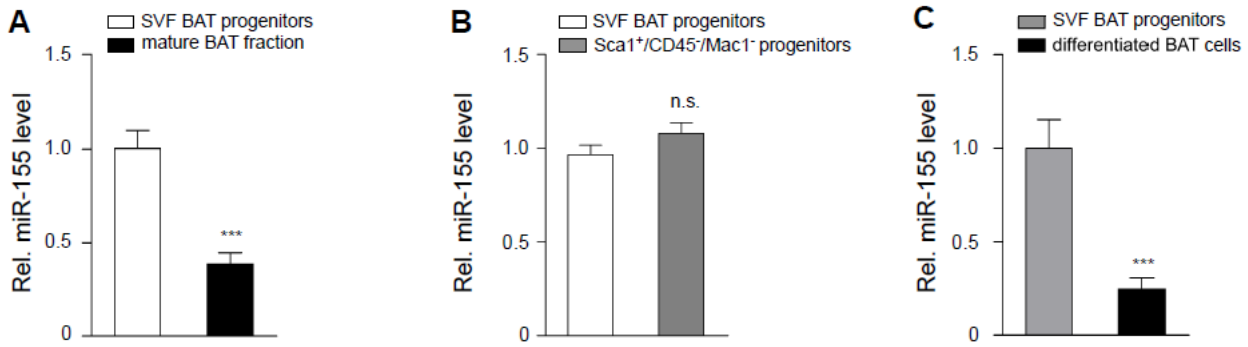

Figure 16. miR-155 regulates brown fat differentiation *ex vivo* and also *in vitro*. qRT-PCR analysis of miR-155 expression **(A)** in BAT tissue samples, the SVF or the mature adipocyte fraction of new-born mice were used. SVF value was set as one; data are represented as means ± SEM (***P<0.001; n=3); **(B)** in BAT cells from the SVF, or Sca-1^{+}, CD-45^{-} and Mac-1^{-} FACS-sorted BAT preadipocytes; **(C)** in preadipocytes and *in vitro* differentiated mature fat cells. The preadipocyte group was set as one data are represented as means ± SEM (n.s., not significant; ***P<0.001; n=3). (All data are normalized to snoRNA202 expression.)

3.2.2. miR-155 inhibits brown adipocyte differentiation *in vitro*

Overexpression of miR-155 has been shown to reduce lipid accumulation *in vitro*, and its expression was down-regulated significantly in mature brown fat *in vivo* as well as *in vitro* (Figure 16A, C). To further investigate the effects of miR-155 in brown adipocytes differentiation *in vitro*, the experiments with lentiviral vectors were performed. Apart from overexpression of miR-155 (LVmiR155), we investigated the effects of a knock-down of endogenous miR-155 by a lentiviral vector carrying a miR-155-specifc octameric decoy target (LVmiRS155) – a so called `sponge´ (Ebert et al., 2007) – that competitively inhibits miR-155. A vector carrying a scrambled miRNA sequence was used as control (LVmiRctrl) (Figure 17A).

To measure miR-155 expression levels in the lentiviral transduced cells, total RNA was isolated 48 h post infection. qRT-PCR data showed, that miR-155 expression was increased 20-fold in LVmiR155 transduced cells. In contrast, transduction with the "sponge" construct (LVmiRS155) resulted in a 70% reduction of miR-155 levels (Figure 17B).

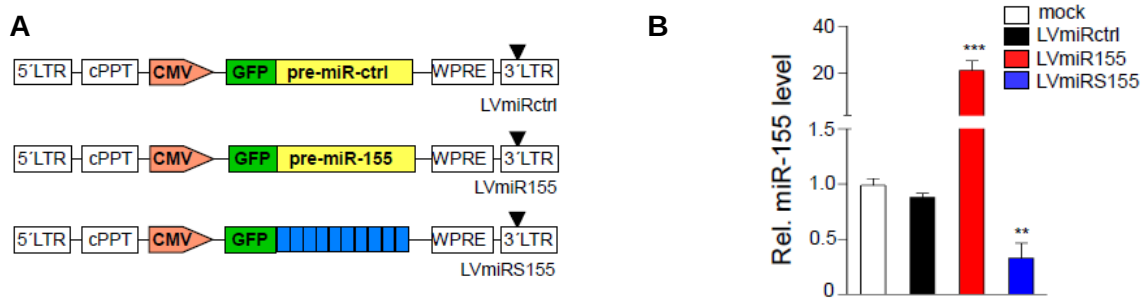

Figure 17. (A) Lentiviral expression vectors; LVmiR155 expresses miR-155 precursors (yellow) coupled to GFP mRNA as reporter (green), LVmiRctrl contains a scrambled, non-targeting sequence (yellow), and LVmiRS155 contains ten repeats of a miR-155 complementary binding site (blue). LTR, long terminal repeat; cPPT, central polypurine tract; CMV, cytomegalovirus promoter; GFP, green fluorescent protein; pre-miR-ctrl, scrambled miRNA sequence; pre-miR-155, precursor miR-155; blue boxes, decoy targets; WPRE, woodchuck hepatitis responsive element; triangle, self-inactivating mutation. **(B)** qRT-PCR analysis of miR-155 expression levels in LVmiR155 and LVmiRS155 transduced preadipocytes (normalized to snoRNA202). Untreated cells (mock) were set as one; data are presented as mean±SEM (***P<0.001; **P<0.01; n=3).

miR-155 overexpressing cells revealed a strong inhibition of lipid accumulation. These results were reflected in decreased tri-glycerol content of differentiated LVmiR155 transduced cells

(Figure 8). In contrast, LVmiRS155 transduced cells displayed a significant increase in lipid droplet number and size as well as in tri-glycerol (TG) content (Figure 18A, B).

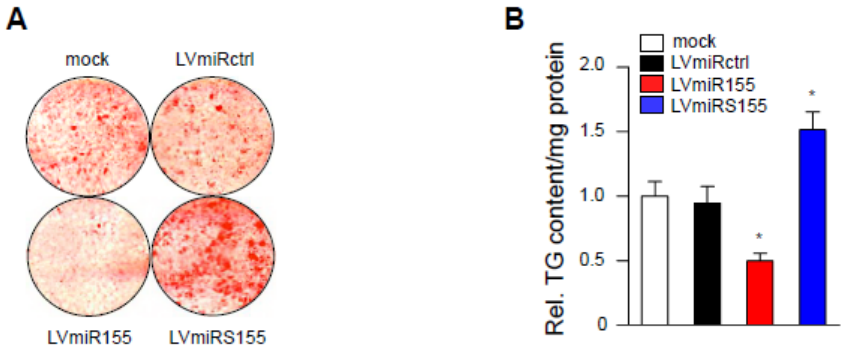

Figure 18. (A) Oil Red O staining of BATi cells overexpressing miR-155 (LVmiR155) or an anti-miR-155 sponge (LVmiRS155) as compared to cells carrying a control scrambled miRNA (LVmiRctrl); mock, uninfected cells. **(B)** TG content of differentiated BAT cells transduced with LVmiRctrl, LVmiR155, and LVmiRS155; mock, uninfected control. TG content was normalized to total protein concentration. Untreated cells were set as one. Data are represented as means ± SEM. (*P<0.05; n=4).

The effect of miR-155 in brown adipocytes differentiation is also validated by data from expression analysis of adipogenic marker genes. Western blotting experiments revealed that overexpression of miR-155 significantly reduced abundance of the adipogenic markers C/EBPα, PPARγ, and aP2, whereas expression of the miR-155 sponge effectively increased abundance of these markers as compared to wt cells or LVmiRctrl transduced cells (Figure 19).

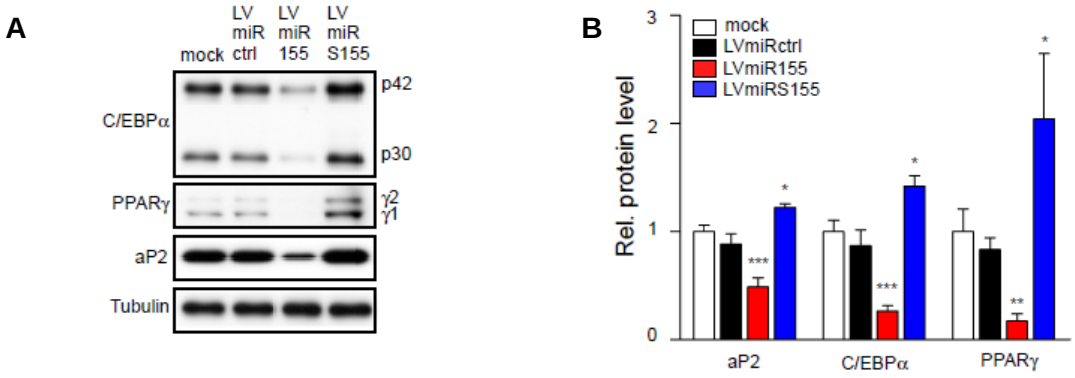

Figure 19. (A) Representative Western blot of fat cell markers C/EBPα, PPARγ, and aP2 in differentiated brown adipocytes transduced with lentiviral vectors LVmiRctrl, LVmiR155, and LVmiRS155, respectively; mock, uninfected control. Tubulin served as loading control. **(B)** Quantification of Western blot analysis of fat cell markers. Uninfected controls (mock) were set as one. Expression data were normalized to Tubulin and are represented as means ± SEM. (*P<0.05; **P<0.01; ***P<0.001; n=4).

Furthermore, three thermogenic markers of brown adipocytes: *UCP1*, *PGC-1α* and *Cidea*, were shown to be reduced in miR-155 overexpressing cells. Interestingly, the opposite effects were observed in the miR-155 knock-down group (LVmiRS155) (Figure 20).

These qRT-PCR data indicated that not only regular fat cell differentiation, but also the brown fat-specific thermogenic program were inhibited by miR-155.

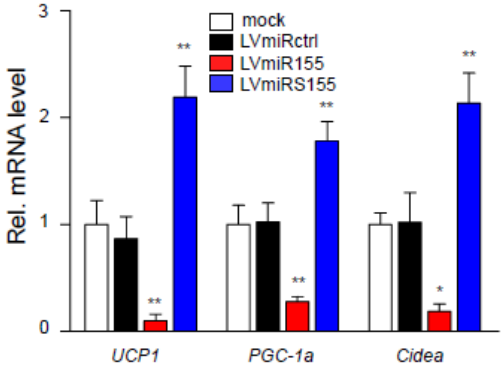

Figure 20. qRT-PCR analysis of the brown thermogenic markers *PGC-1α*, *UCP1*, and *Cidea* in differentiated brown adipocytes transduced with the indicated lentiviral vectors. Untreated cells (mock) were set as one. Data were normalized to HPRT, a reference gene, expression and are represented as means ± SEM. (*P<0.05; **P<0.01; n=4).

Taken together, these data revealed that during brown adipocytes differentiation, miR-155 overexpression showed a strong effect: LVmiR155 transduced cells exhibited a strong reduction of both thermogenic and adipogenic gene expression, less fat droplets, and less TG content. Thus, these data indicate that miR-155 inhibited brown adipocyte differentiation *in vitro*.

3.3 C/EBPβ is the major target of miR-155 in brown adipocyte differentiation

It has been shown that miRNAs can target multiple-mRNAs via binding to partial complementary binding sites. Thereby, one miRNA might be able to influence the translation of many target genes in one certain cell type or tissue. In addition, miRNA abundance and relevance of a given miRNA-target interaction is cell type specific.

To understand the inhibitory role of miR-155 in brown fat differentiation, identification of the major target of miR-155 in brown fat cells is crucial.

3.3.1 miR-155 targets C/EBPβ in brown adipocytes

Databases are currently annotating more than 250 predicted conserved miR-155 target genes in mouse and human UTR (www.targetscan.org). A plethora of validated targets of miR-155 have been reported for hematopoietic and immune cells (O'Connell et al., 2008). Interestingly, C/EBPβ has been identified as a primary target of miR-155 in lymphocytes, myeloid cells and macrophages (Costinean et al., 2009; He et al., 2009; O'Connell et al., 2009; Worm et al., 2009), as well as *in vitro* models of white adipogenesis (Liu et al., 2011). C/EBPβ has a conserved 8-mer binding site for miR-155 in its 3´UTR (Figure 21).

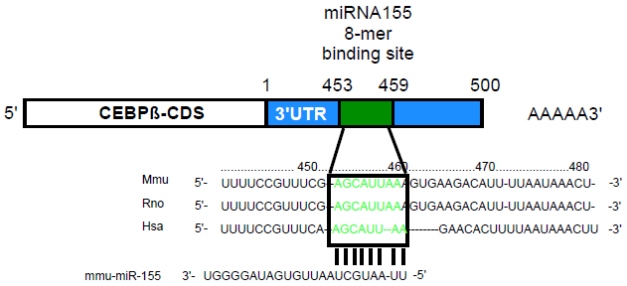

Figure 21. Schematic representation of C/EBPβ mRNA including the 3´UTR containing the predicted miR-155 target region (top). Sequence alignment of the highly conserved miR-155 3´UTR binding site in mice (Mmu), rat (Rno), and human (Hsa) with the seed region of the mature 22nt miR-155 (www.targetscan.org) (bottom).

The transcription factor C/EBPβ is one of the essential regulators of the early phase of adipocyte differentiation. Moreover, recent studies showed that C/EBPβ is not only important in adipogenesis, but is also a crucial factor in the thermogenic program in brown fat (Kajimura et al., 2009). For C/EBPβ, three different polypeptides are generated: two activating forms termed LAP and LAP* (liver-enriched transcriptional activator protein, 35kDa and 38kDa) and one inhibitory form named LIP (liver-enriched transcriptional inhibitory protein, 20kDa) (Nerlov, 2007). All three isoforms arise from one single mRNA transcript by alternative, in-frame translation initiation sites (Calkhoven et al., 2000) and all isoforms are expressed in differentiated brown adipocytes. In our brown fat *in vitro* differentiation procedure, all three C/EBPβ isoforms were strongly induced by induction medium (IM). Especially, LAP was highly abundant after stimulation by IM (Figure 22A). We found that miR-155 down-regulates all three isoforms simultaneously in *in vitro* differentiated brown adipocytes (Figure 22B). This can be explained by the fact that the three C/EBPβ isoforms share the same 3´UTR containing the miR-155 recognition site.

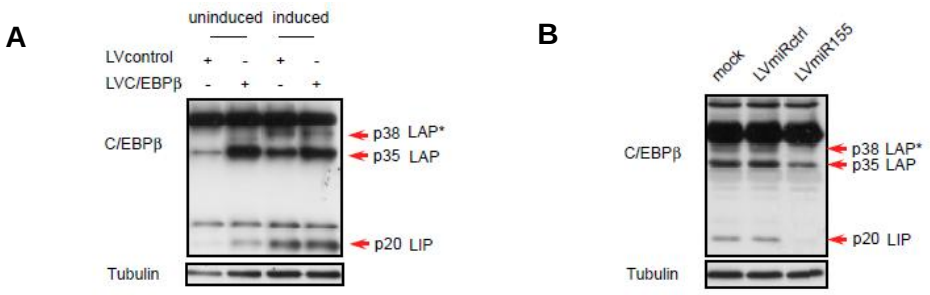

Figure 22. Western blot analysis of C/EBPβ isoform (LAP*/ p38, LAP/ p35, and LIP/ p20) expression **(A)** in BAT cells with or without induction, overexpression of C/EBPβ with lenti-viral transduction (LVC/EBPβ) was set as positive control group; **(B)** in untransduced (mock), LVmiRctrl or LVmiR155 transduced brown mature adipocytes (day 8).

In our next analysis, we were focusing on the LAP isoform, because this is the predominant one in brown adipocytes and has been shown to bind to PRDM16 (Kajimura et al., 2009). Given the importance of C/EBPβ for brown adipogenesis and the inhibitory function of miR-155 on C/EBPβ protein levels in LVmiR155 transduced adipocytes, we further investigated the interaction of miR-155 and C/EBPβ in brown fat differentiation (Figure 23A).

To test direct interaction of miR-155 with C/EBPβ, we generated a luciferase construct carrying the C/EBPβ 3´UTR sequence (Figure 23A top). For these reporter assays we used the the murine HIB-1B brown preadipocyte cell line. HIB-1B cells transduced with LVmiR155 showed a reduced luciferase expression compared to wt or LVmiRctrl transduced cells. Mutagenesis of the miR-155 binding site in the *C/EBPβ* 3´UTR clearly abolished the miR-155 mediated suppression of luciferase activity (Figure 23B bottom).

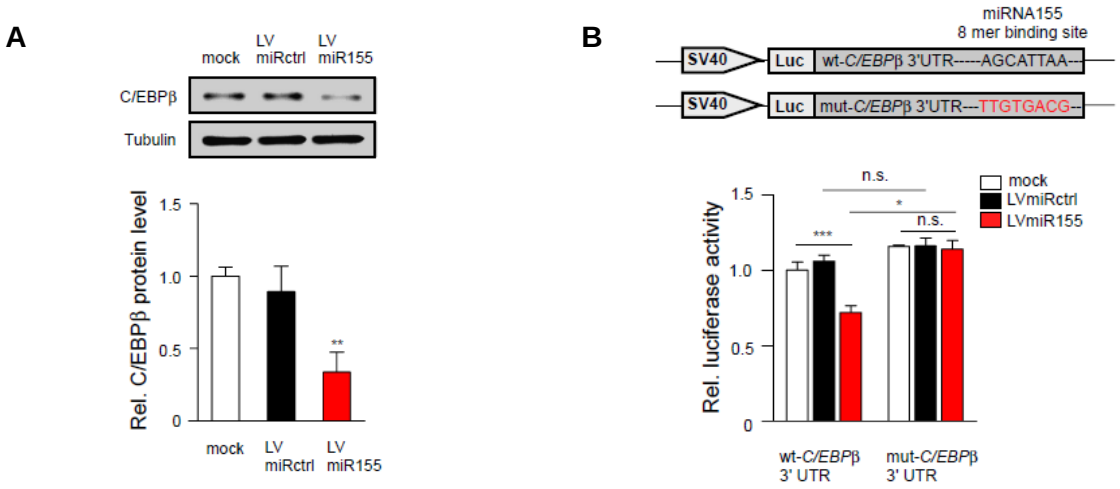

Figure 23. (A) Western Blot analysis (top) of C/EBPβ expression in cells transduced with LVmiRctrl or LVmiR155; mock, uninfected cells. Quantification of Western blot analysis (bottom), tubulin served as loading control. Untreated cells (mock) were set as one. Data are represented as means ± SEM. (**p<0.005; n=3). **(B)** Luciferase assay to examine interaction between miR-155 and its predicted target site in the *C/EBPβ* 3´UTR. Reporter plasmids carrying the wt or mutated *C/EBPβ* 3´UTR (top) were transfected into HIB-1B cells transduced with LVmiRctrl or LVmiR155. Data are represented as means ± SEM. (*p <0.05; *** p <0.001; n.s., not significant, n=3).

In contrast, miR-155 knock-down with the sponge construct resulted in increased C/EBPβ protein levels and significantly increased luciferase reporter expression (Figure 24A, B)

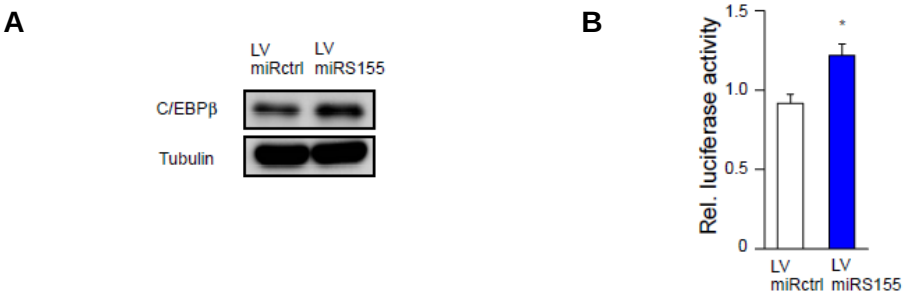

Figure 24. (A) Western blot analysis of C/EBPβ protein levels in LVmiRctrl or LVmiRS155 transduced preadipocytes. Tubulin served as loading control. (**B**) Luciferase assay to analyze miR-155 interaction with the *C/EBPβ* 3´UTR. Reporter plasmids containing the *C/EBPβ* 3´UTR were transfected into LVmiRctrl or LVmiRS155 transduced HIB-1B cells. LVmiRctrl transduced controls were set as one. Data are presented as means ± SEM. (* p <0.05; n=3).

These data clearly suggested that miR-155 is able to directly target C/EBPβ in brown fat differentiation via interaction with its 3´UTR. Next, I addressed the question whether C/EBPβ is

the major target of miR-155, which subsequently inhibits brown adipocyte differentiation. To address this question, rescue experiments were performed: Restoration of C/EBPβ expression levels were supposed to ameliorate the inhibitory effect of miR-155 in brown fat differentiation.

3.3.2 C/EBPβ is able to rescue the inhibitory effect of miR-155 in brown adipocytes

To test the hypothesis of C/EBPβ as the major miR-155 target in brown adipogenesis, miR-155 overexpressing preadipocytes were co-transduced with a lentiviral vector carrying a *C/EBPβ* cDNA that does not contain the miR-155 3´UTR target sequence (LVC/EBPβ). To achieve physiologically relevant levels of C/EBPβ, three different concentrations of LVC/EBPβ were tested (Figure 25A). Western blot analysis revealed, that infection with 1.0 ng LVC/EBPβ resulted in "ectopic" restoration of C/EBPβ levels in LVmiR155 co-transduced cells as compared to the respective controls (Figure 25A) Restoration of C/EBPβ expression levels by LVC/EBPβ rescued the inhibitory effect of miR-155 on lipid accumulation as assessed by Oil Red O staining and measuring cellular TG content (Figure 25B, C).

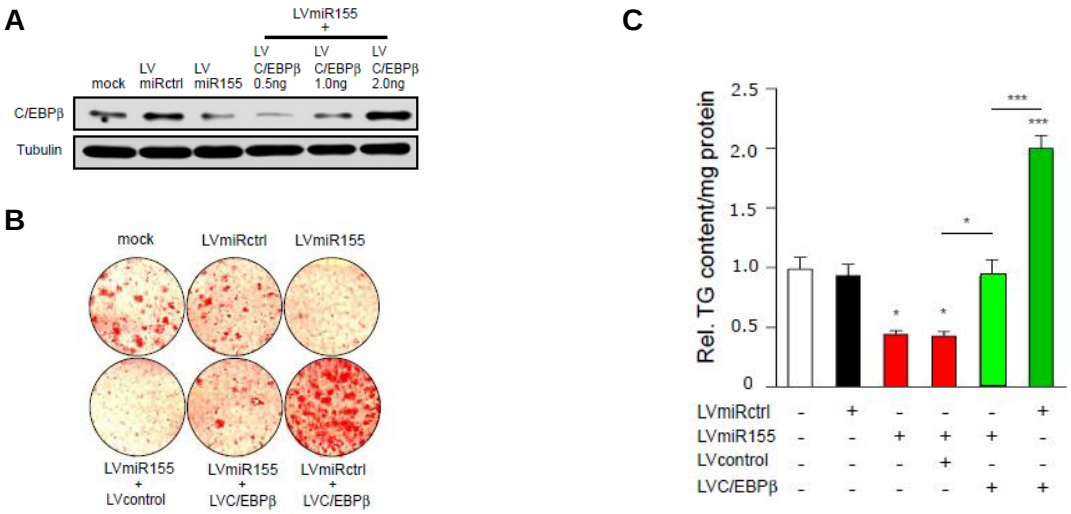

Figure 25. (A) Western blot analysis of C/EBPβ expression in LVmiR155 cells transduced with increasing amounts of LVC/EBPβ to rescue the effect or miR-155 (viral titer was determined using an RT ELISA). Tubulin served as loading control. **(B)** Oil Red O staining of *in vitro* differentiated brown adipocytes infected with different combinations of lentiviral vectors expressing miR-155 (LVmiR155) and/or C/EBPβ (LVC/EBPβ 1 ng RTase); mock, uninfected cells; LVmiRctrl, cells transduced with a control scrambled miRNA lentivirus; LVcontrol, empty vector. **(C)** Triglyceride (TG) content of *in vitro* differentiated brown adipocytes transduced with combinations of lentiviral vectors expressing miR-155 (LVmiR155) and/or C/EBPβ (LVC/EBPβ 1 ng RTase); mock, uninfected cells; LVmiRctrl, cells transduced with a lentivirus carrying a scrambled miRNA; LVcontrol, empty vector; TG content was normalized to total protein concentration. Untreated control was set as one. Data are represented as means ± SEM. (*p<0.05; ***p<0.001; n=3).

In addition, restoration of C/EBPβ protein levels reconstituted expression of the adipogenic markers C/EBPα, PPARγ, and aP2 in miR-155 overexpressing adipocytes to levels comparable to uninfected controls, as assessed by protein as well as by protein expression analysis (Figure 26A, B). The same is true for brown fat specific, thermogenic genes: *PGC-1α* and *UCP1* levels were both rescued by restoration of C/EBPβ in miR-155 overexpressing BAT cells (Figure 26B).

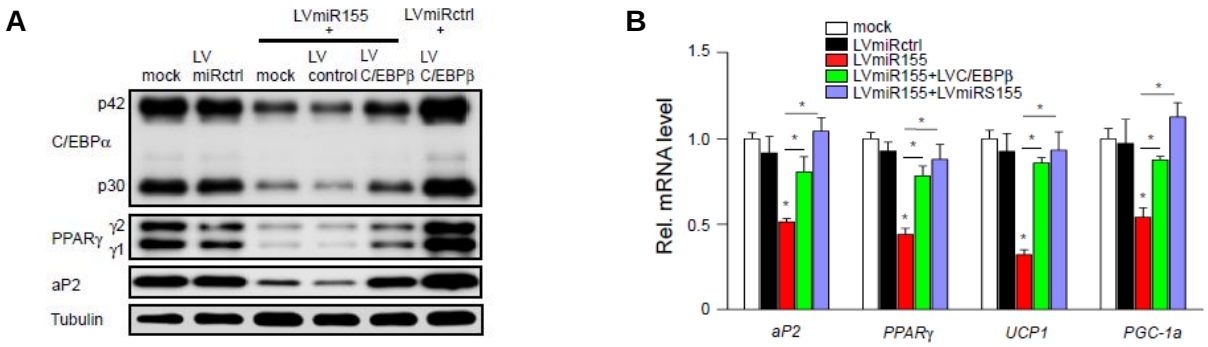

Figure 26. (A) Western Blot analysis of fat cell markers C/EBPα, PPARγ and aP2 of *in vitro* differentiated brown adipocytes transduced with combinations of lentiviral vectors expressing miR-155 (LVmiR155) and/or C/EBPβ (LVC/EBPβ 1 ng RTase); mock, uninfected cells; LVmiRctrl, cells transduced with a control scrambled miRNA lentivirus; LVcontrol, empty vector. Tubulin served as loading control (representative blot out of n=3 is shown). **(B)** Abundance of adipogenic markers *aP2*, *PPARγ* as well as of thermogenic genes *UCP1* and *PGC-1α* as measured by qRT-PCR. Untreated cells (mock) were set as one; data are presented as means ± SEM. (* $p < 0.05$; n=3).

Taken together, these data show that C/EBPβ is able to rescue the miR-155 mediated inhibitory effect on brown adipocyte differentiation. Thus, these data indicate that C/EBPβ is the major target of miR-155 in brown adipocyte, and miR-155 regulates brown adipocyte differentiation via directly targeting C/EBPβ.

3.4 miR-155 is induced by the TGFβ-signaling pathway in brown preadipocytes

To identify the physiological regulators of miR-155 in brown fat differentiation, the detailed time course of miR-155 expression during BAT differentiation was investigated by performing qRT-PCR with RNA samples isolated at day -2, day -1, day 0, day 1, day 2, day 4, and day 7/8 of *in vitro* differentiation. The data revealed that miR-155 expression peaks when cells reach confluency at day -1 or day 0 of the differentiation protocol and decreases continuously after induction of adipogenesis (Figure 27)

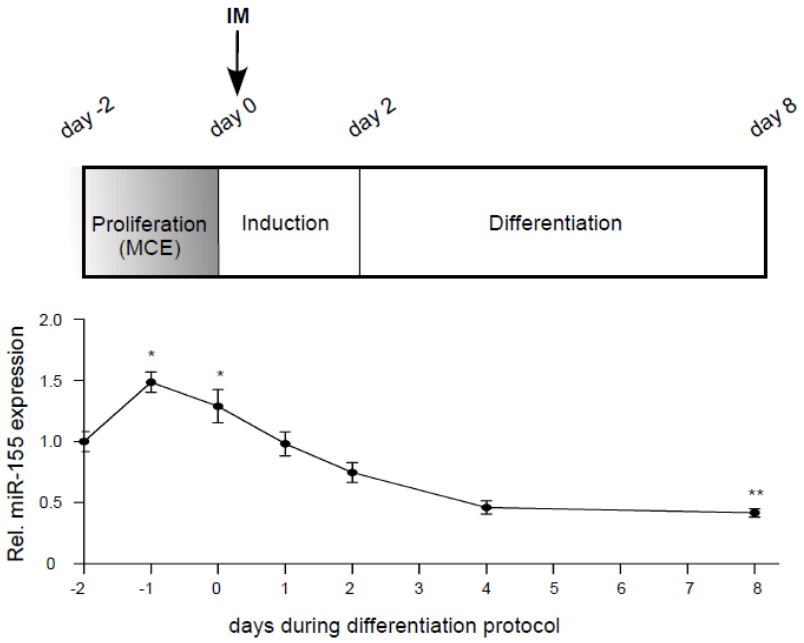

Figure 27. qRT-PCR analysis of miR-155 expression levels in brown fat cells during *in vitro* differentiation procedure (normalized to snoRNA202). Undifferentiated cells (day -2) were set as one. Data are represented as means ± SEM (*$p < 0.05$; **$p < 0.005$; n=5)

Transforming growth factor β 1 (TGFβ1) is known to positively regulate miR-155 via the TGFβ1/Smad pathway in epithelial cells (Kong et al., 2008). Furthermore, TGFβ1 has been shown to potently inhibit adipogenesis in 3T3-L1 cells (Ignotz and Massague, 1985). Therefore, we addressed the question wether TGFβ1/Smad signaling regulates miR-155 expression in BAT cells.

Treatment of preadipocytes with 5ng/ml recombinant TGFβ1 significantly increased miR-155 levels within 24h (Figure 28A), whereas inhibition of TGFβ1/Smad signaling with a

siRNA-Smad4 (Deckers et al., 2006) blocked TGFβ1-mediated miR-155 induction (Figure 28B, C).

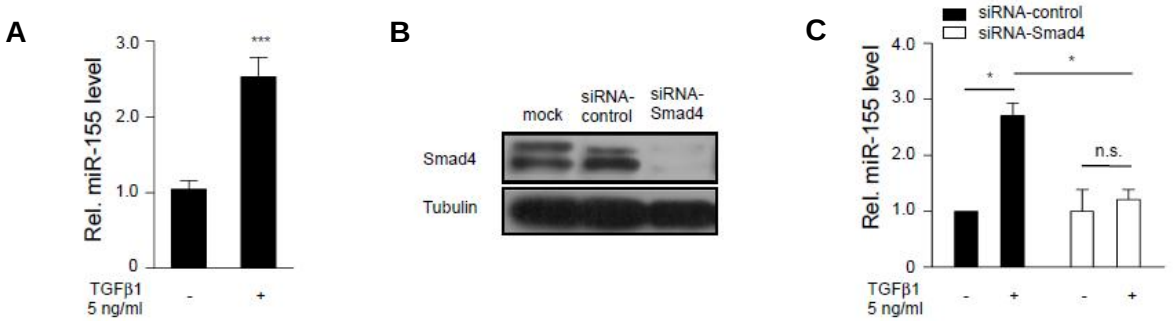

Figure 28. (A) Effect of TGFβ1 (5 ng/ml, 24 h) on miR-155 expression in brown fat cells as measured by qRT-PCR (normalized to snoRNA202 expression). Untreated cells were set as one. Data are represented as means ± SEM. (***p < 0.001; n=3). **(B)** Western blot analysis of Smad4 protein levels in untransduced (mock), control siRNA (RVsictrl) and Smad4 siRNA (RVsiSmad4) transduced preadipocytes. **(C)** qRT-PCR analysis of miR-155 expression in RVsictrl or RVsiSmad4 transduced preadipocytes with or without TGFβ1 treatment (5 ng/ml; 24 h). Untreated, RVsictrl transduced cells served as control. Data are presented as means ± SEM. (*p <0.05; n.s., not significant; n=3).

To investigate TGFβ1 expression during brown fat differentiation, cell culture supernatant was collected once every 2 days. ELISA was performed to measure TGFβ1 concentrations in the medium. Interestingly, we found that TGFβ1 was indeed expressed by brown preadipocytes and is regulated in a differentiation-dependent manner similar to miR-155 at the early stage of differentiation *in vitro* (Figure 29). Strongest induction of TGFβ1 in the medium was measured in the confluent/postconfluent phase of brown adipogenesis at day -2 to day 0, around the time-point of maximal miR-155 expression, followed by a significant decline after cells have entered differentiation phase (day 0 to day 4) (Figure 29).

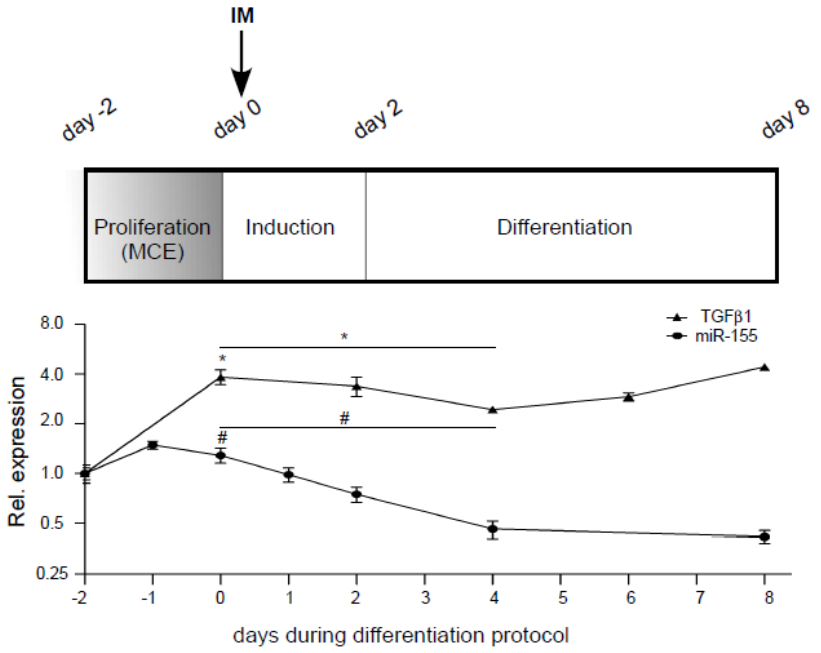

Figure 29. TGFβ1 relative protein concentrations in the cell culture supernatant and intracellular miR-155 expression were measured by ELISA and qRT-PCR during the time course of *in vitro* brown fat cell differentiation. Both values at day-2 were set as one, data are represented as means ± SEM; (*p < 0.05; n=3 in TGFβ1assay; d #p< 0.05; n=5 in miR-155 assay).

These findings were supported by additional analysis with the TGFβ type 1 receptor inhibitor SB-431542 (Inman et al., 2002). 10µM SB-431542 were used for treatment of preadipocytes at the proliferation stage (day -2 to day 0), followed by the regular differentiation procedure. miR-155 expression was measured by qRT-PCR. The data indicated that inhibition of TGFβ1 signaling clearly reduced miR-155 levels and abrogated its induction in proliferating brown preadipocytes (Figure 30).

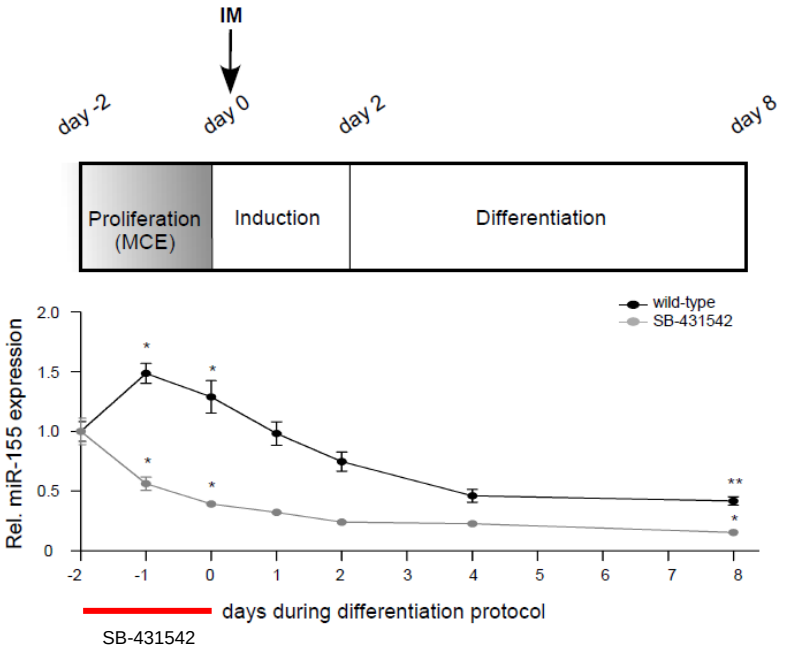

Figure 30. qRT-PCR analysis of miR-155 expression in untreated (black line) or SB-431542 (TGFβ1 receptor inhibitor; 10 µM, 48 h, gray line) treated brown fat cells during *in vitro* differentiation (normalized to snoRNA202 expression). Undifferentiated cells of the respective group at day-2 were set as one. Data are represented as means ± SEM. (*p < 0.05; **p < 0.005; n.s., not significant; n=5).

Moreover, SB-431542 treatment not only reduced miR-155 levels (Figure 31A), but also resulted in enhanced *in vitro* adipogenesis and lipid accumulation (Figure 31B). These pro-adipogenic effects of inhibition of TGFβ-signaling were clearly abolished in LVmiR155-expressing cells indicating that miR-155 is a crucial downstream-effector of TGFβ signaling in brown adipogenesis (Figure 31C).

As previously shown, TGFβ1 shows a similar expression pattern during differentiation as miR-155, with highest expression levels at proliferation stage (Figure 30). Therefore, I aimed to prove that miR-155 is significantly regulated by the TGFβ1 signaling pathway at the proliferative stage to excert its negative effect on brown fat differentiation. Inhibition of the TGFβ1 pathway by SB-431542 was performed at different stages of brown fat differentiation as indicated in Figure 31D.

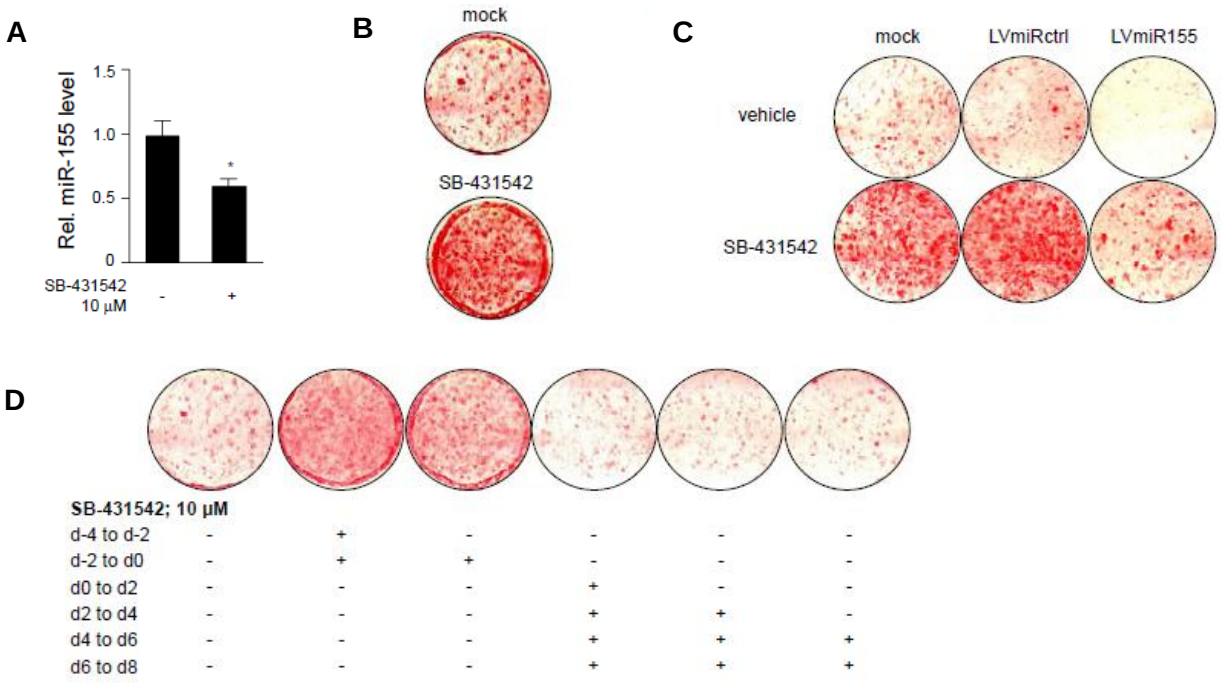

Figure 31. (A) Effect of the TGFβ1 receptor inhibitor SB-431542 (10 µM, 24 h) on miR-155 expression as measured by qRT-PCR (normalized to snoRNA202). Data are represented as means ± SEM (*p < 0.05 as compared to untreated controls; n=3). **(B)** Oil Red O staining of *in vitro* differentiated brown adipocytes treated with SB-431542 (10µM, day -2 to day 0); mock, untreated cells. **(C)** Oil Red O staining of fully differentiated brown adipocytes infected with LVmiRctrl or LVmiR155 and treated with vehicle or SB-431542 (10 µM, day -2 to day 0); mock, uninfected cells; vehicle, distilled water. **(D)** Oil Red O staining (day 8) of brown fat cells treated with 10 µM SB-431542 at indicated time points during *in vitro* differentiation.

Fully differentiated BAT cells were stained with Oil Red O. The staining shows that the most prominent effects of SB-431542 on differentiation were observed with treatment between day -4 to day 0, as well as between day -2 to day 0. However, stimulation with SB-431542 at day 0, when BAT cells were already post-confluent and entering differentiation phase had no obvious effect. This result correlates with the time-point of TGFβ1-mediated induction of miR-155 (from day -2 to day 0).

Thus, this study indicates that the TGFβ1 signaling pathway is a major driver of miR-155 expression in brown preadipocytes.

3.5 miR-155 and C/EBPβ constitute a bistable loop that regulates brown adipocyte differentiation

3.5.1 C/EBPβ regulates the *miR-155* promoter in brown adipocytes

To identify mechanisms that -apart from TGFβ1- might be involved in miR-155 transcriptional regulation in brown fat cells, we examined the miR-155 promoter sequence for transcription factor binding sites. miR-155 is processed from a primary mRNA-coding transcript, the B-cell integration cluster (*BIC*) (Eis et al., 2005; Yin et al., 2008). Computational analysis of the *BIC*/miR-155 promoter sequence revealed few putative C/EBP binding motifs (Figure 32) indicating that miR-155 might be regulated by C/EBPs or even by its own target: C/EBPβ through a feedback mechanism.

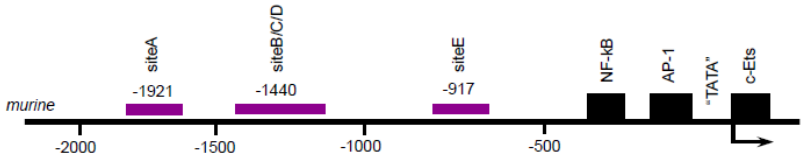

Figure 32. Scheme of the 2 kb murine *BIC/miR-155* promoter with the putative C/EBP binding sites (siteA, siteB/C/D, and siteE) (purple)

In order to address this hypothesis, the expression of both C/EBPβ and miR-155 was "traced" through the whole *in vitro* differentiation procedure. The protein level of C/EBPβ was almost undetectable in preadipocytes. However, C/EBPβ was strongly induced by the adipogenic cocktail (IM) applied at day 0, which corresponds to the time point when miR-155 expression is beginning to decrease (Figure 33). In accordance with the shift of the cells from proliferation to differentiation state, the expression of C/EBPβ was induced while miR-155 was gradually reduced.

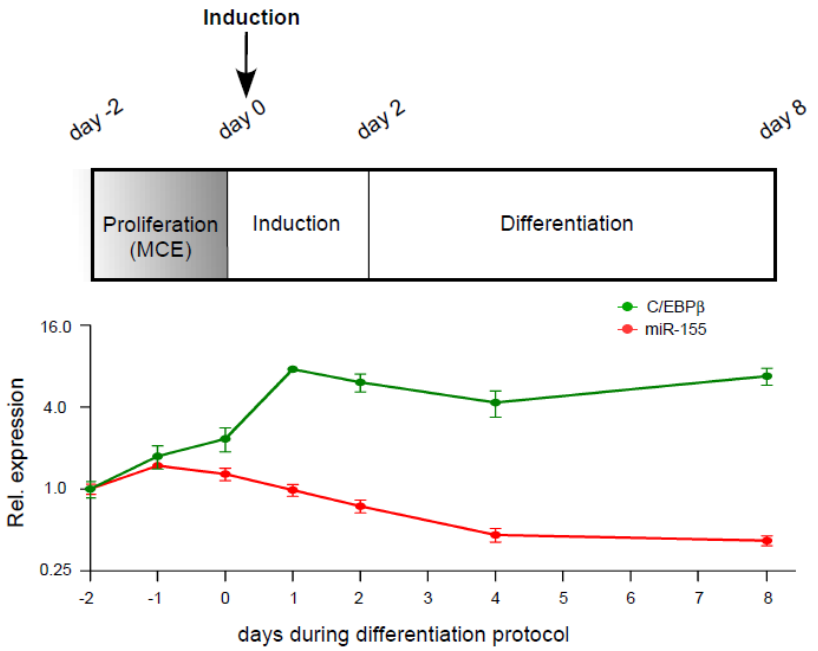

Figure 33. C/EBPβ protein and miR-155 expression were measured by Western-blot and qRT-PCR throughout the brown fat cell differentiation process. Both values at day -2 were set as one; data are represented as means ± SEM.

To further elucidate the role of C/EBPβ in miR-155 expression, gain-of-function experiments were performed: Overexpression of C/EBPβ in brown preadipocytes caused a dramatic downregulation of miR-155 levels as compared to controls (Figure 34A). Next, we used *BIC*/miR-155 promoter luciferase reporter constructs, to analyze transcriptional regulation of miR-155 by C/EBPs in more detail. Lipofectamine transfection of 2 µg C/EBPs (C/EBPα, C/EBPβ, or C/EBPδ) for 48 h led to a strong inhibition of *BIC*/miR-155 promoter activity in HIB-1B cells. Among the C/EBPs, C/EBPβ had the most pronounced effect on the promoter activity (Figure 34B). The same is true, when using 200 ng RTase Lentivirus of the C/EBPβ construct (LVC/EBPβ) to transduce HIB-1B cells (generating a stable C/EBPβ-expressing cell line): *BIC*/miR-155 promoter activity was significantly reduced (Figure 34C). In contrast, siRNA-mediated knock-down of C/EBPβ (siC/EBPβ) (Birsoy et al., 2008) caused a significant increase in miR-155 expression in BAT-cells (Figure 34D, E). These data indicated that C/EBPβ transcriptionally inhibits miR-155 expression.

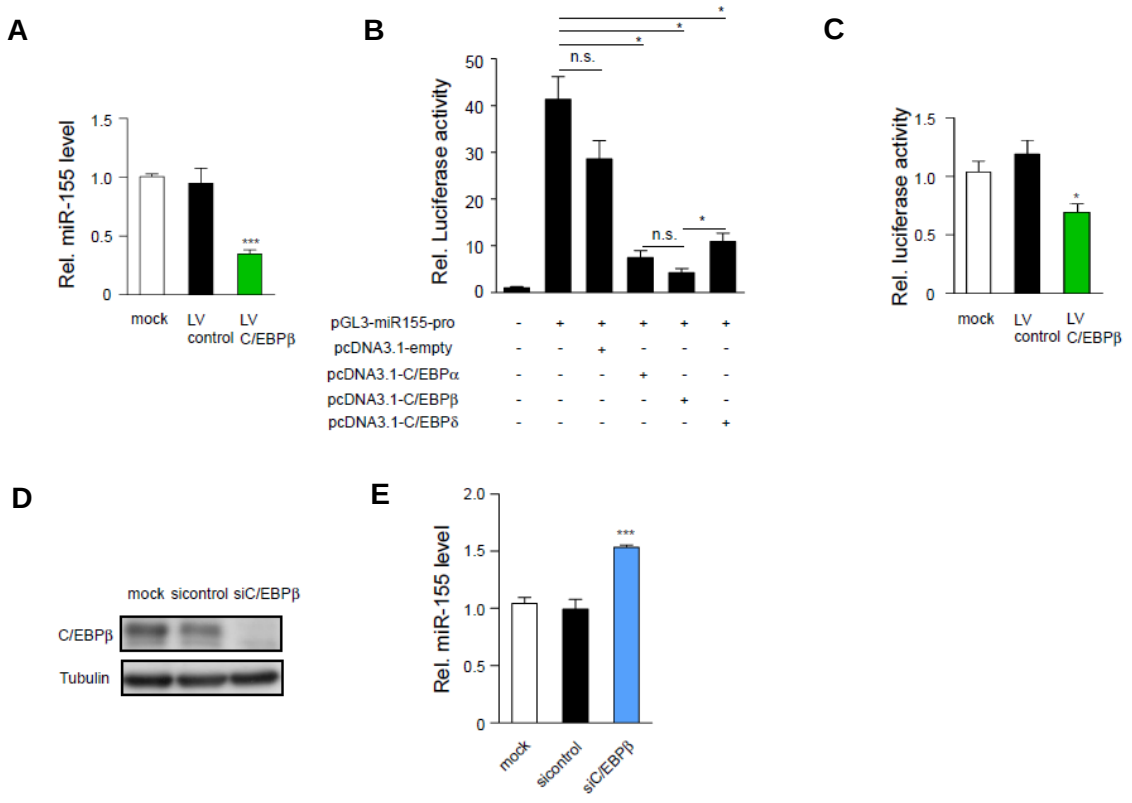

Figure 34. (A) qRT-PCR analysis of miR-155 expression (normalized to sno202) in cells transduced with LVC/EBPβ or control virus (LVcontrol). Untreated controls (mock) were set as one; data are represented as means ± SEM. (***p <0.001; n=3). (**B**) Luciferase assay to analyze regulation of the *BIC/miR-155* promoter by C/EBPs. HIB-1B cells were co-transfected with C/EBPα, C/EBPβ, or C/EBPδ expression vectors and the BIC/miR-155 promoter luciferase construct. Untransfected cells were set as one; data are represented as means ± SEM. (*p <0.05; n=3) **(C)** Luciferase assay to analyze regulation of the *BIC/miR-155* promoter by C/EBPβ. Cells were infected with LVcontrol or LVC/EBPβ 48 h prior to the *BIC/miR-155* promoter luciferase construct transfection. Uninfected controls (mock), transfected with the same reporter construct were set as one; data are represented as means ± SEM. (*p <0.05; n=4). (**D**) Western blot analysis of C/EBPβ expression in preadipocytes 48 h post transduction with sicontrol (control-siRNA) or siC/EBPβ (C/EBPβ-siRNA). (**E**) qRT-PCR analysis of miR-155 levels in preadipocytes 48 h after transduction with sicontrol or siC/EBPβ. miR-155 levels were normalized to snoRNA202; untransduced cells were set as one. Data are presented as means ± SEM (***p < 0.001; n=3).

To further characterize the transcriptional regulation of miR-155 by C/EBPβ, Chromatin Immunoprecipitation (ChIP) assays were performed. Five putative C/EBP binding sites (siteA, siteB, siteC, siteD, and siteE) were identified in the *BIC*/miR-155 promoter sequence by using computational prediction software (http://www.cbrc.jp/research/db/TFSEARCH.html) (Figure 35

top). To identify which binding motif is the major binding site for C/EBPβ in BAT cells, brown preadipocytes were transduced with LVcontrol or LVC/EBPβ for 48 h, followed by chromatin immunoprecipitation assays with C/EBPβ-specific antibodies (ChIP-assay). The ChIP assay revealed a significant enrichment of the siteE containing promoter fragment in C/EBPβ-antibody pull-downs and thus identified the distal siteE in the *BIC*/miR-155 promoter as the critical binding site for C/EBPβ (Figure 35 bottom).

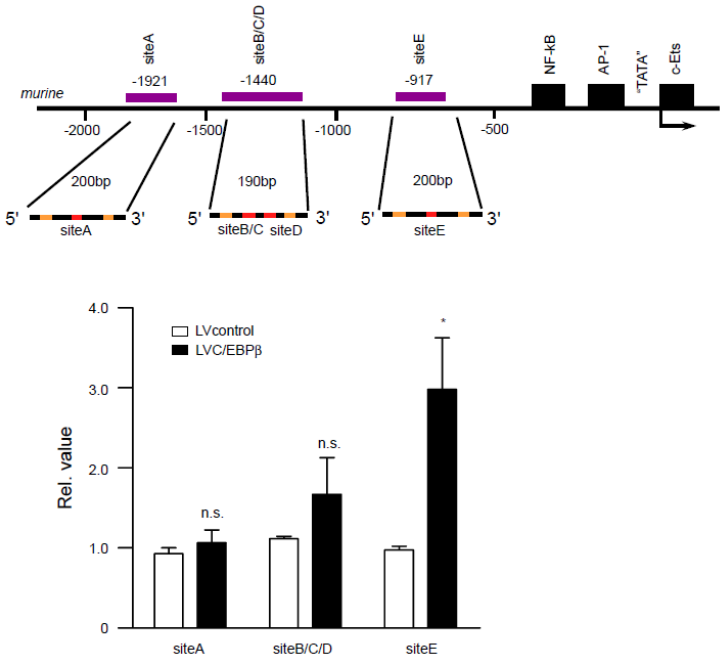

Figure 35. Chromatin immunoprecipitation assay (ChIP) in brown preadipocytes transduced with LVcontrol or LVC/EBPβ 48 h prior the assay. Precipitation was performed with an anti-C/EBPβ antibody or IgG and PolII control antibodies. C/EBPβ bound *BIC/miR-155* promoter fragments were amplified using qRT-PCR primers that span putative binding sites A, B/C/D, or E respectively. Results are normalized to input values. Relative values are represented as means ± SEM. (*p <0.05; n.s., not significant; n=3).

Taken all together, these data indicate that miR-155 in brown adipocytes is regulated by its own major target: C/EBPβ. C/EBPβ interaction with the *BIC/miR-155* promoter resulted in transcriptional repression of miR-155 in BAT cells. Thus, to evidence that miR-155 and C/EBPβ may form a novel bio-stability in the regulation of brown adipocyte differentiation, the further experiments were performed.

Such feedback loops are important in developmental transcriptional regulation and are known to exhibit a bistable behavior (Flynt and Lai, 2008).

3.5.2 miR-155 and C/EBPβ form a negative feed-back loop which regulates brown adipocyte proliferation versus differentiation

To further analyze whether miR-155 and C/EBPβ form a feed-back loop and regulate each other in a direct, dose-dependent manner, preadipocytes were infected with increasing amounts of lentiviruses either expressing miR-155 or C/EBPβ. Stepwise increase in miR-155 levels (Figure 36A) resulted in a dose-dependent reduction of C/EBPβ (Figure 36B). On the other hand, increasing the abundance of C/EBPβ to levels observed after induction of brown fat differentiation with adipogenic hormones resulted in a dose-dependent reduction of miR-155 (Figure 36C, D).

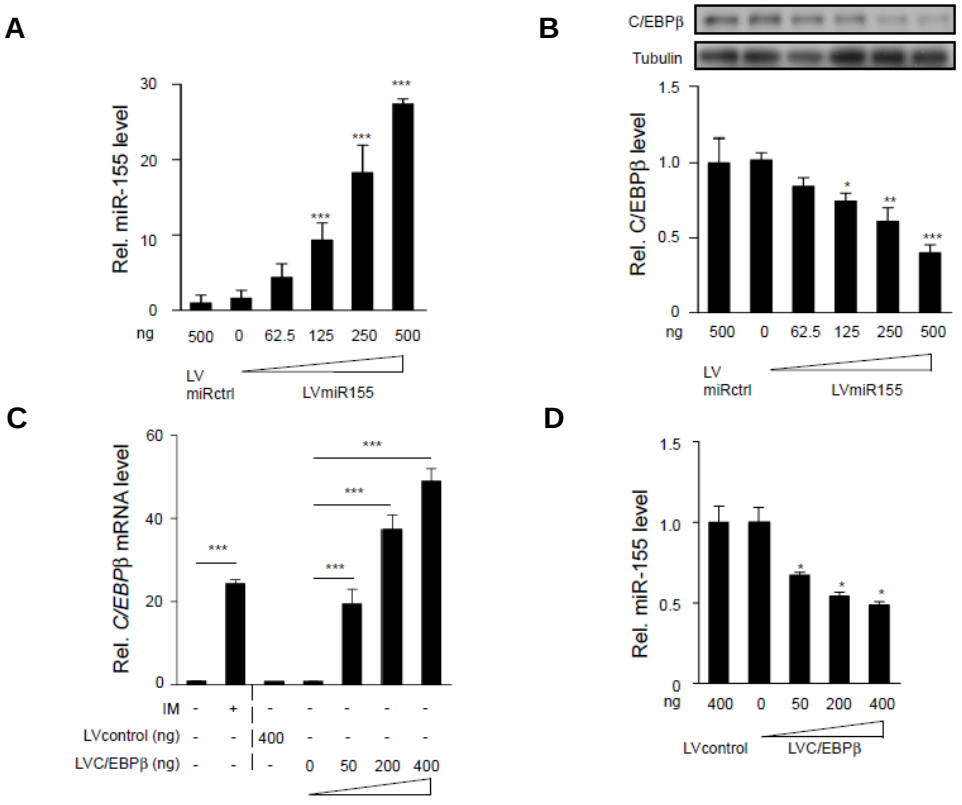

Figure 36. (A) qRT-PCR analysis of miR-155 expression levels in preadipocytes transduced with LVmiRctrl or different amounts of LVmiR155. Data are normalized to sno202 expression, untreated cells

were set as one; data are presented as means ± SEM (***p < 0.001; n=3). **(B)** Western-blot analysis of C/EBPβ protein levels in preadipocytes 48 h post transduction with LVmiRctrl or LVmiR155 (top). Quantification of C/EBPβ protein levels (bottom). Data were normalized to Tubulin; untreated cells were set as one; data are presented as means ± SEM (*p < 0.05; **p < 0.01; ***p < 0.001; n=3). **(C)** qRT-PCR analysis of C/EBPβ mRNA levels in preadipocytes transduced with LVcontrol or LVC/EBPβ as indicated, or stimulated with induction medium (IM) for 8 h Expression was normalized to HPRT; untransduced cells were set as one; data are presented as means ± SEM (***p < 0.001; n=3). **(D)** qRT-PCR analysis of miR-155 expression levels in preadipocytes transduced with LVcontrol or LVC/EBPβ. miR-155 levels were normalized to snoRNA202; untransduced cells were set as one. Data are presented as means ± SEM (*p < 0.05; n=3).

To better understand the relevance of this reciprocal inhibition, we analyzed the influence of miR-155 and C/EBPβ on the differentiation state of brown fat cells. miR-155 overexpression correlated with decreased cellular TG content and enhanced proliferation in BAT cells (Figure 37A). In contrast, C/EBPβ overexpression had the opposite effects resulting in strongly increased TG levels and significant reduction of proliferation (Figure 37B). In both approaches, TG levels and proliferation rates were regulated in a clearly LVmiR155/ LV/CEBPβ dose-dependent manner.

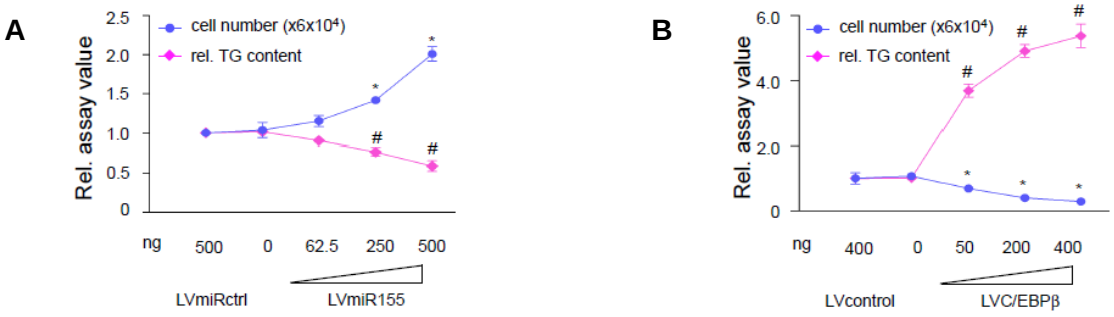

Figure 37. TG content and cell number of brown adipocytes transduced with different doses of **(A)** LVmiR155 (0 ng, 62.5 ng, 250 ng, 500 ng RTase/well in 6-well plates) or **(B)** LVC/EBPβ (0 ng, 50 ng, 200 ng, 400 ng RTase/well in 6-well plates). TG content was normalized to total protein concentration. LVmiRctrl transduced cells were set as one. All data are represented as means ± SEM. (#p <0.05; n=3 in TG assay, *p <0.05; n=3 in proliferation assay).

Preadipocyte factor 1 (Pref-1), a trans-membrane protein highly expressed in undifferentiated preadipocytes (Wang and Sul, 2009), was highly expressed in miR-155 overexpressing cells (Figure 38A, B). In contrast, cells with low miR-155 (Figure 38A) or high C/EBPβ levels (Figure 38B) displayed strongly reduced Pref-1 abundance.

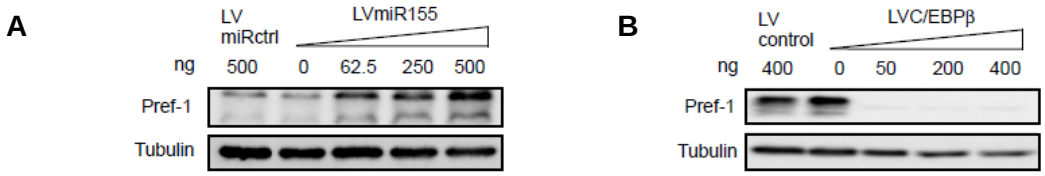

Figure 38. Western-blot analysis of Pref-1 expression in preadipocytes transduced with **(A)** LVmiRctrl and LVmiR-155 or **(B)** LVcontrol and LVC/EBPβ at different dosages. Tubulin served as loading control.

Taken all these data together, these data indicate that miR-155 and C/EBPβ constitute a bistable system/loop that either maintains preadipocytes in a proliferative, undifferentiated stem cell state or initiates the brown adipogenic differentiation and thermogenesis program.

3.6 miR-155 inhibits brown fat differentiation *in vivo*

To study the function of miR-155 *in vivo*, we generated transgenic mice overexpressing miR-155 under control of the ubiquitous phosphoglycerate kinase (*PGK*) promoter (miR155TG) (Figure 39) using lentiviral transgenesis (Lois et al., 2002; Pfeifer et al., 2002).

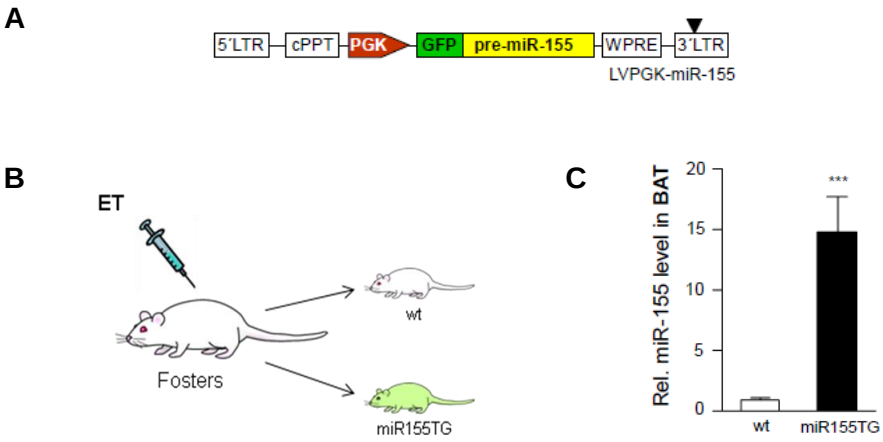

Figure 39. (A) Schematic representation of the lentiviral construct (LVPGK-miR-155) used for generation of miR-155 transgenic animals. LTR, long terminal repeat; cPPT, central polypurine tract; PGK, phosphoglycerate 1 promoter; GFP, green fluorescent protein; pre-miR155, precursor miR-155; WPRE, woodchuck hepatitis responsive element; triangle, self-inactivating mutation. **(B)** miR-155 transgenic embryos mixed with wt embryos were transplanted **(ET)** to foster mice **(C)** qRT-PCR analysis of miR-155 expression levels in the interscapular brown adipose tissue (BAT) from one week old wt or miR-155 transgenic (miR155TG) mice, generated by transduction of preimplantation embryos with LVPGK-miR-155. miR-155 levels were normalized to snoRNA202. Data of wt were set as one; data are represented as means ± SEM (***$P < 0.001$, n=3).

One week old miR155TG animals displayed significantly reduced size and weight of BAT compared to their wt littermates (Figure 40A, B). Hematoxylin and eosin (H&E) staining on BAT revealed that the size and number of lipid droplets in interscapular BAT of miR155TG were clearly reduced, similar to the *in vitro* situation (Figure 40C). This finding corresponded with a significantly reduced TG content (Figure 40D) and reduced expression of the key adipogenic and thermogenic factors (Figure 40E, F).

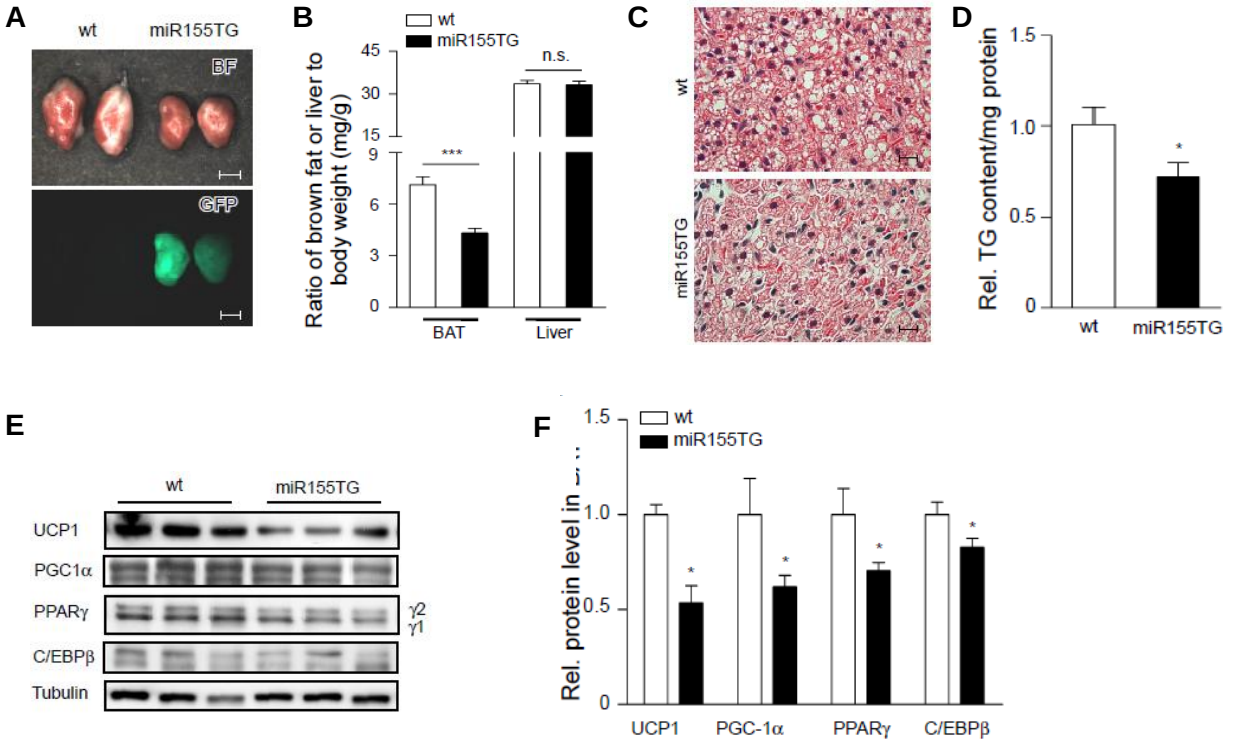

Figure 40. (A) Interscapular brown adipose tissue isolated from one week old wt or LVPGKmiR155 transgenic mice. Shown are bright field (left) and fluorescent images (right); GFP is co-expressed with miR-155 in transgenic mice; (scale bar = 2 mm). **(B)** Ratios of interscapular BAT and liver weight to total body weight of one week old wt and miR155TG mice. Data are presented as means ± SEM (***P < 0.001; ns: not significant; wt group n=6, miR155TG group n=6). **(C)** Hematoxylin and eosin staining of BAT sections from one week old wt and miR-155TG littermates; (scale bar, 15 µm). **(D)** TG content of interscapular BAT isolated from one week old wt or miR155TG mice. TG content was normalized to total protein concentration of lysates. wt was set as one, and data are represented as means ± SEM (*p <0.05;**p <0.01 n=3). **(E)** Western Blot analysis of UCP1, PGC-1α, PPARγ and C/EBPβ expression in BAT isolated from one week old wt and miR-155TG littermates; each protein levels from three representative animals per group are shown. Tubulin served as loading control. **(F)** Densitometric quantification of UCP1, PGC-1α, PPARγ and C/EBPβ expression levels, normalized to tubulin. Data of the wt group were set as one. Data are represented as means ± SEM (*p <0.05; n=6).

Remarkably, miR155TG mice displayed a significant reduction of BAT–derived thermogenesis as measured by infrared thermography (Haas et al., 2009; Hodges et al., 2008). Interscapular surface temperature of one week old pups was 1.5°C± 0.9°C lower in miR155TG mice compared to wt animals (Figure 41 A, B).

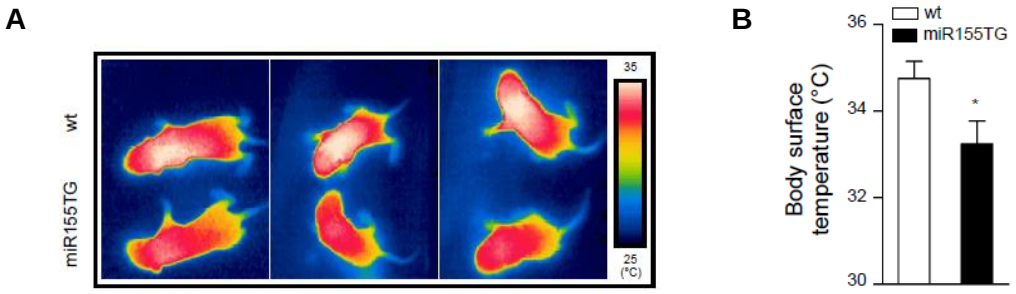

Figure 41. (A) Infrared thermographic analysis of the body surface temperature in four day old wt and miR155TG littermates. Three representative pairs are shown. **(B)** Statistical analysis of body surface temperature in wt and miR155TG littermates; wt: 34.75±0.39°C; miR155TG: 33.24±0.53°C. Data are represented as means ± SEM. (*p <0.05; n=5).

Also at 10 weeks of age, miR155TG mice exhibited a significantly reduced interscapular BAT mass and clearly lower levels of thermogenic markers in BAT. In contrast, size and weight of inguinal WAT and visceral WAT were not affected by miR-155 overexpression (Figure 42A, B, C), albeit similar levels of miR-155 expression were reached in WAT and BAT (Figure 42D, E). miR155TG animals do not show significant alterations in body weight or food intake (Figure 42F, G). These data indicate a preferential effect of miR-155 on BAT development, which is reminiscent of the alterations observed in C/EBPβ-deficient mice (Tanaka et al., 1997).

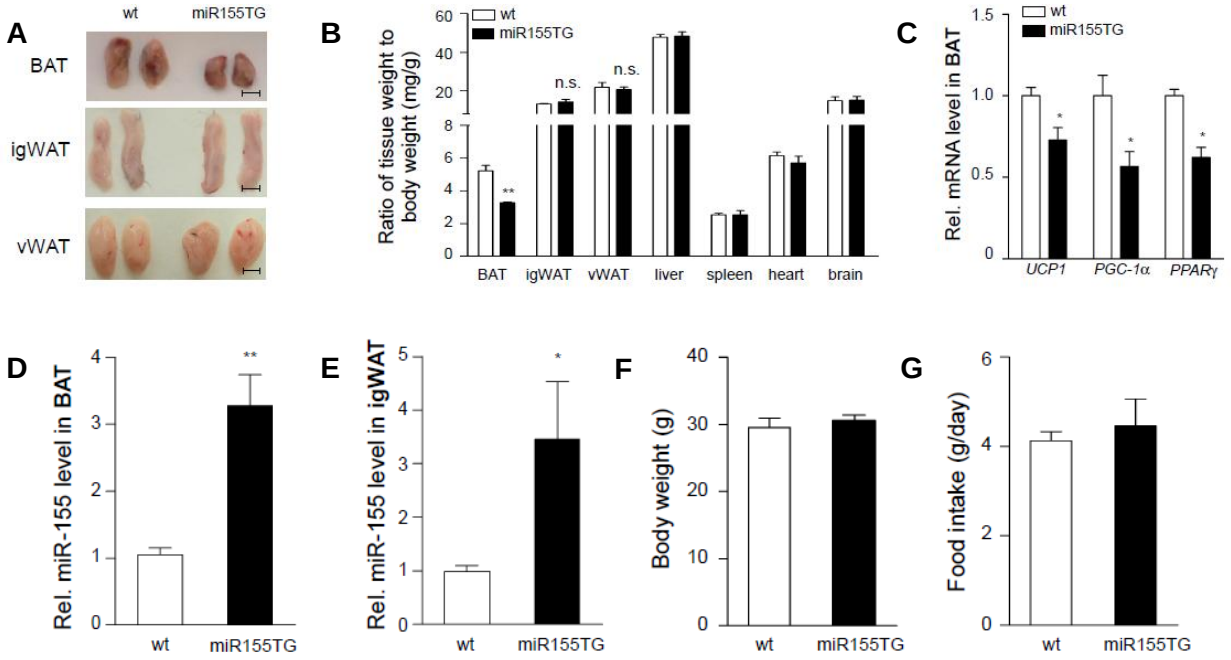

Figure 42. (A) Interscapular brown adipose tissue (BAT) (scale bar = 3 mm), inguinal white adipose tissue (igWAT), and visceral white adipose tissue (vWAT) (Scale bar = 4 mm) were isolated from ten week old wt or miR155TG littermates. Two representative littermates are shown. **(B)** Statistics of BAT, igWAT, vWAT, spleen, heart, brain and liver weights relative to total body weight in ten week old wt and miR155TG littermates. Data are presented as means ± SEM (*p <0.05; **p <0.01; n.s., not significant; wt group n=3, miR155TG group n=3). **(C)** qRT-PCR analysis of brown thermogenic/adipogenic genes in interscapular BAT of wt or miR155TG littermates at ten weeks of age: *UCP1*, *PGC-1α*, *PPARγ.* Data are presented as means ± SEM (*p <0.05; **p <0.01; n.s., not significant; wt group n=3, miR155TG group n=3). (**D, E**) qRT-PCR analysis of miR-155 expression levels in (**D**) interscapular BAT, or in (**E**) igWAT from ten week old wt or miR155TG mice. miR-155 levels were normalized to snoRNA202. wt was set as one; data are represented as means ± SEM (*p <0.05;**p <0.01 n=3). (**F**) Body weight and (**G**) daily food intake of wt and miR155TG littermates at 10-13 weeks of age (wt group n=5, miR155TG group n=9).

To study whether the observed phenotype in BAT is cell-autonomous, we generated an additional, BAT-specific mouse model using the *UCP1* promoter to drive miR-155 expression (LVUCP1miR155) (Figure 43A). Transduction of brown preadipocytes with LVUCP1miR155 clearly reduced *in vitro* differentiation demonstrating the functionality of the UCP1-miR-155 construct in brown fat cells (Figure 43B). One week old LVUCP1miR155 transgenic animals (Figure 43C), showed a phenotype very similar to the miR155TG mice with ubiquitous miR-155 expression: Body surface temperature and BAT weight were significantly decreased (Figure 43D, E). In addition, size and number of lipid droplets in BAT (Figure 43F), as well as expression of

PPARγ and UCP1 were clearly reduced (Figure 43G, H). Thus, both transgenic animal models demonstrate that miR-155 overexpression *in vivo* impairs BAT function.

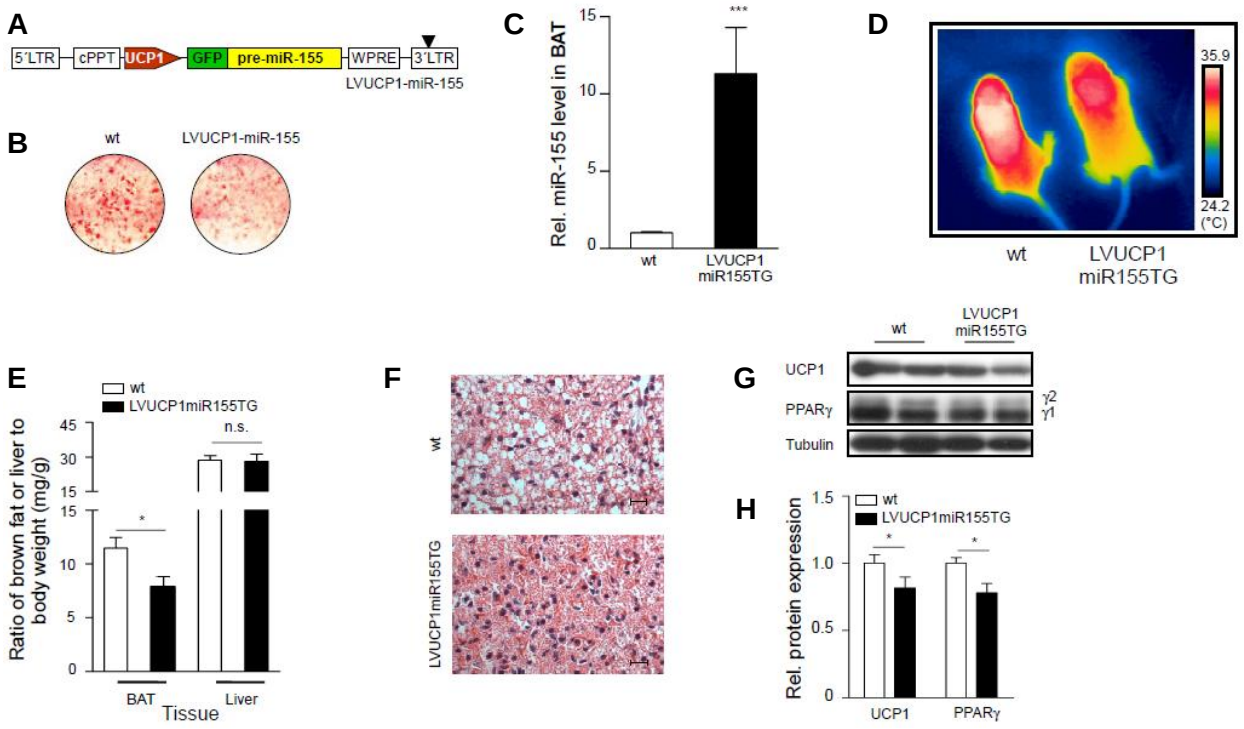

Figure 43. (**A**) Schematic representation of the lentiviral construct (LVUCP1miR155) for brown fat-specific expression of miR-155. LTR, long terminal repeat; cPPT, central polypurine tract; UCP1, uncoupling protein 1 promoter; GFP, green fluorescent protein; pre-miR-155, precursor miR-155; WPRE, woodchuck hepatitis responsive element; triangle, self-inactivating mutation. (**B**) Oil Red O staining of differentiated brown adipocytes transduced with LVUCP1-miR-155 as compared to wt cells. (**C**) qRT-PCR analysis of miR-155 expression levels in one week old wt and miR-155 transgenic (LVUCP1miR155TG) mice generated by transduction of preimplantation embryos with LVUCP1miR155. miR-155 levels were normalized to snoRNA202. Data are represented as means ± SEM. (***p < 0.001; wt group n=7, LVUCP1miR155TG group n=7). (**D**) Body surface temperature of wt and LVUCP1miR155TG mice was measured by infrared thermography. (**E**) Ratios of BAT and liver weight versus total body weight. Data are represented as means ± SEM. (*p < 0.05; n.s., not significant; wt group n=7, LVUCP1miR155TG group n=7). (**F**) Hematoxylin and eosin staining of BAT sections from one week old wt and LVUCP1miR155TG littermates; (scale bar, 15 µm). (**G**) Western Blot analysis of UCP1 and PPARγ protein levels in BAT isolated from wt and LVUCP1miR155TG littermates. Tubulin served as loading control. 2 representative pairs are shown. (**H**) Densitometric quantification of Western blot analysis (right). Proteins expression was normalized to Tubulin. Data are presented as means ± SEM. (*p < 0.05; wt group n=7, LVUCP1miR155TG group n=7).

3.7 Role of miR-155 in white adipocytes

3.7.1 miR-155 regulates white adipocyte "browning" *in vitro*

To assess the effects of miR-155 on white fat cells, we isolated SVF cells from murine inguinal WAT of 10-12 weeks old wt male mice and overexpressed miR-155 using three different concentrations of LVmiR155 (60, 180 and 500 ng RTase per well in 6 well-plates). In addition, we knocked-down miR-155 with the "sponge" construct and used siC/EBPβ to analyze directly the effect of C/EBPβ. Overexpression of miR-155 at high levels (500 ng RTase) (Figure 44A) significantly reduced lipid-droplet accumulation, TG-content (Figure 44B, C), and adipogenic marker (*aP2*, *PPARγ*, and *C/EBPα*) levels in white adipocytes (Figure 44D), whereas transduction with LVmiRS155 resulted in enhanced differentiation (Figure 44A-D). Interestingly, we not only found regular adipogenic markers, but also thermogenic markers regulated by miR-155: UCP1, the major brown fat specific marker, was strongly enhanced by knock-down of miR-155 even in WAT cells (Figure 44E). Therefore, we proceeded to study the crucial role of miR-155 in WAT cells and its possible role in "browning".

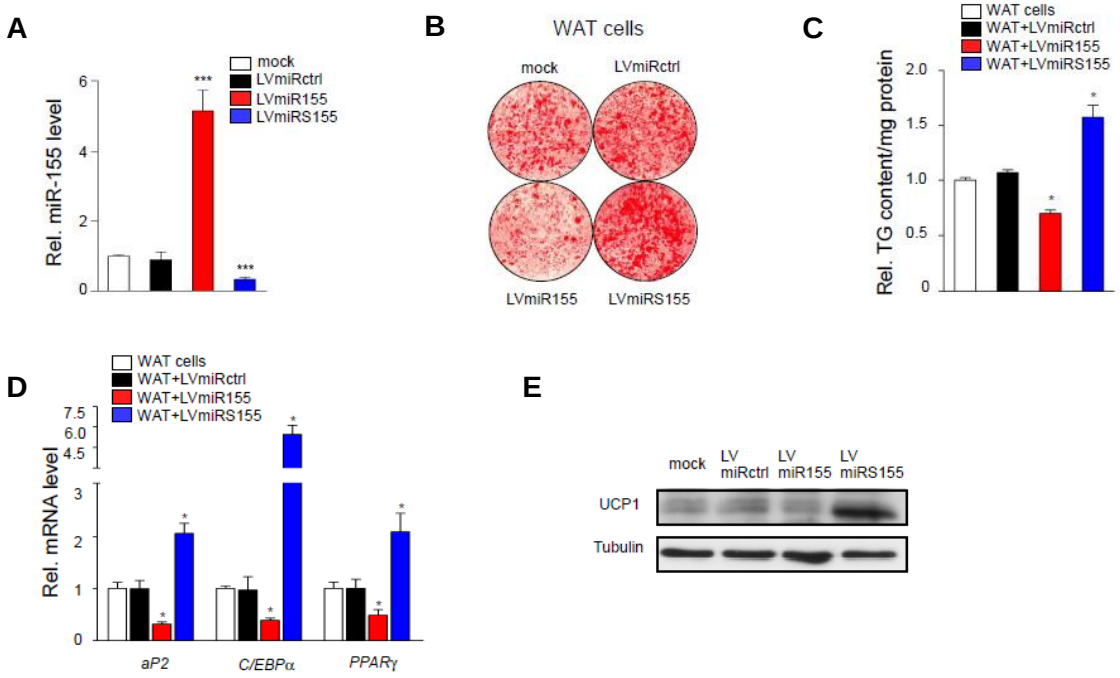

Figure 44. (A) qRT-PCR analysis of miR-155 expression levels in LVmiRctrl, LVmiR155 or LVmiRS155 transduced white preadipocytes (normalized to snoRNA202). Untransduced cells (mock) were set as one. Data are represented as means ± SEM (***p <0.001; n=3). **(B)** Oil Red O staining of fully differentiated white adipocytes (WAT) overexpressing miR-155 (LVmiR155) or an anti-miR-155

sponge (LVmiRS155) as compared to cells carrying a control scrambled miRNA (LVmiRctrl); mock, uninfected cells. **(C)** TG content of fully differentiated white adipocytes transduced with LVmiRctrl, LVmiR155, and LVmiRS155; mock, uninfected control. TG content was normalized to total protein concentration. Untreated cells were set as one. Data are represented as means ± SEM. (*p <0.05; ***p <0.001; n=3). **(D)** qRT-PCR analysis of *aP2, C/EBPα,* and *PPARγ* mRNA in fully differentiated white adipocytes transduced with indicated lentiviruses. Untreated cells were set as one. Data are presented as mean±SEM (*p <0.05; n=3). (**E**) Western Blot analysis of UCP1 protein levels in LVmiRctrl, LVmiR155 or LVmiRS155 transduced fully differentiated white adipocytes at day 9. Tubulin served as loading control.

Given the prominent effect of miR-155 on the development of the thermogenic program in brown adipocytes, we examined whether miR-155 might also have similar effects in WAT progenitors. Importantly, inhibition of endogenous miR-155 dramatically induced expression of *UCP1* more than 20-fold (Figure 45). Remarkably, the increase in *UCP1* expression induced by the miR-155 sponge was even higher than the effect of norepinephrine (NE), a well-known inducer of "browning" (Cinti, 2009), and was identical to the effect of C/EBPβ overexpression (Figure 44). *PGC-1α* and *Cidea* were almost undetectable in mature WAT cells; however, both were significantly increased by knock-down of miR-155. In contrast, transduction with LVmiR155 further decreased the already low expression levels of *UCP1* in mature WAT cells (Figure 45).

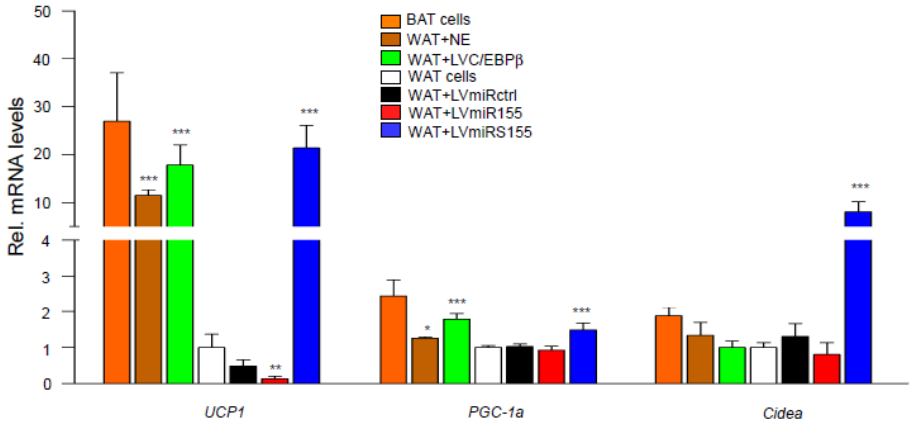

Figure 45. qRT-PCR analysis of *UCP1*, *PGC-1α* and *Cidea* mRNA levels in differentiated white adipocytes transduced with LVC/EBPβ, LVmiR155, LVmiRS155, LVmiRctrl or treated with 5 μM norepinephrine (NE). Differentiated BAT cells were used as positive control. Untreated white fat cells were set as one. Data were normalized to *HPRT* housekeeping gene expression and are represented as means ± SEM. (*p <0.05; **p <0.01; ***p <0.001; n=3).

3.7.2 miR-155 and C/EBPβ are specific regulators in brown adipocyte differentiation

To address the question, whether the miR-155/C/EBPβ circuit is of general relevance for both brown and white fat differentiation, or if this interaction is rather specific for brown fat, we performed also transduction experiments at low- and medium-dose of LVmiR155 in BAT and WAT-derived adipocytes (Figure 46A-D). In parallel, we performed low- and medium-dose knock-down experiments with LVsiC/EBPβ, as well as LVmiRS155.

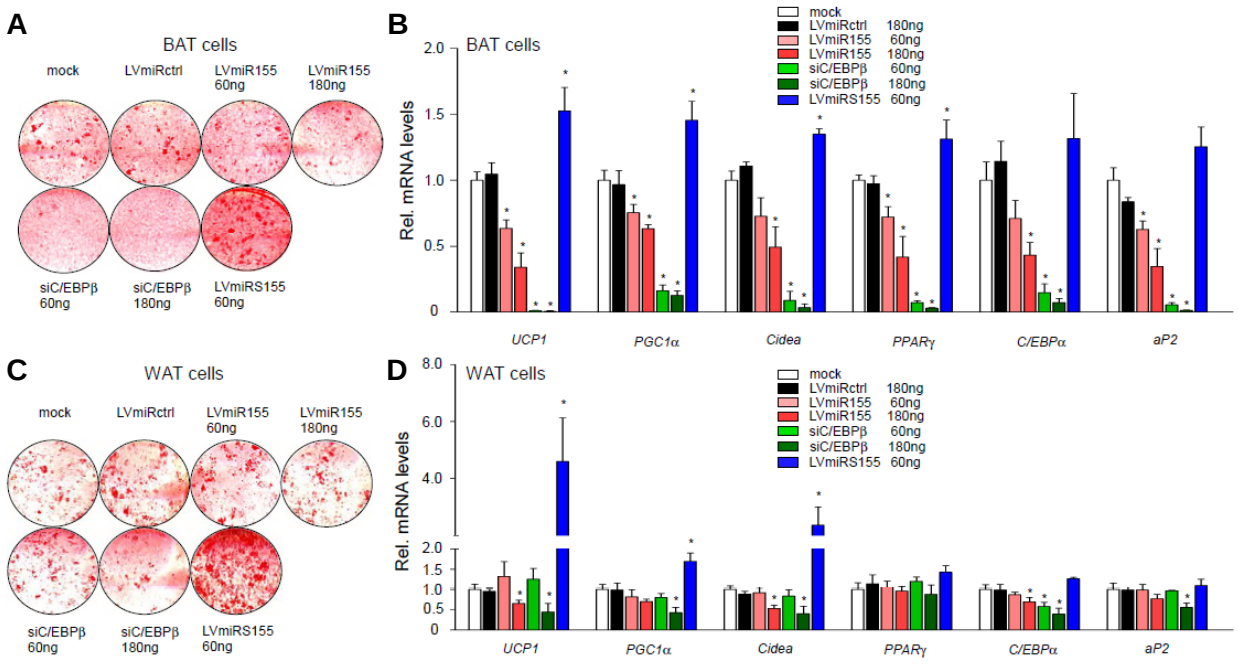

Figure 46. (A, B) Oil Red O staining **(A)** and qRT-PCR analysis **(B)** of *UCP1, PGC-1α, Cidea*, *PPARγ*, *C/EBPα,* and *aP2* mRNA of brown adipocytes transduced with a low (60 ng) or medium (180 ng) dosage of control-miR (LVmiRctrl), miR-155 (LVmiR155) or anti-C/EBPβ siRNA (siC/EBPβ), or low dosage of anti-miR-155 sponge (LVmiRS155); mock, uninfected cells. Uninfected cells were set as one. Expression data are normalized to *HPRT*, and data are represented as means± SEM. (*p <0.05; n=3). **(C, D)** Oil Red O staining **(C)** and qRT-PCR analysis **(D)** of *UCP1, PGC-1α, Cidea*, *PPARγ*, *C/EBPα,* and *aP2* mRNA of white adipocytes transduced with with a low (60 ng) or medium (180 ng) dosage of control-miR (LVmiRctrl), miR-155 (LVmiR155) or anti-C/EBPβ siRNA (siC/EBPβ), or low dosage of anti-miR-155 sponge (LVmiRS155); mock, uninfected cells. Uninfected cells were set as one. Expression data are normalized to *HPRT*, and data are represented as means± SEM. (*p <0.05; n=3).

In brown fat cells, we found a significant inhibition of differentiation already at the low dose (60 ng) of miR-155 with a 28% decrease in expression of PPARγ and reduced Oil Red O staining. The thermogenic program (as determined by measurement of *UCP1*, *PGC-1α* and *Cidea* levels) was also significantly suppressed by low levels of miR-155 (Figure 46A, B). In contrast, the low

concentration of miR-155 had no significant effect on any of the marker genes tested during white fat cell differentiation (Figure 46C, D). Accordingly, knock-down of C/EBPβ had a stronger striking impact on marker expression in brown versus white fat cells. The low concentration of siC/EBPβ reduced adipogenic as well as thermogenic markers by 83.7 to 98.9% in brown adipocytes, but had no significant effect in white adipocytes (Figure 46A-D).

The medium dose (180 ng) of miR-155 caused a significant reduction of the thermogenic marker gene expression, but was still not sufficient to significantly affect all adipogenic markers in white fat cells. siC/EBPβ significantly inhibited white adipocyte differentiation at medium concentrations (maximum suppression 55.6-60.1% at 180ng) (Figure 46D). The effects of medium dose siC/EBPβ were much more pronounced in brown fat cells resulting in a 87.1 to 99.3% reduction of marker gene expression (Figure 46B). All these data point towards higher sensitivity of brown adipocytes for miR-155- and C/EBPβ-dependent regulation and a predominant role of the miR-155/C/EBPβ interaction in brown fat.

Moreover, knocking-down miR-155 with low-dose sponge lentivirus, LVmiRS155, still enhanced thermogenic genes (*UCP1*, *PGC-1α* and *Cidea*) in brown adipocytes. Importantly, these thermogenic genes were also highly increased in low-dose LVmiRS155 treated white adipocytes.

Thus, taken all together, the data demonstrate that the miR-155/C/EBPβ regulatory feedback loop has a specific effect in brown adipocytes. Furthermore, knock-down of miR-155 reprograms white adipocytes to brown fat-like adipocytes which effect is similar to the C/EBPβ effect in the white fat cell line HIB-1B (Karamanlidis et al., 2007).

3.8 miR-155 regulates cold-induced thermogenesis in adipose tissue and "browning" of WAT *in vivo*

To analyze the effect of miR-155 suppression on WAT browning and BAT recruitment *in vivo*, we used *Bic/miR-155* knock-out (miR-155$^{-/-}$) mice (Thai et al., 2007). BAT activation was studied by exposing mice to cold (4°C, 4 h). BAT activity and interscapular body surface temperature was analyzed using infrared thermography, and core body temperature was

measured with a 4610 rectal thermometer. Interscapular temperature of miR-155$^{-/-}$ mice was significantly higher (38.4°C ± 0.66°C) as compared to the wt littermates (35°C ± 0.37°C) after cold exposure indicating that inducible thermogenesis of BAT is significantly increased in the absence of miR-155 (Figure 47A, B).

In addition, analysis of body core temperature revealed a significant difference between miR-155$^{-/-}$ and wt mice already at room temperature. After 4 h cold exposure, core temperature dropped by 3 ± 0.39 °C in wt but only 0.8 ± 0.3 °C in miR-155$^{-/-}$ mice (Figure 47C).

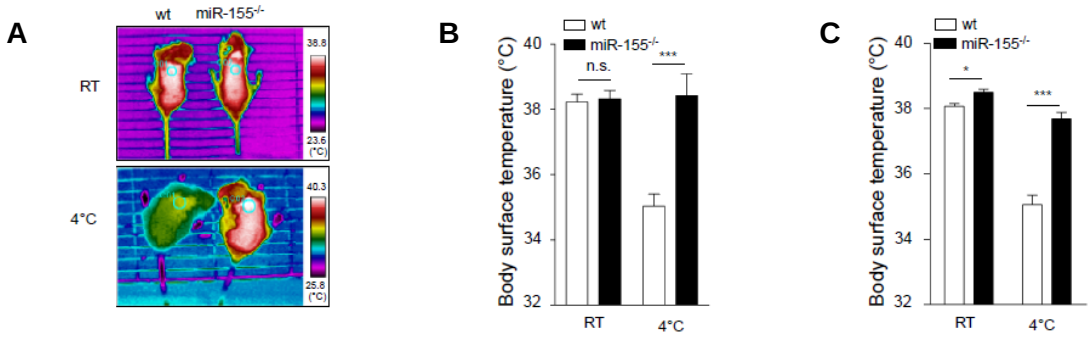

Figure 47. (A) Representative infrared thermographic image of 12-16 week old male wt and miR-155$^{-/-}$ littermates kept at 4°C for 4 h. **(B)** Statistical analysis of body surface temperature as measured by infrared thermography. Data are represented as means ± SEM. (*p <0.05; n.s., not significant; wt group n=7, miR-155$^{-/-}$ group n=5). **(C)** Statistical analysis of rectal body core temperature measurement of 12-16 weeks old wt, or miR-155$^{-/-}$ littermates exposed to either RT or 4 °C. Data are represented as means ± SEM (*p <0.05; ***p <0.001) (wt group n=14, miR-155$^{-/-}$ group n=12).

For a more detailed analysis, the animals were sacrificed and the organs and tissues were isolated. Analysis of BAT morphology revealed fewer lipid droplets in miR-155$^{-/-}$ mice after 4 °C treatment (Figure 48A). Exposure to cold increased lipolytic activity and cellular respiration to a greater extent in miR-155$^{-/-}$ mice than in wt mice (Figure 48B, C), which could explain the reduced lipid content of miR-155$^{-/-}$ BAT. Moreover, miR-155$^{-/-}$ mice exhibited increased expression of *UCP1* and *PGC-1a* (Figure 48D).

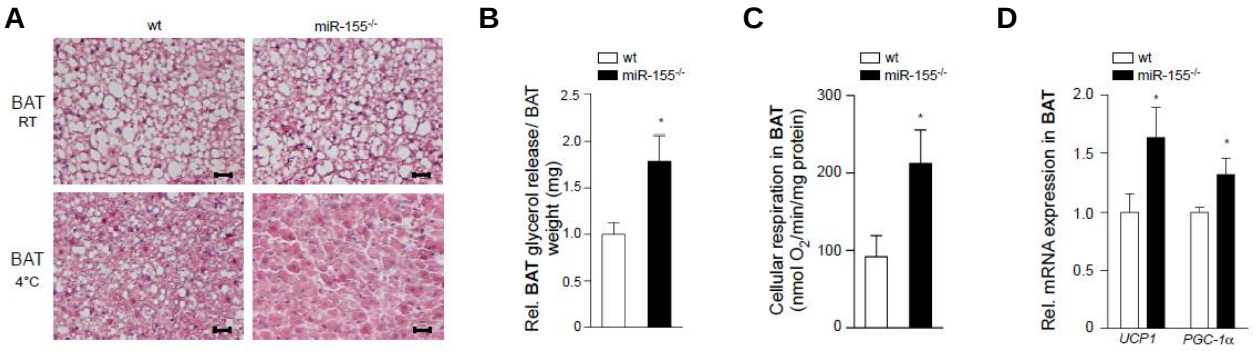

Figure 48. (A) Hematoxylin and eosin staining of interscapular BAT sections from wt and miR-155$^{-/-}$ littermates kept at room temperature (RT) or post cold exposure (4 °C, 4 h) (scale bar, 50 µm). **(B)** Lipolysis assay of BAT from 12 week old wt and miR-155$^{-/-}$ littermates kept in 4 °C for 4 h (*p <0.05; n=4). **(C)** *Ex vivo* Oxygraph measurement of cellular mitochondrial respiration in BAT from 12 to 16 weeks old wt or miR-155$^{-/-}$ littermates exposed to 4 °C (**P*<0.05; wt group n=6, miR-155$^{-/-}$ group n=5). **(D)** qRT-PCR analysis of *UCP1* and *PGC-1α* expression in BAT of 12 to 16 week old wt or miR-155$^{-/-}$ littermates after cold exposure (**P*<0.05; n=4).

Given the impact of miR-155 on the development of a brown fat-like thermogenic program in white adipocytes (Figure 45 and Fig. 46C, D), we studied whether cold-induced WAT browning is affected by loss of miR-155 *in vivo.* igWAT of miR-155$^{-/-}$ mice kept at ambient temperature was clearly morphologically different from wt mice (Figure 49A). miR-155$^{-/-}$ igWAT contained clusters of adipocytes with brown adipocyte-like multilocular lipid droplets (Figure 49A). After cold exposure, the induction of a brown fat phenotype in WAT was clearly enhanced in miR-155$^{-/-}$ mice. Exposure to cold for only 4 h resulted in the predominance of small adipocytes with multilocular lipid droplets in the igWAT of miR155$^{-/-}$ mice. Furthermore, we found a stronger induction of UCP1 and *PGC-1a* expression, and enhanced cellular respiration in miR155$^{-/-}$ mice compared to wt littermates (Figure 49B, C). Body weight of 12-16 week old miR-155$^{-/-}$ mice was significantly lower, whereas food intake of these animals was not altered when compared to wt littermates (Figure 49D, E).

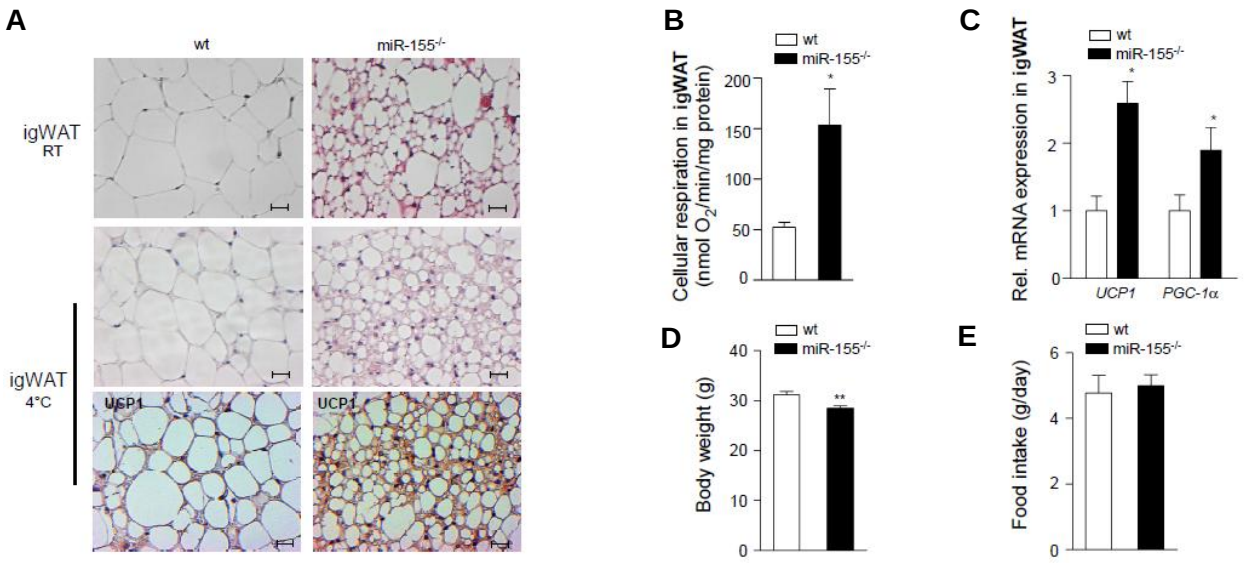

Figure 49. (A) Representative hematoxylin and eosin staining of igWAT sections from wt and miR-155$^{-/-}$ littermates at room temperature or post cold exposure (top). Immunohistochemical staining for UCP1 abundance in respective igWAT sections (bottom) (scale bar, 50 µm). **(B)** *Ex vivo* Oxygraph measurement of cellular mitochondrial respiration in igWAT of wt and miR-155$^{-/-}$ littermates at 12 to 16 weeks of age (**P*<0.05; wt group n=6, miR-155$^{-/-}$ group n=5). **(C)** qRT-PCR analysis of *UCP1* and *PGC-1α* in igWAT from 12 to 16 week old wt or miR-155$^{-/-}$ littermates exposed to 4 °C for 4 h (**P*<0.05; wt group n=4, miR-155$^{-/-}$ group n=4). **(D)** Body weight and **(E)** daily food intake of wt and miR-155$^{-/-}$ littermates at 12-16 weeks of age. Data are represented as means ± SEM (***P*<0.01; wt group n=12, miR-155$^{-/-}$ group n=16).

Importantly, we found that even heterozygous miR-155 (miR-155$^{+/-}$) mice that express about 50% less miR-155 than wt mice (Figure 50A) presented an altered phenotype with significantly enhanced thermogenesis and cellular respiration (Figure 50B-E). Ex vivo respiration rates of miR-155$^{+/-}$ BAT and igWAT were significantly increased but did not reach levels as high as in miR-155$^{-/-}$ animals (Figure 50E, F). These findings show that changes of miR-155 – even at moderate levels - induce activation of the thermogenic program in brown and white adipose tissue depots.

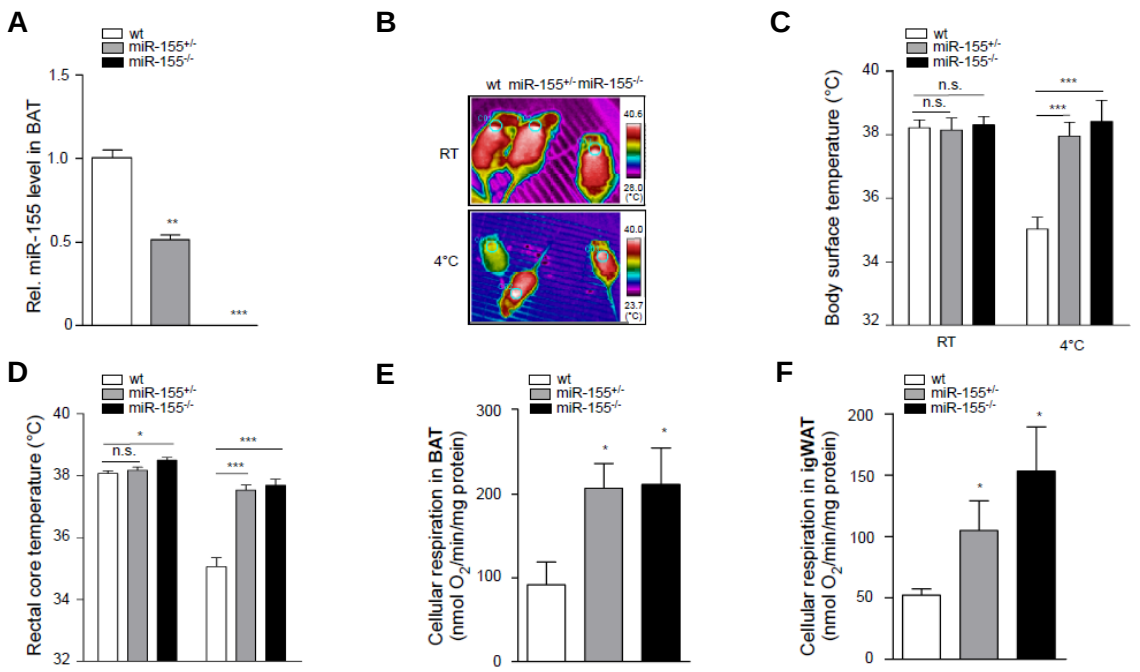

Figure 50. (A) RT-PCR analysis of miR-155 expression levels in interscapular brown adipose tissue (BAT) from 16 week old mice. Data are normalized to sno202RNA expression; data of wt group were set as one; data are represented as means ± SEM (***P*<0.01; *** *P*<0.001; wt group n=3, miR-155$^{+/-}$ group n=3, and miR-155$^{-/-}$ group n=3). **(B)** Infrared thermography analysis of body surface temperature of 12-16 week old wt, miR-155$^{+/-}$ or miR-155$^{-/-}$ littermates exposed to 4 °C. **(C)** Statistical analysis of body surface temperature. Data are represented as means ± SEM (**P*<0.05; n.s., not significant) (wt group n=7, miR-155$^{+/-}$ group n=5, and miR-155$^{-/-}$ group n=5). **(D)** Statistical analysis of rectal body core temperature measurement of 12-16 week old wt, miR-155$^{+/-}$ or miR-155$^{-/-}$ littermates exposed to either RT or 4 °C. Data are represented as means ± SEM (**P*<0.05; *** *P*<0.001; n.s., not significant) (wt group n=14, miR-155$^{+/-}$ group n=14, and miR-155$^{-/-}$ group n=12). **(E, F)** *Ex vivo* Oxygraph measurement of cellular mitochondrial respiration in **(E)** interscapular BAT, or in **(F)** igWAT of wt, miR-155$^{+/-}$ and miR-155$^{-/-}$ littermates at 12-16 weeks of age. Data are represented as means ± SEM (**P*<0.05; ***P*<0.01; ****P*<0.001; n.s., not significant; wt group n=6, miR-155$^{+/-}$ group n=6, and miR-155$^{-/-}$ group n=5).

4. Discussion

4.1. miR-155 works as inhibitor of brown adipose tissue

The recent findings of metabolically active BAT in adults (Enerback, 2010; Nedergaard and Cannon, 2010) considerably raised the interest in brown fat cell development. Brown adipocytes of the "classical" interscapular BAT depot originate from Myf5-positive progenitors (Kajimura et al., 2010). In addition, beige cells with multilocular morphology and UCP1 expression have been described in WAT that are not derived from Myf5-positive precursor cells (Petrovic et al., 2010). The development of these beige cells is induced by cold-exposure or β3-agonists (Seale et al., 2008), such as NE (norepinephrine). Apart from these factors several other stimuli have been described that enhance recruitment of beige cells including prostaglandins, the transcription factor FOXC2 and PPARγ agonists (thiazolidinediones) (Cinti, 2009; Yang et al., 2003), as well as natriuretic peptides and cGMP (Bordicchia et al., 2012; Jennissen et al., 2012). So far not much was known about miRNA-based regulation of brown and beige adipocytes.

miRNAs control the expression of a large part of the human and murine genome. Up to 30% of the human genes are regulated by miRNAs, thereby modulating diverse biological cellular processes. Initial studies revealed differential expression of miRNAs in white and brown adipocytes and that muscle-specific miRNAs are expressed in brown adipocytes (Walden et al., 2009). A recent study by (Sun et al., 2011) found that the miR193b-365 cluster enhances brown adipogenesis of mesenchymal progenitors mainly by suppression of myogenic genes during *in vitro* differentiation.

Using a genome-wide deep sequencing approach, I identified miRNAs that are differentially expressed in brown adipocyte differentiation *in vitro*. Among the miRNAs enriched in preadipocytes, miR-155 was of special interest as it efficiently inhibited adipogenesis, was strongly reduced in mature brown fat cells and was enriched in brown adipose tissue as compared to white adipose tissue.

miR-155 has been shown to regulate gene expression in the hematopoietic system, such as B-cells, T-cells, macrophages as well as immune response cells or cancer cells (O'Connell et al., 2010). In our study, we demonstrate that miR-155 has a significant inhibitory effect in fat tissue,

especially in brown adipose tissue. miR-155 is able to inhibit brown fat differentiation, as well as thermogenic function of brown fat cells. Thus, miR-155 was to the best of our knowledge the first miRNA inhibitor of brown fat adipogenesis until miR-133a has been shown that it is another miRNA inhibitor (Trajkovski et al., 2012a). Similar to the situation in cancer, where oncogenic miRNAs that promote tumor formation or growth and tumor-suppressive, anti-oncogenic miRNAs have been identified (Pfeifer and Lehmann, 2010), we propose that an interplay of "pro-adipogenic" miRNAs – such as miR-193b-365 (Sun et al., 2011) and "anti-adipogenic" miRNAs like miR-155 orchestrates brown fat differentiation.

4.2. miR-155 targets C/EBPβ, the crucial transcriptional factor in brown adipose differentiation

Brown and white differentiation processes share many transcriptional regulators (Seale et al., 2007). For example, PPARγ has been clearly identified as a master regulator of both white and brown adipogenesis and the interplay between PPARγ and members of the C/EBP family are critical for general adipocyte development. However, the effects of PPARγ and of individual members of the C/EBP family are not identical and there appears to be a specificity of certain C/EBPs for white versus brown fat. C/EBPα is required for differentiation of white, but not brown, adipose tissue (Linhart et al., 2001). The analysis of C/EBPβ and C/EBPβ/C/EBPδ knockout mice revealed a predominant role of C/EBPβ in BAT (Tanaka et al., 1997) with only little effect of C/EBPβ-deficiency on white adipocyte development and function.

But how can C/EBPβ be essential for establishment of a brown fat phenotype when it has been demonstrated that it can also initiate the adipogenic differentiation program in white adipose precursors? This puzzle might be explained by (i) differences in the temporal dynamics of C/EBPβ expression in brown versus white cells, with sustained C/EBPβ exposure resulting in the brown phenotype (Karamanlidis et al., 2007) and / or (ii) by its interaction with the transcriptional coregulator PRDM16. PRDM16 and C/EBPβ are co-enriched in BAT and form a transcriptional complex that controls the cell fate switch to brown fat cells (Kajimura et al., 2009; Seale et al., 2008). In the context of overexpression of C/EBPβ alone induces a brown fat cell-like phenotype in white adipocytes (Karamanlidis et al., 2007).

C/EBPβ, the crucial pro-adipogenic transcription factor, had been identified as a major miR-155 target in other cell types including white preadipocytes (He et al., 2009; Skarn et al., 2011; Worm et al., 2009). Its 3'UTR contains one conserved 8mer miR-155 "seed" binding site (www.targetscan.org). Interestingly, in our study we found that miR-155 also efficiently inhibited C/EBPβ expression in brown preadipocytes. miR-155 transduced brown adipocytes revealed reduced protein levels of all three C/EPBβ isoforms: LAP, LAP*, and LIP. Both LAPs have been shown to be important in BAT cell differentiation (Nerlov, 2007). Transduction of miR-155 in BAT cells with lentiviral vectors carrying C/EBPβ restored LAP protein levels. This C/EBPβ restorage rescued brown fat cell differentiation back to the wild type situation. It demonstrates that C/EBPβ is the major target of miR-155 in brown fat precursor cells.

Moreover, luciferase reporter assays have shown that miR-155 directly binds to the C/EBPβ mRNA 3'UTR which is shared by all three C/EBPβ isoforms, resulting in reduced reporter activity. Mutating the putative miR-155 8mer binding site in the 3'UTR of C/EBPβ rescued the reduced reporter activity back to wild type control levels.

An intricate network of regulators controls C/EBPβ expression and function. Among these are adipogenic hormones like insulin, transcription factors (e.g. CREB, Plac8, Forkhead TFs and HOXC8), as well as post-transcriptional regulators (e.g. KSR1 and TRB3) (Bezy et al., 2007; Jimenez-Preitner et al., 2011; Kortum et al., 2005; Mori et al., 2012; Seale et al., 2009). miR-155-based post-transcriptional regulation of C/EBPβ adds another level of regulation. miR-155 shows an interesting temporal expression pattern with high levels during preadipocyte proliferation and mitotic clonal expansion (MCE), but decreasing expression during maturation. The expression changes of miR-155 during brown fat differentiation highlights its decisive function in the temporal regulation of C/EBPβ which expresses at low level during proliferation or MCE stage of preadipocytes, and is increasing during the differentiation. Similar regulatory patterns have been described for Plac8-dependent regulation of C/EBPβ expression (Jimenez-Preitner et al., 2011). Therefore, the correct timing of C/EBPβ expression is crucial for adipogenic differentiation.

4.3. miR-155 expression is regulated by the TGFβ1 signaling pathway in BAT

The transcription factor TGFβ1 was shown to positively regulate miR-155 via the TGFβ/Smad pathway in epithelial cells (Kong et al., 2008). Furthermore, TGFβ has been shown to potently inhibit adipogenesis in 3T3L1 cells (Choy et al., 2000; Ignotz and Massague, 1985). Therefore, we tested whether TGFβ1 is involved in the regulation of miR-155 expression in brown adipocytes.

Remarkably, TGFβ1 expression was regulated in a differentiation-dependent manner very similar to miR-155 in the *in vitro* adipogenesis experiments. Strongest induction of TGFβ1 was measured in the confluent/postconfluent phase at day 0, around the time-point of maximal miR-155 expression. TGFβ1 expression levels decreased significantly after cells had entered differentiation phase (day 0-day 4), which indicates that TGFβ1 is not essential at the early stage of differentiation in BAT cells.

In addition, we could show a direct effect of TGFβ1 on miR-155 transcription: Treatment of preadipocytes with TGFβ1 (5ng/ml) induced a significant increase in miR-155 levels within 24h. When we treated BAT cells with the TGFβ1 receptor inhibitor SB-431542 to block TGFβ1 signaling, miR-155 levels were strongly reduced, resulting in enhanced BAT cell differentiation. Taken together all experimental data, it demonstrates that miR-155 is regulated by TGFβ1 pathway signaling in preadipocytes. Previous studies have shown transcriptional induction of miR-155 by the TGFβ/Smad pathway in epithelial cells (Kong et al., 2008). In brown preadipocytes, however, our data also suggest that TGFβ1 regulates miR-155 via Smad4.

Although TGFβ1 levels are increasing at late stage ofdifferentiation (day 8), miR-155 expression remains at low levels in mature brown fat cells. These results indicate that miR-155 is not only regulated by TGFβ1, but also by other miR-155 inhibitory factors which are presumably strongly expressed at the late stage of differentiation. Therefore, we sought to identify other mechanisms/signals that – apart from TGFβ- are involved in miR-155 regulation.

4.4. C/EBPβ and miR-155 form a bistable feedback loop in BAT

To investigate which factor regulates miR-155 at the stage of BAT cell differentiation, we have analyzed the BIC/miR-155 promoter region for relevant transcription factor binding sites. Interestingly, we identified 5 putative binding sites for transcription factors of the C/EBP family which are essential transcription factors in BAT cell differentiation. The experimental results demonstrated that all C/EBPs are able to repress the BIC/miR-155 promoter activity via binding to the BIC/miR-155 promoter. Among the C/EBPs, C/EBPβ reduced the activity most strongly and can therefore be considered the most prominent regulator of BIC/ miR-155 transcription in brown adipocytes.

Thus, importantly, we found a reciprocal negative regulation or double negative feedback loop (Figure 51) between miR-155 and C/EBPβ that integrates pro- and anti-adipogenic cues during brown fat cell differentiation. One such anti-adipogenic cue is TGFβ1 which is secreted by proliferating precursor cells and induces miR-155 expression. High levels of miR-155 inhibit C/EBPβ expression, thereby suppressing premature differentiation and keeping preadipocytes in an undifferentiated proliferative state. Pro-adipogenic hormones induce expression of C/EBPβ, which in turn inhibits transcription of *BIC*/miR-155. Thus, this double negative feedback mechanism leads to robust commitment to one of two possible states establishing a bistable system (Flynt and Lai, 2008). A similar bistable system has been described for the developing *Drosophila* eye (Li and Carthew, 2005) where miR-7 inhibits the transcription factor Yan, which in turn represses miR-7 transcription. The miR-155/C/EBPβ bistable loop might have evolved to convert weak or only transiently available external signals to a strong response ensuring a uniform response of precursor cells to signals that either prohibit or induce adipogenesis.

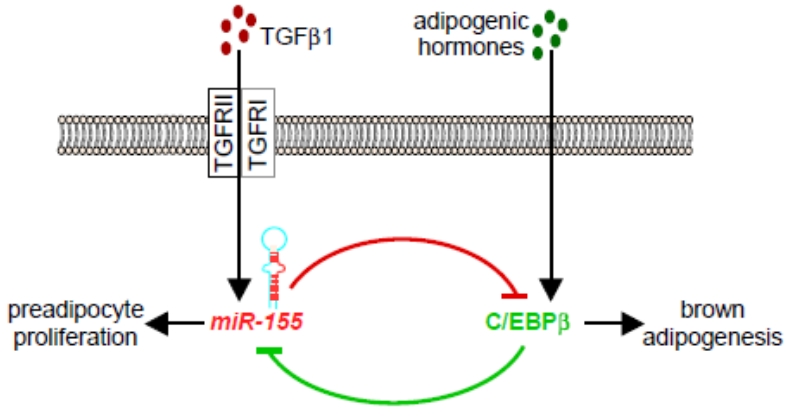

Figure 51. miR-155 and C/EBPβ form a self-inhibitory feedback loop that tightly regulates brown adipogenesis. miR-155 expression is induced by TGFβ1 signaling and mediates translational repression of C/EBPβ by binding to its 3´UTR. In turn, C/EBPβ is induced by adipogenic hormones and inhibits transcription of miR-155. Thereby, miR-155 and C/EBPβ constitute a bistable system for the regulation of adipogenesis and thermogenesis by either maintaining preadipocytes in an undifferentiated precursor state (mitotic clonal expansion) or initiating the brown adipogenic program.

4.5. miR-155 regulates brown fat differentiation *in vivo*

To gain further insight into the function of miR-155, we transduced preimplantation embryos with miR-155 carrying lentivirus to generate miR-155 transgenic mice (Pfeifer et al., 2002). These transgenic animals showed reduced BAT mass, altered BAT morphology characterized by a strong reduction of lipid droplets and TG content, and significantly reduced UCP1 expression. This phenotype corresponds to the impaired differentiation of miR-155 overexpressing preadipocytes observed *in vitro*. Interestingly, the level of miR-155 overexpression achieved in the miR155TG mice caused only a slight - albeit significant - reduction of C/EBPβ indicating that the major effect of miR-155 transgenesis is not a mere suppression of C/EBPβ but rather a destabilization of the miR-155-C/EBPβ feedback loop tipping the balance towards an un-differentiated state. To measure BAT activation/thermogenesis *in vivo*, we analyzed the interscapular body surface temperature by infrared thermographic imaging as well as body core temperature. In line with reduced brown fat differentiation and reduced UCP1 levels, we found significantly reduced BAT thermogenesis in miR-155 transgenic mice. In addition, we found a significant increase in body core temperature in miR-155 transgenic mice after cold exposure.

BAT-specific expression of miR-155 using the *UCP1* promoter resulted in the same effects indicating that the observed phenotype is cell-autonomous. Thus, miR-155 overexpression leads to severe impairment of the thermogenic program and energy expenditure in BAT. Concerning the effect of miR-155 on WAT development, the *in vitro* data show that miR-155 expressed at high levels can inhibit differentiation of SVF cells isolated from murine WAT, of human MSCs (Skarn et al., 2011) and of 3T3L1 cells (Liu et al., 2011). In contrast to BAT, we found no significant changes in WAT weight in the miR-155 transgenic mice, although both tissues expressed similar levels of miR-155. Overall, the phenotype of miR-155 transgenics strikingly resembles the phenotypic hallmarks of the C/EBPβ$^{-/-}$ mice (Tanaka et al., 1997).

4.6. miR-155 regulates "browning" of white fat cells

Most importantly, our study unravels a decisive function of miR-155 in controlling the phenotypic switch of white to brown fat-like cells (beige cells): miR-155 depletion activates the thermogenic program in white adipocytes *in vitro* (Figure 52).

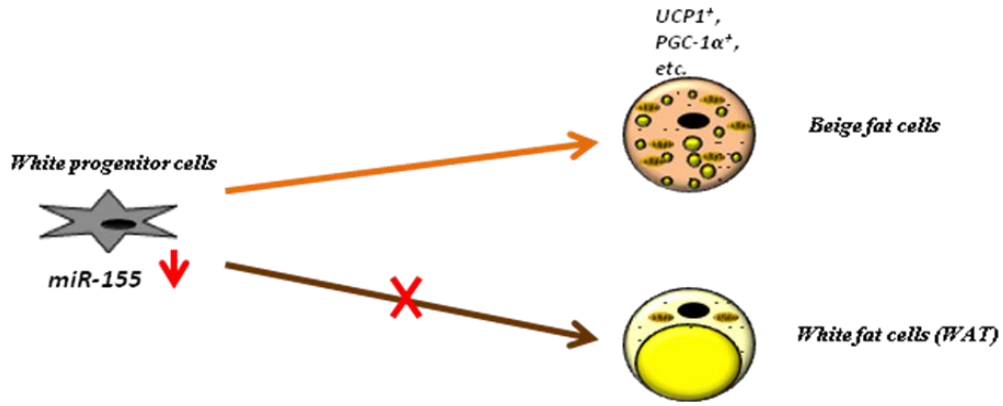

Figure 52. Scheme of the fate of miR-155 expression decreased or deleted white progenitor cells. Brown-specific genes are increased in mature miR-155 knock-down fat cells which were differentiated from white progenitor cells. Fat Droplets are shown in yellow, and mitochondria are shown in brown.

Consequently, miR-155$^{-/-}$ mice show an increased ability to adapt to cold exposure and recruit inducible brown/beige cells in white fat depots. Thus, miR-155 is a key regulator of brown adipocyte identity in brown as well as in white fat, which is tightly linked by a bistable feedback

loop system to C/EBPβ. Knock-down or knock-out of miR-155 enhances thermogenic gene expression in both BAT and WAT. In contrast, transduction of low or medium dosage LVmiR-155 had a much stronger effect on thermogenic and adipogenic gene expression in brown compared to white adipocytes. Furthermore, thermogenic genes are more sensitive to gain- or loss- of miR-155, both in brown and white fat. These data characterize miR-155 as a predominantly brown-fat specific regulator of thermogenesis.

Taken together, miR-155 not only plays a role in differentiation of white adipocytes (Liu et al., 2011), but also has a key function in the regulation of the thermogenic system. When expression of miR-155 is decreased or depleted in white fat progenitors, those progenitors will develop towards preadipocytes with an increased thermogenic potential. These white preadipocytes are able to differentiate to brown like adipocytes (beige adipocytes). These cells expose similar thermogenic functions as brown adipocytes (Ohno et al., 2012; Seale et al., 2008; Seale et al., 2011; Trajkovski et al., 2012b; Vegiopoulos et al., 2010).

Concerning a potential role of miR-155 in humans it is of interest that miR-155 expression has been associated with adipose tissue dysfunction and obesity (Kloting et al., 2009). Obese T2D patients exhibited a strong correlation between increased adipocyte diameter and miR-155 expression. Furthermore, miR-155 expression is significantly correlated to the number of macrophages infiltrating subcutaneous fat depots (Kloting et al., 2009). Adipose tissue macrophages in insulin-resistant subjects are known to secrete higher levels of TGFβ. Thus, macrophage-derived TGFβ might induce miR-155 expression in adipocytes, thereby inhibiting the recruitment of inducible brown/brite cells. Since reduction of miR-155 by 50% in haploinsufficient mice already enhances differentiation and recruitment of both beige adipocytes and BAT cells, therapeutic attempts to reduce miR-155 might be a promising approach to treat obesity in humans.

5. Summary

Brown adipose tissue (BAT) is the primary site of energy expenditure by non-shivering heat and plays an important role in the regulation of metabolic balance in human adults. Recent studies have shown that the energy-storing white adipose tissue (WAT) is able to switch to a brown-like/beige phenotype with similar capacities regarding thermogenesis and energy expenditure like BAT. This process is called “browning”and is mainly induced by cold exposure.

MicroRNAs (miRNAs) are non-coding, post-transcriptional regulators of gene expression. Each miRNA is predicted to target not only one, but up to hundreds of target genes. Therefore, miRNAs are part of a complex regulatory network that tightly regulates expression of ~30% of the human proteome. MiRNAs play an important role in white fat cell differentiation and are deregulated in obese subjects. In contrast, knowledge about the function of miRNAs in brown and beige adipocytes is very limited.

To identify differentially regulated miRNAs with a decisive function in brown adipogenesis, we performed a genome-wide deep sequencing screen comparing preadipocytes of murine BAT with *in vitro* differentiated mature brown fat cells. A selected number of candidate miRNAs were validated by qRT-PCR. Optimized lentiviral expression vectors were used to over-express miRNAs and perform extensive *in vitro* analysis.

The candidate miR-155 is significantly downregulated during brown adipocyte differentiation. Overexpression of miR-155 resulted in strong inhibition of *in vitro* adipocyte differentiation as assessed by lipid droplet staining, triglyceride content measurement as well as by measuring the abundance of adipogenic (C/EBPα, PPARγ and aP2) and thermogenic (UCP1 and PGC-1α) markers.

miR-155 is induced by TGFβ1 during early adipogenesis and is regulated via the TGFβ1/Smad4 signaling pathway. Furthermore, we identified a double negative feedback loop in which miR-155 suppresses the transcription factor C/EBPβ that is essential for early adipogenic commitment. Importantly, C/EBPβ reciprocally represses transcription of miR-155 resulting in a bistable system that tightly controls differentiation of brown adipocytes. Besides, I demonstrate that this

novel miR-155-C/EBPβ feedback loop not only regulates the differentiation of brown adipocytes, but also the capacity of "browning" in WAT cells.

In vivo studies with two types of miR-155 overexpressing transgenic mice model, as well as with knock-out mice model demonstrated that the miR-155-C/EBPβ bistable system is essential for normal brown fat development and function: miR-155 transgenic mice exhibited a strongly reduced BAT mass with decreased lipid content, reduced expression of adipogenic and thermogenic marker proteins, and impaired energy expenditure. In contrast, WAT mass (igWAT, vWAT) of these animals was comparable to wild type mice. These data demonstrate that miR-155 overexpression *in vivo* has a rather specific function in BAT development and is affecting less white adipose tissue depots. Furthermore, studies in miR-155 deficient mice revealed an important role of this miRNA for the "browning" capacity of white adipose tissue.

Taken together, our results show that miRNAs are important regulators of brown adipocyte differentiation: They can either inhibit or promote adipogenesis. miR-155 is a crucial regulator in brown adipogenic differentiation. It has been shown to inhibit fat differentiation via a newly identified miR-155-C/EBPβ regulatory feedback loop. Blockage of miR-155 enhances the differentiation of BAT and the "browning" capability of white adipocytes, resulting in increased energy expenditure. Therefore, therapeutic targeting of miR-155 may be a promising future strategy to fight obesity and metabolic diseases in humans.

6. Curriculum vitae

Personal Data:

Name:	Chen, Yong
Gender:	Male
Date of Birth:	Nov 3rd, 1981
Birth Place:	Wuhan, China
Nationality:	China .P.R
Marital Status:	Married
Current address:	MechenStr. 66
	53129, Bonn

Education background:

09.1988---09.1994	The Elementary School of Tongji Medical College, Wuhan, China
09.1994---09.1997	The Junior High School of Tongji Medical College, Wuhan, China
09.1997---09.2000	The 11th High School of Wuhan city, Wuhan, China
09.2000---10.2005	Tongji Medical College of Huazhong University of Science and Technology, Wuhan, China Specialty: Medicine
10.2005---03.2008	Martin Luther University, Halle (Saale), Germany Specialty: Master of Biomedical Engineering

Professional career:

06.2007---03.2008	Master thesis at Martin Luther University Halle, Department of Internal Medicine, Hematology and Oncology (PD Dr G Behre) Title: "miRNA profiling in human mesenchymal stem cells modulated by C/EBPα during adipogenesis"
03.2008---02.2009	Scientific Staff at Martin-Luther University Halle, Department of Internal Medicine, Hematology and Oncology (PD Dr G Behre)
03.2009---now	Scientific Staff at Rheinische Friedrich-Wilhelms University Bonn, Institute of Pharmacology and Toxicology (Prof. Dr. A. Pfeifer) Title: "Role of miRNAs in brown fat differentiation"
03.2010---08.2012	Stipends of "NRW international Graduate Research School BIOTECH-PHARMA at Friedrich-Wilhelms University Bonn"

7. Publications and Abstracts

7.1. Publications

miR-155 regulates differentiation of brown and beige adipocytes via a bistable circuit.
Chen Y, Siegel F, Kipschull S, Haas B, Fröhlich H, Meister G, Pfeifer A.
Nat Commun. 4:1769 doi: 10.1038/ncomms2742 (2013)

Cyclic GMP and protein kinase G control a Src-containing mechanosome in osteoblasts. Rangaswami H, Schwappacher R, Marathe N, Zhuang S, Casteel DE, Haas B, **Chen Y,** Pfeifer A, Kato H, Shattil S, Boss GR, Pilz RB.
Sci Signal. 2010 Dec 21; 3(153):ra91

AML1/ETO induced survivin expression inhibits transcriptional regulation of myeloid differentiation. Balkhi MY, Christopeit M, **Chen Y**, Geletu M, Behre G.
Exp Hematol. 2008 Nov; 36(11):1449-60

7.2. Abstracts

Yong Chen, Franziska Siegel, Steffanie Kipschull, Alexander Pfeifer. "miR-155 regulates differentiation of brown and beige adipocytes". Heidelberg, Germany, 13th -16th of Sep, 2012

Franziska Siegel, Yong Chen, Steffanie Kipschull, Alexander Pfeifer. "miRNA regulate brown fat differentiation". Santa Fe, USA, 30th of Jan, 2012

Yong Chen, Franziska Siegel, Steffanie Kipschull, Bodo Haas, Alexander Pfeifer. "miRNA controls brown fat differentiation". Tsukuba, Japan, 2nd of Nov, 2011

Yong Chen, Franziska Siegel, Steffanie Kipschull, Bodo Haas, Alexander Pfeifer. "Brown fat differentiation is controlled by miRNAs". Bonn, Germany, 12th of Sep, 2011

8. References

Amanda, B., Manuela, M., Antonia, M., Claudio, M., and Gregorio, B. (2010). Posturography measures and efficacy of different physical treatments in somatic tinnitus. Int Tinnitus J 16, 44-50.

Bentwich, I., Avniel, A., Karov, Y., Aharonov, R., Gilad, S., Barad, O., Barzilai, A., Einat, P., Einav, U., Meiri, E., Sharon, E., Spector, Y., and Bentwich, Z. (2005). Identification of hundreds of conserved and nonconserved human microRNAs. Nat Genet 37, 766-770.

Berezikov, E., and Plasterk, R.H. (2005). Camels and zebrafish, viruses and cancer: a microRNA update. Hum Mol Genet 14 Spec No. 2, R183-190.

Bezy, O., Vernochet, C., Gesta, S., Farmer, S.R., and Kahn, C.R. (2007). TRB3 blocks adipocyte differentiation through the inhibition of C/EBPbeta transcriptional activity. Mol Cell Biol 27, 6818-6831.

Birsoy, K., Chen, Z., and Friedman, J. (2008). Transcriptional regulation of adipogenesis by KLF4. Cell Metab 7, 339-347.

Bobis, S., Jarocha, D., and Majka, M. (2006). Mesenchymal stem cells: characteristics and clinical applications. Folia Histochem Cytobiol 44, 215-230.

Bordicchia, M., Liu, D., Amri, E.Z., Ailhaud, G., Dessi-Fulgheri, P., Zhang, C., Takahashi, N., Sarzani, R., and Collins, S. (2012). Cardiac natriuretic peptides act via p38 MAPK to induce the brown fat thermogenic program in mouse and human adipocytes. J Clin Invest 122, 1022-1036.

Calkhoven, C.F., Muller, C., and Leutz, A. (2000). Translational control of C/EBPalpha and C/EBPbeta isoform expression. Genes Dev 14, 1920-1932.

Chen, P.Y., and Meister, G. (2005). microRNA-guided posttranscriptional gene regulation. Biol Chem 386, 1205-1218.

Choy, L., and Derynck, R. (2003). Transforming growth factor-beta inhibits adipocyte differentiation by Smad3 interacting with CCAAT/enhancer-binding protein (C/EBP) and repressing C/EBP transactivation function. J Biol Chem 278, 9609-9619.

Choy, L., Skillington, J., and Derynck, R. (2000). Roles of autocrine TGF-beta receptor and Smad signaling in adipocyte differentiation. J Cell Biol 149, 667-682.

Cinti, S. (2009). Transdifferentiation properties of adipocytes in the adipose organ. Am J Physiol Endocrinol Metab 297, E977-986.

Collet, A.J., and Des Biens, G. (1975). Evolution of mesenchymal cells in fetal rat lung. Anat Embryol (Berl) 147, 273-292.

Costinean, S., Sandhu, S.K., Pedersen, I.M., Tili, E., Trotta, R., Perrotti, D., Ciarlariello, D., Neviani, P., Harb, J., Kauffman, L.R., Shidham, A., and Croce, C.M. (2009). Src homology 2 domain-containing inositol-5-phosphatase and CCAAT enhancer-binding protein beta are targeted by miR-155 in B cells of Emicro-MiR-155 transgenic mice. Blood 114, 1374-1382.

Cypess, A.M., Lehman, S., Williams, G., Tal, I., Rodman, D., Goldfine, A.B., Kuo, F.C., Palmer, E.L., Tseng, Y.H., Doria, A., Kolodny, G.M., and Kahn, C.R. (2009). Identification and importance of brown adipose tissue in adult humans. N Engl J Med 360, 1509-1517.

Deckers, M., van Dinther, M., Buijs, J., Que, I., Lowik, C., van der Pluijm, G., and ten Dijke, P. (2006). The tumor suppressor Smad4 is required for transforming growth factor beta-induced epithelial to mesenchymal transition and bone metastasis of breast cancer cells. Cancer Res 66, 2202-2209.

Dull, T., Zufferey, R., Kelly, M., Mandel, R.J., Nguyen, M., Trono, D., and Naldini, L. (1998). A third-generation lentivirus vector with a conditional packaging system. J Virol 72, 8463-8471.

Ebert, M.S., Neilson, J.R., and Sharp, P.A. (2007). MicroRNA sponges: competitive inhibitors of small RNAs in mammalian cells. Nat Methods 4, 721-726.

Eis, P.S., Tam, W., Sun, L., Chadburn, A., Li, Z., Gomez, M.F., Lund, E., and Dahlberg, J.E. (2005). Accumulation of miR-155 and BIC RNA in human B cell lymphomas. Proc Natl Acad Sci U S A 102, 3627-3632.

Enerback, S. (2010). Brown adipose tissue in humans. Int J Obes (Lond) 34 Suppl 1, S43-46.

Fazi, F., Rosa, A., Fatica, A., Gelmetti, V., De Marchis, M.L., Nervi, C., and Bozzoni, I. (2005). A minicircuitry comprised of microRNA-223 and transcription factors NFI-A and C/EBPalpha regulates human granulopoiesis. Cell 123, 819-831.

Flynt, A.S., and Lai, E.C. (2008). Biological principles of microRNA-mediated regulation: shared themes amid diversity. Nat Rev Genet 9, 831-842.

Gesta, S., Tseng, Y.H., and Kahn, C.R. (2007). Developmental origin of fat: tracking obesity to its source. Cell 131, 242-256.

Gregory, R.I., Chendrimada, T.P., and Shiekhattar, R. (2006). MicroRNA biogenesis: isolation and characterization of the microprocessor complex. Methods Mol Biol 342, 33-47.

Haas, B., Mayer, P., Jennissen, K., Scholz, D., Berriel Diaz, M., Bloch, W., Herzig, S., Fassler, R., and Pfeifer, A. (2009). Protein kinase G controls brown fat cell differentiation and mitochondrial biogenesis. Sci Signal 2, ra78.

He, M., Xu, Z., Ding, T., Kuang, D.M., and Zheng, L. (2009). MicroRNA-155 regulates inflammatory cytokine production in tumor-associated macrophages via targeting C/EBPbeta. Cell Mol Immunol 6, 343-352.

Hodges, M.R., Tattersall, G.J., Harris, M.B., McEvoy, S.D., Richerson, D.N., Deneris, E.S., Johnson, R.L., Chen, Z.F., and Richerson, G.B. (2008). Defects in breathing and thermoregulation in mice with near-complete absence of central serotonin neurons. J Neurosci 28, 2495-2505.

Ignotz, R.A., and Massague, J. (1985). Type beta transforming growth factor controls the adipogenic differentiation of 3T3 fibroblasts. Proc Natl Acad Sci U S A 82, 8530-8534.

Inman, G.J., Nicolas, F.J., Callahan, J.F., Harling, J.D., Gaster, L.M., Reith, A.D., Laping, N.J., and Hill, C.S. (2002). SB-431542 is a potent and specific inhibitor of transforming growth factor-beta superfamily type I activin receptor-like kinase (ALK) receptors ALK4, ALK5, and ALK7. Mol Pharmacol 62, 65-74.

Jennissen, K., Haas, B., Mitschke, M.M., Siegel, F., and Pfeifer, A. (2013). Analysis of cGMP Signaling in Adipocytes. Methods Mol Biol 1020, 175-192.

Jennissen, K., Siegel, F., Liebig-Gonglach, M., Hermann, M.R., Kipschull, S., van Dooren, S., Kunz, W.S., Fassler, R., and Pfeifer, A. (2012). A VASP-Rac-soluble guanylyl cyclase pathway controls cGMP production in adipocytes. Sci Signal 5, ra62.

Jimenez-Preitner, M., Berney, X., Uldry, M., Vitali, A., Cinti, S., Ledford, J.G., and Thorens, B. (2011). Plac8 Is an Inducer of C/EBPbeta Required for Brown Fat Differentiation, Thermoregulation, and Control of Body Weight. Cell Metab.

Kajimura, S., Seale, P., Kubota, K., Lunsford, E., Frangioni, J.V., Gygi, S.P., and Spiegelman, B.M. (2009). Initiation of myoblast to brown fat switch by a PRDM16-C/EBP-beta transcriptional complex. Nature 460, 1154-1158.

Kajimura, S., Seale, P., and Spiegelman, B.M. (2010). Transcriptional control of brown fat development. Cell Metab 11, 257-262.

Karamanlidis, G., Karamitri, A., Docherty, K., Hazlerigg, D.G., and Lomax, M.A. (2007). C/EBPbeta reprograms white 3T3-L1 preadipocytes to a Brown adipocyte pattern of gene expression. J Biol Chem 282, 24660-24669.

Kloting, N., Berthold, S., Kovacs, P., Schon, M.R., Fasshauer, M., Ruschke, K., Stumvoll, M., and Bluher, M. (2009). MicroRNA expression in human omental and subcutaneous adipose tissue. PLoS One 4, e4699.

Kong, W., Yang, H., He, L., Zhao, J.J., Coppola, D., Dalton, W.S., and Cheng, J.Q. (2008). MicroRNA-155 is regulated by the transforming growth factor beta/Smad pathway and contributes to epithelial cell plasticity by targeting RhoA. Mol Cell Biol 28, 6773-6784.

Kortum, R.L., Costanzo, D.L., Haferbier, J., Schreiner, S.J., Razidlo, G.L., Wu, M.H., Volle, D.J., Mori, T., Sakaue, H., Chaika, N.V., Chaika, O.V., and Lewis, R.E. (2005). The molecular scaffold kinase suppressor of Ras 1 (KSR1) regulates adipogenesis. Mol Cell Biol 25, 7592-7604.

Kozomara, A., and Griffiths-Jones, S. (2010). miRBase: integrating microRNA annotation and deep-sequencing data. Nucleic Acids Res 39, D152-157.

Krutzfeldt, J., Poy, M.N., and Stoffel, M. (2006). Strategies to determine the biological function of microRNAs. Nat Genet 38 Suppl, S14-19.

Krutzfeldt, J., Rosch, N., Hausser, J., Manoharan, M., Zavolan, M., and Stoffel, M. (2011). MicroRNA-194 is a target of transcription factor 1 (Tcf1, HNF1alpha) in adult liver and controls expression of frizzled-6. Hepatology 55, 98-107.

Kuznetsov, A.V., Veksler, V., Gellerich, F.N., Saks, V., Margreiter, R., and Kunz, W.S. (2008). Analysis of mitochondrial function in situ in permeabilized muscle fibers, tissues and cells. Nat Protoc 3, 965-976.

Lee, R.C., Feinbaum, R.L., and Ambros, V. (1993). The C. elegans heterochronic gene lin-4 encodes small RNAs with antisense complementarity to lin-14. Cell 75, 843-854.

Lee, Y., Kim, M., Han, J., Yeom, K.H., Lee, S., Baek, S.H., and Kim, V.N. (2004). MicroRNA genes are transcribed by RNA polymerase II. EMBO J 23, 4051-4060.

Lewis, B.P., Burge, C.B., and Bartel, D.P. (2005). Conserved seed pairing, often flanked by adenosines, indicates that thousands of human genes are microRNA targets. Cell 120, 15-20.

Li, X., and Carthew, R.W. (2005). A microRNA mediates EGF receptor signaling and promotes photoreceptor differentiation in the Drosophila eye. Cell 123, 1267-1277.

Linhart, H.G., Ishimura-Oka, K., DeMayo, F., Kibe, T., Repka, D., Poindexter, B., Bick, R.J., and Darlington, G.J. (2001). C/EBPalpha is required for differentiation of white, but not brown, adipose tissue. Proc Natl Acad Sci U S A 98, 12532-12537.

Liu, S., Yang, Y., and Wu, J. (2011). TNFalpha-induced up-regulation of miR-155 inhibits adipogenesis by down-regulating early adipogenic transcription factors. Biochem Biophys Res Commun 414, 618-624.

Liu, Z., Sall, A., and Yang, D. (2008). MicroRNA: An emerging therapeutic target and intervention tool. Int J Mol Sci 9, 978-999.

Lois, C., Hong, E.J., Pease, S., Brown, E.J., and Baltimore, D. (2002). Germline transmission and tissue-specific expression of transgenes delivered by lentiviral vectors. Science 295, 868-872.

Lowell, B.B., and Flier, J.S. (1997). Brown adipose tissue, beta 3-adrenergic receptors, and obesity. Annu Rev Med 48, 307-316.

Lund, E., Guttinger, S., Calado, A., Dahlberg, J.E., and Kutay, U. (2004). Nuclear export of microRNA precursors. Science 303, 95-98.

Monticelli, S., Ansel, K.M., Xiao, C., Socci, N.D., Krichevsky, A.M., Thai, T.H., Rajewsky, N., Marks, D.S., Sander, C., Rajewsky, K., Rao, A., and Kosik, K.S. (2005). MicroRNA profiling of the murine hematopoietic system. Genome Biol 6, R71.

Mori, M., Nakagami, H., Rodriguez-Araujo, G., Nimura, K., and Kaneda, Y. (2012). Essential role for miR-196a in brown adipogenesis of white fat progenitor cells. PLoS Biol 10, e1001314.

Mraz, M., and Pospisilova, S. (2012). MicroRNAs in chronic lymphocytic leukemia: from causality to associations and back. Expert Rev Hematol 5, 579-581.

Nedergaard, J., Bengtsson, T., and Cannon, B. (2007). Unexpected evidence for active brown adipose tissue in adult humans. Am J Physiol Endocrinol Metab 293, E444-452.

Nedergaard, J., and Cannon, B. (2010). The changed metabolic world with human brown adipose tissue: therapeutic visions. Cell Metab 11, 268-272.

Nedergaard, J., and Cannon, B. (2013). How brown is brown fat? It depends where you look. Nat Med 19, 540-541.

Nerlov, C. (2007). The C/EBP family of transcription factors: a paradigm for interaction between gene expression and proliferation control. Trends Cell Biol 17, 318-324.

O'Connell, R.M., Chaudhuri, A.A., Rao, D.S., and Baltimore, D. (2009). Inositol phosphatase SHIP1 is a primary target of miR-155. Proc Natl Acad Sci U S A 106, 7113-7118.

O'Connell, R.M., Kahn, D., Gibson, W.S., Round, J.L., Scholz, R.L., Chaudhuri, A.A., Kahn, M.E., Rao, D.S., and Baltimore, D. (2010). MicroRNA-155 promotes autoimmune inflammation by enhancing inflammatory T cell development. Immunity 33, 607-619.

O'Connell, R.M., Rao, D.S., Chaudhuri, A.A., Boldin, M.P., Taganov, K.D., Nicoll, J., Paquette, R.L., and Baltimore, D. (2008). Sustained expression of microRNA-155 in hematopoietic stem cells causes a myeloproliferative disorder. J Exp Med 205, 585-594.

Ohno, H., Shinoda, K., Spiegelman, B.M., and Kajimura, S. (2012). PPARgamma agonists induce a white-to-brown fat conversion through stabilization of PRDM16 protein. Cell Metab 15, 395-404.

Pasquinelli, A.E., Reinhart, B.J., Slack, F., Martindale, M.Q., Kuroda, M.I., Maller, B., Hayward, D.C., Ball, E.E., Degnan, B., Muller, P., Spring, J., Srinivasan, A., Fishman, M., Finnerty, J., Corbo, J., Levine, M., Leahy, P., Davidson, E., and Ruvkun, G. (2000). Conservation of the sequence and temporal expression of let-7 heterochronic regulatory RNA. Nature 408, 86-89.

Pelled, G., G, T., Aslan, H., Gazit, Z., and Gazit, D. (2002). Mesenchymal stem cells for bone gene therapy and tissue engineering. Curr Pharm Des 8, 1917-1928.

Petrovic, N., Walden, T.B., Shabalina, I.G., Timmons, J.A., Cannon, B., and Nedergaard, J. (2010). Chronic peroxisome proliferator-activated receptor gamma (PPARgamma) activation of epididymally derived white adipocyte cultures reveals a population of thermogenically competent, UCP1-containing adipocytes molecularly distinct from classic brown adipocytes. J Biol Chem 285, 7153-7164.

Pfeifer, A., Ikawa, M., Dayn, Y., and Verma, I.M. (2002). Transgenesis by lentiviral vectors: lack of gene silencing in mammalian embryonic stem cells and preimplantation embryos. Proc Natl Acad Sci U S A 99, 2140-2145.

Pfeifer, A., and Lehmann, H. (2010). Pharmacological potential of RNAi - focus on miRNA. Pharmacol Ther 126, 217-227.

Preall, J.B., He, Z., Gorra, J.M., and Sontheimer, E.J. (2006). Short interfering RNA strand selection is independent of dsRNA processing polarity during RNAi in Drosophila. Curr Biol 16, 530-535.

Reinhart, B.J., Slack, F.J., Basson, M., Pasquinelli, A.E., Bettinger, J.C., Rougvie, A.E., Horvitz, H.R., and Ruvkun, G. (2000). The 21-nucleotide let-7 RNA regulates developmental timing in Caenorhabditis elegans. Nature 403, 901-906.

Rodriguez, A., Griffiths-Jones, S., Ashurst, J.L., and Bradley, A. (2004). Identification of mammalian microRNA host genes and transcription units. Genome Res 14, 1902-1910.

Rosen, E.D., Hsu, C.H., Wang, X., Sakai, S., Freeman, M.W., Gonzalez, F.J., and Spiegelman, B.M. (2002). C/EBPalpha induces adipogenesis through PPARgamma: a unified pathway. Genes Dev 16, 22-26.

Rosen, E.D., and MacDougald, O.A. (2006). Adipocyte differentiation from the inside out. Nat Rev Mol Cell Biol 7, 885-896.

Sacchetti, B., Funari, A., Michienzi, S., Di Cesare, S., Piersanti, S., Saggio, I., Tagliafico, E., Ferrari, S., Robey, P.G., Riminucci, M., and Bianco, P. (2007). Self-renewing osteoprogenitors in bone marrow sinusoids can organize a hematopoietic microenvironment. Cell 131, 324-336.

Saito, M., Okamatsu-Ogura, Y., Matsushita, M., Watanabe, K., Yoneshiro, T., Nio-Kobayashi, J., Iwanaga, T., Miyagawa, M., Kameya, T., Nakada, K., Kawai, Y., and Tsujisaki, M. (2009). High incidence of metabolically active brown adipose tissue in healthy adult humans: effects of cold exposure and adiposity. Diabetes 58, 1526-1531.

Saraf, A., and Mikos, A.G. (2006). Gene delivery strategies for cartilage tissue engineering. Adv Drug Deliv Rev 58, 592-603.

Schulz, T.J., Huang, T.L., Tran, T.T., Zhang, H., Townsend, K.L., Shadrach, J.L., Cerletti, M., McDougall, L.E., Giorgadze, N., Tchkonia, T., Schrier, D., Falb, D., Kirkland, J.L., Wagers, A.J., and Tseng, Y.H. (2010). Identification of inducible brown adipocyte progenitors residing in skeletal muscle and white fat. Proc Natl Acad Sci U S A 108, 143-148.

Seale, P., Bjork, B., Yang, W., Kajimura, S., Chin, S., Kuang, S., Scime, A., Devarakonda, S., Conroe, H.M., Erdjument-Bromage, H., Tempst, P., Rudnicki, M.A., Beier, D.R., and Spiegelman, B.M. (2008). PRDM16 controls a brown fat/skeletal muscle switch. Nature 454, 961-967.

Seale, P., Conroe, H.M., Estall, J., Kajimura, S., Frontini, A., Ishibashi, J., Cohen, P., Cinti, S., and Spiegelman, B.M. (2011). Prdm16 determines the thermogenic program of subcutaneous white adipose tissue in mice. J Clin Invest 121, 96-105.

Seale, P., Kajimura, S., and Spiegelman, B.M. (2009). Transcriptional control of brown adipocyte development and physiological function--of mice and men. Genes Dev 23, 788-797.

Seale, P., Kajimura, S., Yang, W., Chin, S., Rohas, L.M., Uldry, M., Tavernier, G., Langin, D., and Spiegelman, B.M. (2007). Transcriptional control of brown fat determination by PRDM16. Cell Metab 6, 38-54.

Shi, X., Shi, W., Li, Q., Song, B., Wan, M., Bai, S., and Cao, X. (2003). A glucocorticoid-induced leucine-zipper protein, GILZ, inhibits adipogenesis of mesenchymal cells. EMBO Rep 4, 374-380.

Shivdasani, R.A. (2006). MicroRNAs: regulators of gene expression and cell differentiation. Blood 108, 3646-3653.

Skarn, M., Namlos, H.M., Noordhuis, P., Wang, M.Y., Meza-Zepeda, L.A., and Myklebost, O. (2011). Adipocyte Differentiation of Human Bone Marrow-Derived Stromal Cells Is Modulated by MicroRNA-155, MicroRNA-221, and MicroRNA-222. Stem Cells Dev.

Sun, L., Xie, H., Mori, M.A., Alexander, R., Yuan, B., Hattangadi, S.M., Liu, Q., Kahn, C.R., and Lodish, H.F. (2011). Mir193b-365 is essential for brown fat differentiation. Nat Cell Biol 13, 958-965.

Tanaka, T., Yoshida, N., Kishimoto, T., and Akira, S. (1997). Defective adipocyte differentiation in mice lacking the C/EBPbeta and/or C/EBPdelta gene. EMBO J 16, 7432-7443.

Thai, T.H., Calado, D.P., Casola, S., Ansel, K.M., Xiao, C., Xue, Y., Murphy, A., Frendewey, D., Valenzuela, D., Kutok, J.L., Schmidt-Supprian, M., Rajewsky, N., Yancopoulos, G., Rao, A., and Rajewsky, K. (2007). Regulation of the germinal center response by microRNA-155. Science 316, 604-608.

Trajkovski, M., Ahmed, K., Esau, C.C., and Stoffel, M. (2012a). MyomiR-133 regulates brown fat differentiation through Prdm16. Nat Cell Biol 14, 1330-1335.

Tseng, Y.H., Kokkotou, E., Schulz, T.J., Huang, T.L., Winnay, J.N., Taniguchi, C.M., Tran, T.T., Suzuki, R., Espinoza, D.O., Yamamoto, Y., Ahrens, M.J., Dudley, A.T., Norris, A.W., Kulkarni, R.N., and Kahn, C.R. (2008). New role of bone morphogenetic protein 7 in brown adipogenesis and energy expenditure. Nature 454, 1000-1004.

van Marken Lichtenbelt, W.D., Vanhommerig, J.W., Smulders, N.M., Drossaerts, J.M., Kemerink, G.J., Bouvy, N.D., Schrauwen, P., and Teule, G.J. (2009). Cold-activated brown adipose tissue in healthy men. N Engl J Med 360, 1500-1508.

Vegiopoulos, A., Muller-Decker, K., Strzoda, D., Schmitt, I., Chichelnitskiy, E., Ostertag, A., Berriel Diaz, M., Rozman, J., Hrabe de Angelis, M., Nusing, R.M., Meyer, C.W., Wahli, W., Klingenspor, M., and Herzig, S. (2010). Cyclooxygenase-2 controls energy homeostasis in mice by de novo recruitment of brown adipocytes. Science 328, 1158-1161.

Velu, V.K., Ramesh, R., and Srinivasan, A.R. (2012). Circulating MicroRNAs as Biomarkers in Health and Disease. J Clin Diagn Res 6, 1791-1795.

Virtanen, K.A., Lidell, M.E., Orava, J., Heglind, M., Westergren, R., Niemi, T., Taittonen, M., Laine, J., Savisto, N.J., Enerback, S., and Nuutila, P. (2009). Functional brown adipose tissue in healthy adults. N Engl J Med 360, 1518-1525.

Walden, T.B., Timmons, J.A., Keller, P., Nedergaard, J., and Cannon, B. (2009). Distinct expression of muscle-specific microRNAs (myomirs) in brown adipocytes. J Cell Physiol 218, 444-449.

Wang, Y., and Sul, H.S. (2009). Pref-1 regulates mesenchymal cell commitment and differentiation through Sox9. Cell Metab 9, 287-302.

Wightman, B., Ha, I., and Ruvkun, G. (1993). Posttranscriptional regulation of the heterochronic gene lin-14 by lin-4 mediates temporal pattern formation in C. elegans. Cell 75, 855-862.

Worm, J., Stenvang, J., Petri, A., Frederiksen, K.S., Obad, S., Elmen, J., Hedtjarn, M., Straarup, E.M., Hansen, J.B., and Kauppinen, S. (2009). Silencing of microRNA-155 in mice during acute inflammatory response leads to derepression of c/ebp Beta and down-regulation of G-CSF. Nucleic Acids Res 37, 5784-5792.

Wu, Z., Rosen, E.D., Brun, R., Hauser, S., Adelmant, G., Troy, A.E., McKeon, C., Darlington, G.J., and Spiegelman, B.M. (1999). Cross-regulation of C/EBP alpha and PPAR gamma controls the transcriptional pathway of adipogenesis and insulin sensitivity. Mol Cell 3, 151-158.

Yadav, H., Quijano, C., Kamaraju, A.K., Gavrilova, O., Malek, R., Chen, W., Zerfas, P., Zhigang, D., Wright, E.C., Stuelten, C., Sun, P., Lonning, S., Skarulis, M., Sumner, A.E., Finkel, T., and Rane, S.G. (2011). Protection from obesity and diabetes by blockade of TGF-beta/Smad3 signaling. Cell Metab 14, 67-79.

Yadav, H., and Rane, S.G. (2012). TGF-beta/Smad3 Signaling Regulates Brown Adipocyte Induction in White Adipose Tissue. Front Endocrinol (Lausanne) 3, 35.

Yang, X., Enerback, S., and Smith, U. (2003). Reduced expression of FOXC2 and brown adipogenic genes in human subjects with insulin resistance. Obes Res 11, 1182-1191.

Yin, Q., Wang, X., McBride, J., Fewell, C., and Flemington, E. (2008). B-cell receptor activation induces BIC/miR-155 expression through a conserved AP-1 element. J Biol Chem 283, 2654-2662.

Zhou, Z., Yon Toh, S., Chen, Z., Guo, K., Ng, C.P., Ponniah, S., Lin, S.C., Hong, W., and Li, P. (2003). Cidea-deficient mice have lean phenotype and are resistant to obesity. Nat Genet 35, 49-56.